Design and Performance Analysis of MIMO Based WLANs

Von der Fakultät für Elektrotechnik und Informationstechnik der Rheinisch-Westfälischen Technischen Hochschule Aachen zur Erlangung des akademischen Grades eines Doktors der Ingenieurwissenschaften genehmigte Dissertation

vorgelegt von

Diplom-Ingenieurin
Jelena Mirković

aus Kikinda, Serbien

Berichter: Universitätsprofessor Dr.-Ing. Bernhard Walke
Universitätsprofessor Dr. rer.nat. Friedrich K. Jondral

Tag der mündlichen Prüfung: 2. Dezember 2008

AACHENER BEITRÄGE ZUR MOBIL- UND TELEKOMMUNIKATION

Herausgeber:
Universitätsprofessor Dr.-Ing. Bernhard Walke

Bibliografische Information Der Deutschen Bibliothek
Die Deutsche Bibliothek verzeichnet diese Publikation in der Deutschen Nationalbibliografie; detaillierte bibliografische Daten sind im Internet über http://dnb.ddb.de abrufbar.

1. Auflage 2009
ISBN: 3-86130-938-6
Aachener Beiträge zur Mobil- und Telekommunikation; Band 58

Wissenschaftsverlag Mainz
Süsterfeldstr. 83, 52072 Aachen
Telefon: 02 41 / 2 39 48 oder 02 41 / 87 34 34
Fax: 02 41 / 87 55 77
www.verlag-mainz.de

Herstellung: Druckerei Mainz GmbH,
Süsterfeldstr. 83, 52072 Aachen
Telefon 02 41 / 87 34 34; Fax: 02 41 / 87 55 77

Gedruckt auf chlorfrei gebleichtem Papier

"D82 (Diss. RWTH Aachen)"

ABSTRACT

Multiple Input - Multiple Output (MIMO) refers to the use of multiple antennas at receiver and transmitter in order to improve the performance of communication link and the whole system. It is receiving growing attention for application in wireless networks, reflected in the vivid activities related to MIMO in standardization bodies for different systems, e.g. IEEE 802.11n and 802.16 (Worldwide Interoperability for Microwave Access (WiMAX)), High-Speed Packet Access Evolution (HSPA+) and 3rd Generation Partnership Project (3GPP) Long Term Evolution (LTE).

Application of MIMO poses several challenges to system design, not only on Physical Layer (PHY), but also on Medium Access Control (MAC) layer, such as signaling methods, channel estimation and Channel State Information (CSI) feedback. Also, adapting channel aware scheduling algorithms to the layered structure of the MIMO channel promises high performance gains.

MAC layer design and performance evaluation of MIMO based Wireless Local Area Networks (WLANs) are addressed in this thesis. Single-User - Distributed Coordination Function (SU-DCF) and Multi-User - Distributed Coordination Function (MU-DCF) are proposed as extensions of the IEEE 802.11 Distributed Coordination Function (DCF). Orthogonal Frequency Division Multiple Access (OFDMA) signaling is introduced in order to efficiently exchange control frames and reduce the overhead that MU-DCF suffers from.

Performance evaluation of these two protocols, by means of achievable throughput, provided fairness, and delay characteristic, on both link and system level is presented, revealing the benefits and drawbacks of Single-User (SU) and Multi-User (MU) transmission strategies. Cases of both uninformed transmitter and informed transmitter that applies different channel aware scheduling algorithms are studied, investigating the impact of MU diversity and channel uncertainty on the performance of the scheduling algorithms.

Abstract

KURZFASSUNG

Multiple Input - Multiple Output (MIMO) verweist auf Verwendung von mehreren Antennen beim Sender und Empfänger um die Leistung der Verbindung und des ganzen Systems zu verbessern. Die Verwendung von MIMO in der drahtlosen Kommunikation zieht viel Aufmerksamkeit auf sich, sichtbar in vielen Aktivitäten in der Standardisierung für verschiedene Systeme, z. B. IEEE 802.11n und 802.16 (Worldwide Interoperability for Microwave Access (WiMAX)), High-Speed Packet Access Evolution (HSPA+) und 3rd Generation Partnership Project (3GPP) Long Term Evolution (LTE).

Die Verwendung von MIMO stellt mehrere Herausforderungen für den Systementwurf dar, nicht nur auf Schicht-1, sonden auch auf Schicht-2, wie Signalisierungsmethoden, Kanalschätzung und die Übertragung von Kanalzustandsinformation. Zusätzlich verspricht die Anpassung der adaptiven Zuteilungsalgorithmen die die MIMO Kanal Schichtstruktur berücksichtigen, hohe Leistungsteigerung.

Diese Arbeit befasst sich mit dem Entwurf und der Leistungbewertung der Schicht-2 von MIMO basierten drahtlosen Netzen. Single-User - Distributed Coordination Function (SU-DCF) und Multi-User - Distributed Coordination Function (MU-DCF) werden als Erweiterungen von IEEE 802.11 Distributed Coordination Function (DCF) vorgeschlagen. Orthogonal Frequency Division Multiple Access (OFDMA) Signalisierung wird eingeführt, um die Effizienz zu steigern und den Overhead, unter dem MU-DCF stark leidet, zu reduzieren.

Die Leistung von SU-DCF und MU-DCF wird anhand von Durchsatz, Fairness und Paketverzögerung auf Link- und Systemebene bewertet. Dabei werden die Vorteile und Nachteile der beiden Verfahren deutlich herausgestellt. Untersucht werden sowohl der Fall von Sendern ohne, als auch der von Sendern mit Kanalzustandsinformation, die die verschiedenen Zuteilungsalgorithmen verwenden. Damit wird der Einfluss von Mehrbenutzer-Diversität und Ungenauigkeit der Kanalzustandsinformation auf die Leistung der Zuteilungalgorithmen bewertet.

CHAPTER 1

Introduction

Contents

Multiple Input - Multiple Output (MIMO) is a wide set of multiple antenna technologies that can significantly increase the capacity of wireless networks, without additional bandwidth or increased transmission power. They are widely recognized as technologies essential for meeting, at relatively low cost, ever growing network requiremens, such as higher data rate, high mobility, QoS support, higher security, support for diversity and plurality of devices and services, etc.

1.1 Multiple Antennas in Wireless Communications

Antenna arrays were used from the beginning of 20^{th} century for radar applications and later also for Angle-of-Arrival (AoA) estimation (e.g. MUSIC [Schmidt, 1986] and ESPRIT algorithms [Roy et al., 1986]). Their application in wireless communications started with 1984 and work of Jack Winters [Winters, 1984]. Many other valuable contributions have followed, such as introduction of Bell Labs Layered Space Time (BLAST) scheme [Foschini, 1996], Orthogonal Space-Time Block Coding (OSTBC) in [Tarokh et al., 1999a] and MIMO channel Shannon capacity published by Telatar in [Telatar, 1999].

Based on the optimization criterion set by the applied algorithm, MIMO technologies can be divided into three classes: methods to increase the link/system capacity (Spatial Multiplexing (SMUX)), methods to increase the robustness of the communication link (Space-Time Coding (STC)), and methods to reduce co-channel interference (beamforming and Space Division Multiple Access (SDMA)).

1.1.1 MIMO in Standards

Being a technology that for relatively low price dramatically improves the network performance, the interest of industry in it is very high. This is reflected in the vivid activities related to MIMO in standardization bodies for different systems.

Standards and systems that are currently under development include different MIMO technologies. Basicly, those are beamforming in combination with SDMA, STC and SMUX, although different organizations and companies tend to use different names. Examples of new systems that will eventually or already do include MIMO are 3rd Generation Partnership Project (3GPP) Long Term Evolution (LTE) and High-Speed Packet Access Evolution (HSPA+) for cellular radio systems, IEEE 802.16 and Worldwide Interoperability for Microwave Access (WiMAX) for Wireless Metropolitan Area Networks (WMANs), and IEEE 802.11n for Wireless Local Area Networks (WLANs).

1.1.2 Boosting the link level performance

In SMUX schemes, multiple streams are transmitted simultaneously, each one using a dedicated transmit antenna. The receiver also has multiple antennas that receive a signal that is a sum of the transmitted signals that have propagated different paths. Provided rich multipath scattering, by applying an appropriate algorithm the original symbols are separated. Thus, the throughput increases with a factor equal to the number of transmitted streams.

SMUX and STC are typically combined with Orthogonal Frequency Division Multiplexing (OFDM) or Orthogonal Frequency Division Multiple Access (OFDMA) that efficiently handle the Inter-Symbol Interference (ISI) created by multi-path channel. In this combination, coding not only over time and space is possible, but also coding over frequency to provide additional diversity.

1.1.3 Higher Layer Aspects

MIMO based Physical Layer (PHY) provides the transmission channel with a layered structure that gives another degree of freedom in scheduling transmissions. Thus, a cross-layer approach that provides efficient management of the channels spatial layers, can significantly increase the networks performance on both link and system level.

Cross-layer design gets another dimension compared to conventional, single-antenna systems, and that is spatial dimension. Therefore e.g. with properly designed scheduling algorithm and fine-grained resource allocation, there is a high potential for boosting the network performance.

1.2 Objectives

In this work MAC layer aspects and potentials for improvement of a system with MIMO based PHY are investigated.

MIMO based PHY poses several challenges to system design. In particular, on MAC layer they include signaling methods, channel estimation and Channel State Information (CSI) feedback. Opportunistic scheduler algorithms developed for single antenna systems directly applied in MIMO systems do not fully exploit the potentials offered by MIMO channel. Their design and performance evaluation under channel uncertainty are also addressed in this work.

1.3 Contributions of this Thesis

The major contributions of this thesis can be summarized in the following:

- Two Medium Access Control (MAC) protocols, namely Single-User - Distributed Coordination Function (SU-DCF) and Multi-User - Distributed Coordination Function (MU-DCF), are designed, adapted to support MIMO technology (Single-User (SU) and Multi-User (MU) respectively) in IEEE 802.11 based WLANs.

- OFDMA based signaling (instead of TDMA based) is proposed. This type of signaling significantly reduces the overhead in MU environment.
- Comprehensive analysis of MIMO based PHY, with varying number of spatial streams, by means of distribution of post-processing SNR for each stream is provided.
- A model for saturation throughput calculation of the proposed systems under different traffic types (with different packet length and packet interarrival time distribution) is developed.
- Comprehensive comparison of MU and SU transmission strategies is provided, that includes the system capacity, fairness provision and delay characteristic. Their benefits and drawbacks are highlighted.
- Several SU and MU channel aware schedulers are developed that have different degrees of freedom when allocating available resources and their performace comparison is provided, in particular the ability to exploit MU diversity.
- The degree of impact of channel uncertainty on the performance of the channel aware schedulers is investigated.

1.4 Outline

This thesis has the following structure: Chapter 2 provides an overview of main radio propagation phenomena and propagation channel characterization.

In Chapter 3, basic concepts of MIMO technology are described. This includes classification of MIMO processing techniques and MIMO systems. Special attention is payed to MIMO channel capacity and channel modeling. This chapter also provides a survey of receiver and transmitter algorithms for MIMO communications.

Chapter 4 containts an overview of IEEE 802.11-2007 standard, that is a basis for the system analyzed in this thesis, and of IEEE 802.11n standard, that is also closely related to this topic.

A detailed description of the system analyzed in this thesis is given in Chapter 5, highlighting MAC layer features essential for efficient support of MIMO in ad-hoc networks.

The remaining of this thesis deals with performance evaluation of the described system. Chapter 6 contains a description of MIMO schemes that are in the focus of this work. Particular attention is payed to the performace of the receiver algorithms. The number of spatial streams is varied, and as a metric for evaluation and comparison, post-processing Signal-to-Noise Ratio (SNR) and achievable gross bitrate are used.

In the focus of Chapter 7 is the system level performance evaluation in case of uninformed transmitter (the transmitter that does not have channel knowledge). The developed model for saturation throughput calculation is presented and used for the evaluation for an example parameter set. Fair service provision is also addressed, and used for comprehensive delay analysis in the remaining of the chapter.

Chapter 8 analyzes the system performance in case of informed transmitter (the transmitter that has some form of channel knowledge). Several channel adaptive schedulers are developed and evaluated, with different degrees of freedom, and different ability to exploit multiuser diversity. The performance of the schedulers is also investigated in the presence of channel uncertainty. In addition to that, the achievability of CSI feedback provision is discussed.

Finally, Chapter 9 containts the summary and conclusion of this thesis and outlines the issues to deal with in the scope of future research activities.

CHAPTER 2

Radio Propagation

Contents

In the this chapter, a survey of the main radio propagation phenomena is given, namely pathloss, and shadowing and different types of small-scale fading. An overview of main parameters for channel characterization is also given.

2.1 Radio Propagation Mechanisms

The mechanisms of radio propagation can generally be attributed to the basic propagation mechanisms: reflection, diffraction, and scattering. Reflection occurs as the propagating wave impinges upon an object that is large compared to its wavelength (e.g. walls, earth etc.). Diffraction occurs when the radio path between the transmitter and receiver is obstructed by surface with sharp irregular edges. Waves are formed e.g. around building edges or obstacles so that radio waves can propagate through areas even though there is no Line-of-Sight (LoS) path between transmitter and receiver. Scattering happens when objects small compared to the wavelength of the propagating wave are located between the transmitter and receiver, and when in addition their density is high [Rappaport, 2001].

In a wireless mobile communication system, a signal can travel from transmitter to receiver over multiple reflective paths. This phenomenon, referred to as multipath propagation, can cause fluctuations in the received signal's amplitude, phase, and angle of arrival, giving rise to the terminology multipath fading. For the purpose of characterization of the channel, the classification of fading types is given in Figure 2.1 [Sklar, 2001].

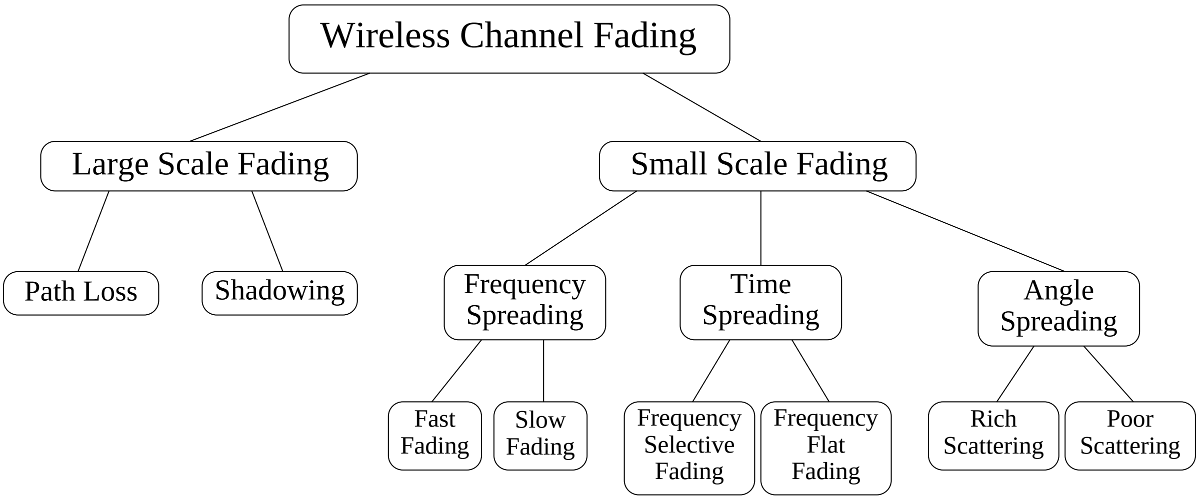

Figure 2.1: Fading classification

Fading can be classified into large- and small-scale fading. Large-scale fading describes the (variable) attenuation of the received signal over large distances. On the other hand, small-scale fading refers to the dramatic changes of the received power level over small distance, or short periods of time. Large- and small-scale fading differently affect the signal level, as illustrated in Figure 2.2: pathloss gives the average behavior over distance, shadowing accounts for environmental variations, and the deep fades are a consequence of multipath fading. The different fading types are described more in detail in the remaining of this chapter.

2.2 Large-Scale Fading

2.2.1 Pathloss

The attenuation of power of electromagnetic waves propagating through space is pathloss. The simplest approach to model pathloss is to assume the propagation through space free of all objects that might absorb or reflect Radio Frequency (RF) energy. The free space propaga-

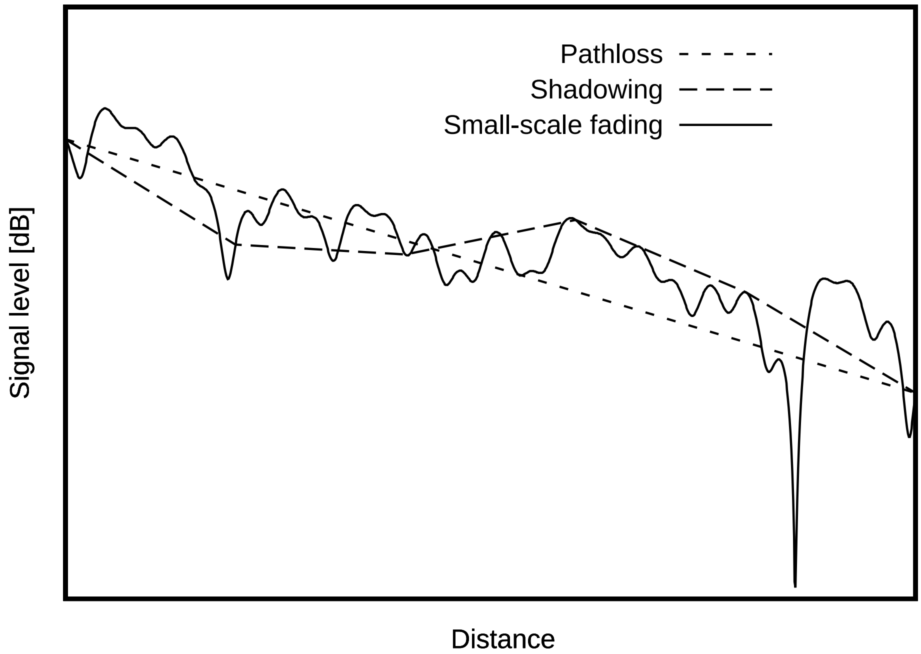

Figure 2.2: Signal power fluctuations and impact of large- and small-scale fading types

tion model also assumes that, within this region, the atmosphere behaves as a perfectly uniform and nonabsorbing medium and treats the earth infinitely far away from the propagating signal (or, equivalently, as having a reflection coefficient that is negligible). In the idealized free-space model, the attenuation of RF energy between the transmitter and receiver follows an inverse-square law. In that case, the attenuation $L_s(d)$ [Sklar, 2001, Sklar, 1997a, Proakis, 2001] is given by the following expression:

$$L_s(d) = \left(\frac{4\pi d}{\lambda}\right)^2, \tag{2.1}$$

where d is the distance between the transmitter and receiver, and λ is the wavelength of the propagating signal. This idealized propagation model is not suitable for most practical channels.

Okumura-Hata model is one of the most widely used empirical propagation prediction models. It was developed through works of Y. Okumura [Okumura et al., 1968] and M. Hata [Hata, 1980]. The model is based on the results of extensive measurements in urban and suburban areas of Japan. The propagation models for both indoor and outdoor radio channels indicate that the mean pathloss, $L_p(d)$, as a function of distance between transmitter and receiver d is proportional to an n^{th}-power of d, relative to a reference distance d_0:

$$\overline{L_p}(d)(dB) = L_s(d_0)(dB) + 10nlog\left(\frac{d}{d_0}\right). \tag{2.2}$$

The reference distance d_0 corresponds to a point located in the far field of the transmit antenna. Typically, the value of d_0 is taken to be 1 km for large cells, 100 m for microcells, and 1 m for indoor channels. $\overline{L_p}(d)$ is the average pathloss (over a multitude of different sites) for a given value of d.

The value of the pathloss exponent n depends on the radio frequency, antenna heights, and propagation environment. The more obstructions are present in the propagation environment, the higher the value of n is. Therefore, typical values of pathloss exponent are higher for indoor scenario compared to outdoor scenarios. In free space, where signal propagation follows an inverse-square law, n is equal to 2, as shown in Equ. (2.1). The value of the pathloss exponent n can also be lower than 2, e.g. in the presence of a very strong guided-wave phenomenon (such as urban streets).

2.2.2 Shadowing

The attenuation on a given distance is affected by prominent terrain contours (hills, forests, billboards, clumps of buildings, and so on) between the transmitter and the receiver. The receiver is often said to be "shadowed" by such objects. Large-scale fading (attenuation or pathloss) can be considered to be a spatial average over the small-scale fluctuations of the signal. It is generally evaluated by averaging the received signal over 10-30 wavelengths, in order to decouple the small-scale fluctuations from the large-scale shadowing effects (typically log-normal).

In Equ. (2.2), the only average value of the signal attenuation is given. It has been shown by measurements the pathloss $L_p(d)$ on at distance d is a random variable having a log-normal distribution about the mean distant-dependent value $\overline{L_p}(d)$ [Sklar, 2001, Sklar, 1997a], thus it can be expressed as follows:

$$L_p(d)(dB) = L_s(d_0)(dB) + 10nlog_{10}(\frac{d}{d_0}) + X_\sigma(dB), \tag{2.3}$$

where X_σ is a zero-mean, Gaussian random variable with standard deviation σ. Being site and distance dependent, the value of X_σ is determined from the measurements [Sklar, 2001, Okumura et al., 1968, Hata, 1980].

2.3 Small-Scale Fading

Small-scale fading refers to the dramatic changes in signal amplitude and phase for small changes of the position of the transmitter and/or receiver (as small as a half wavelength). Small-scale fading manifests itself as:

- time-spreading of the signal,
- time-variant behavior of the channel, and
- angular spreading of the arriving multipath components.

If the received signal is a result of superposition of multiple componenets traversing non-LoS paths from the transmitter to the receiver, small-scale fading is called Rayleigh fading. The envelope of such a received signal has Rayleigh distribution. In case of a dominant nonfading signal component is present, such as a LoS propagation path, the small-scale fading envelope is described by a Rician distribution. Superimposed on large-scale fading, small-scale fading fully describes the signal amplitude, phase and angle of arrival at the receiver.

2.3.1 Doppler Spread - Time Variable Fading

In the mobile radio communications, the time variability of the propagation channel is the consequence of motion between the transmitter and receiver. The paths that the components of the received signal traverse change, as well as the number of the components that reach the receiver. This leads to variability of the signal amplitude and phase at the receiver.

The channel variability is caused not only by moving transmitter and receiver, but also by mobility in the environment. Since the channel characteristics are dependent on the positions of the transmitter and receiver, time variance in this case is equivalent to spatial variance [Sklar, 2001].

The characterization of time variant nature of the radio channel can be done by Doppler shift, denoted f_d (also referred to in the literature by several different names: Doppler spread, fading rate, fading bandwidth, or spectral broadening) [Rappaport, 2001, Sklar, 2001]:

$$f_d = \frac{V}{\lambda}, \tag{2.4}$$

where V is the relative velocity, and λ is the wavelength of the transmitted symbol. The Doppler shift of each signal component is generally different from that of other paths and depends on the angle between the direction in which the receiver/transmitter is moving and the direction of the signal propagation. Therefore, the effect on the received signal manifests itself as a Doppler spreading of the transmitted signal frequency, rather than a shift by a fixed value.

The alternative characterization of time variant channel can be done in time domain, with the coherence time. Coherence time is the time over which the two received signals have strong potential for amplitude correlation [Rappaport, 2001]. The coherence time and the Doppler shift are reciprocally related [Sklar, 2001, Sklar, 1997a, Rappaport, 2001]:

$$T_0 \approx \frac{1}{f_d} \tag{2.5}$$

When T_0 is defined as the time duration over which the channels response has a correlation of at least 0.5, the relationship between T_0 and f_d is given by the following expression [Sklar, 2001, Rappaport, 2001]:

$$T_0 \approx \frac{9}{16\pi f_d} \tag{2.6}$$

A widely-used rule of thumb for modern digital communications is the definition of the coherence time as geometric mean of Equ. (2.5) and (2.6) [Sklar, 2001, Rappaport, 2001]:

$$T_0 \approx \sqrt{\frac{9}{16\pi f_d^2}} \tag{2.7}$$

By the rapidity of the time-variability in the context of the transmitted symbol rate, the propagation channel can be characterized as fast fading or slow fading.

In case that for the channel coherence time T_0 it applies that $T_0 < T_s$, where T_s is the transmitted symbol duration, the channel can be characterized as fast fading. On the fast fading channel, the channel changes over duration of one symbol period with high probability, which leads to distortion of the baseband pulse shape and irreducible error rate. The distortion is a consequence of low correlation of the received signals components throughout time. Such distorted pulses cause synchronization problems (failure of phase-locked-loop receivers), in addition to difficulties in adequately designing a matched filter [Sklar, 2001].

A channel can be characterized as slow fading if $T_0 > T_s$. In this case, the received signal's components are correlated over time needed to transmit one symbol. Therefore, the transmitted symbol will with high probability be received without distortions. The primary degradation in a slow-fading channel is loss in SNR [Sklar, 2001].

2.3.2 Delay Spread - Frequency Selective Fading

For a typical wireless channel, the received signal is a superposition of several multipath components. Since these components travel different paths from the transmitter to the receiver, they also arrive at different times at the receiver. In order to characterize this phenomenon, maximum excess delay is used. For a single transmitted impulse, the the maximum excess delay T_m is defined as the time between the first and last received component, after which the signal power of individual components falls below some threshold level relative to the strongest component. The threshold level might be chosen at 10 dB or 20 dB below the level of the strongest component.

Depending on the relationship between the channel maximum excess delay time T_m, and symbol time T_s, the fading can be characterized as frequency-selective fading, and frequency nonselective or flat fading, as mentioned in Figure 2.1.

A channel is said to exhibit frequency-selective fading if $T_m > T_s$. In this case, the time when received multipath components of a symbol arrive at the receiver exceeds the symbols time duration. This category of fading causes ISI. Mitigating the distortion in the case of frequency-selective fading is possible because many of the multipath components are resolvable by the receiver [Sklar, 2001].

If $T_m < T_s$, the channel is exhibiting frequency-flat fading. In this case, all of the received multipath components of a symbol arrive within the symbol time duration, hence there is no channel-induced ISI distortion. There is still performance degradation, due to destructive superposition of the individual multipath components that can yield a reduction in SNR. For loss in SNR due to flat fading, the appropriate mitigation technique is to improve the received SNR or use more robust transmission techniques [Sklar, 2001, Sklar, 1997b].

Similarly as in case of Doppler spread and coherence time, delay spread can be characterized by the coherence bandwidth f_0 in frequency domain. The coherence bandwidth is the range of frequencies over which two frequency components have a strong potential for amplitude correlation [Rappaport, 2001]. That is, a signal's spectral components in that range are affected by the channel in a similar manner. Coherence bandwith f_0 and maximum excess delay T_m are reciprocally related [Sklar, 2001, Rappaport, 2001]:

$$f_0 \approx \frac{1}{T_m}. \tag{2.8}$$

An overview of time variable and frequency selective fading and techniques to mitigate the fading effects is given in [Sklar, 1997a, Sklar, 1997b].

2.3.3 Angle Spread - Space Selective Fading

Characterization of fading channels has traditionally be studied by assuming the omnidirectional azimuthal propagation model [Jakes, 1974, Clarke, 1968], that is not often the case in practice. Particularly, if smart antennas are applied, such characterization does not suffice.

Signal multipath components arrive at the receiver from a number of azimuthal directions. In Figure 2.3 it is illustrated the LoS component of the signal arriving from the direction θ_0 relative to imaginary positive x-axis, and a number of (reflected, defracted, scattered) components arriving within an angle θ_{BW}. This distribution of multipath power is described by the function $p(\theta)$, where θ is the azimuthal angle. In the limit of very small $d\theta$, the term $p(\theta)d\theta$ represents the power of a single multipath plane wave received from the θ direction by the receiver [Durgin and Rappaport, 1998, Rappaport, 2001].

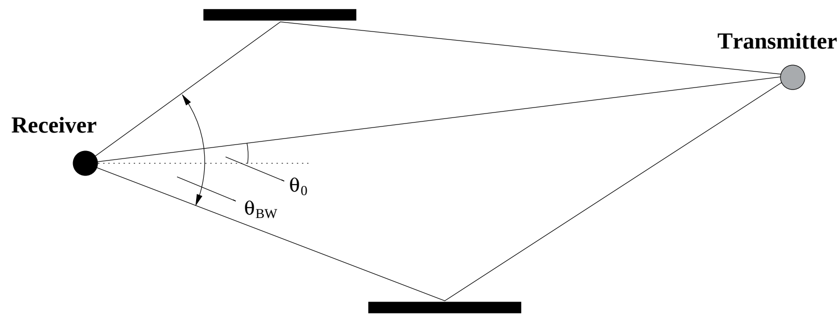

Figure 2.3: Angle spread of the multipath components at the receiver

Angle spread causes space selective fading, causing the varying signal amplitude depending on the spatial location of the antenna. Space selective fading is characterized by the coherence distance D_C which is the spatial separation for which the autocorrelation coefficient of the spatial fading drops to 0.7. Coherence distance is inversely proportional to the angle spread [Paulray et al., 2003].

Characterization of angular spread can be done at both transmitter and receiver side. The angular spread is very sensitive to the antenna height and the nature of the scattering environment. Measurements have shown that the angle spread increases as the antenna height is lowered, as well as that it is higher in urban areas compared to the suburban and rural areas [Rappaport, 2001, Durgin and Rappaport, 1998, Gans, 1972, Liberti and Rappaport, 1999].

CHAPTER 3

MIMO Communications

Contents

This chapter cover the fundamental information theory results and basic concepts of MIMO communications. An introduction to the topic is given, including a classification of MIMO systems and the signal models used throughout this work. The channel capacity in case of multiple antennas at the receiver and/or transmitter are given, followed by different approaches in modeling MIMO channels. The last part of this chapter contains a classification and an overview of receiver and transmitter algorithms applied in MIMO systems.

3.1 Multiple Antennas in Wireless Communications

The benefits of applying multiple antennas in a wireless system are multifold. They can be applied to e.g. increase range, boost the capacity, improve the robustness of a communication link, or reduce co-channel interference. In Figure 3.1 a coarse classification of MIMO systems based on the type of signal processing is given.

Two basic types can be recognized: beamforming techniques, and STC. Beamforming, as its name indicates, are algorithms that steer antenna radiation beams in the direction of the intended station, and at the same

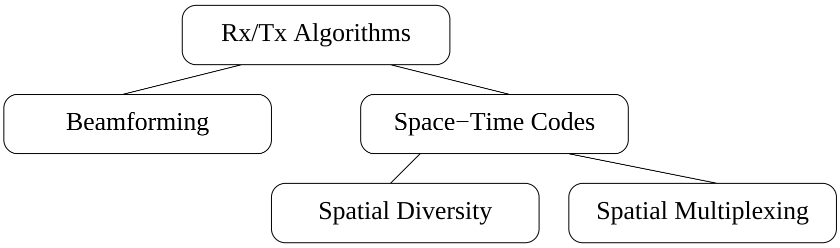

Figure 3.1: Classification of MIMO processing techniques

time avoiding interference to the other stations. STC in the general case assumes omnidirectional radiation. In different configurations, they can be used for increasing the range and robustness of the communication link - Spatial Diversity (SDIV) schemes, or to increase the link capacity - SMUX schemes.

The performace of these algorithms heavily depends on the fading characteristics in the given environment. Hence, beamforming algorithms give best performance under highly correlated fading. STC, on the other hand, is beneficial in the rich scattering environment, where the signals received by different antennas are not correlated. More details are given in Section 3.5.

On the link level, different gains can be exploited in multiple antenna systems: array gain, SDIV gain, SMUX gain, or co-channel interference reduction [Paulray et al., 2003, Paulray et al., 2004]. Array gain is the average increase of signal power at the receiver after processing at the transmitter and the receiver. Array gain is proportional to the number of transmit and receive antennas, and in order to exploiting transmit/receive array gain requires the channel knowledge at the transmitter/receiver.

Diversity is an efficient technique to mitigate fading in wireless links. Unlike time and frequency diversity, SDIV has the advantage that it neither prolongs the duration of the transmission nor requires more bandwidth. SDIV gain can be characterized by diversity order. Maximum diversity order that can be obtained over a MIMO link is $M_t \cdot M_r$, where M_t is the number of transmit and M_r is the number of receive antennas.

SMUX gain can be exploited if multiple antennas are used for simultaneous transmission of multiple data streams, without additional power, time or bandwidth. Theoretically, the capacity of the channel can be increased linearly by $min(M_t, M_r)$. The expressions corresponding to SISO, SIMO, MISO and MIMO channel capacities are given in Section 3.3.

3.2 Classification of Multiple Antenna Systems

Figure 3.2 illustrates different antenna configurations of a wireless link. Single Input - Single Output (SISO) corresponds to the traditional wireless

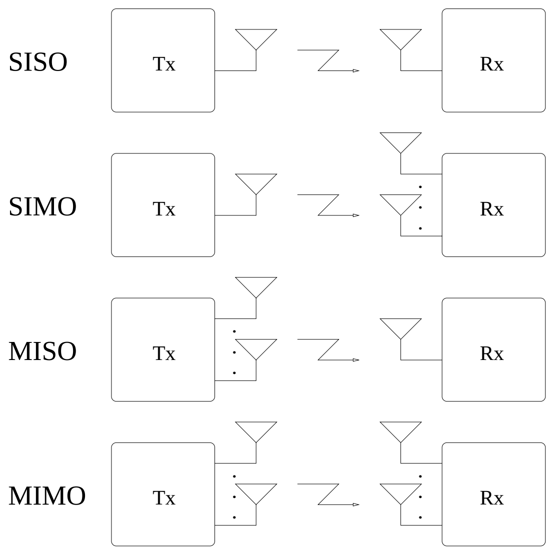

Figure 3.2: Overview of different MIMO systems

link. In Single Input - Multiple Output (SIMO) and in Multiple Input - Single Output (MISO) systems, multiple antennas are present only at one side: at the receiver or at the transmitter, whereas in MIMO systems both transmitter and receiver are equipped with multiple antennas.

In another, more general view of MIMO systems, so called virtual MIMO, or cooperative MIMO, multiple antennas at the transmitter are not necessarily located at one station, multiple stations with coordinated transmissions appear to the receiver as one, and simulate a MIMO transmission.

3.2.1 Signal Models

Throughout this work, the following signal models are used (E is the total received energy, and M_t and M_r are numbers of transmit and receive antennas):

SISO channel:

$$y = \sqrt{E} h s + n, \tag{3.1}$$

where y is the received signal,
h is the channel transfer function,
s is the transmitted symbol, and
n is the noise at the receiver;

SIMO channel:

$$\mathbf{y} = \sqrt{E} \mathbf{h} s + \mathbf{n}, \tag{3.2}$$

where $\mathbf{y} = [y_1 \dots y_{M_r}]^T$ is the received signal vector,
$\mathbf{h} = [h_1 \dots h_{M_r}]^T$ is the channel transfer function vector,
s is the transmitted symbol, and
$\mathbf{n} = [n_1 \dots n_{M_r}]^T$ is the noise vector at the receiver;

MISO channel:

$$y = \sqrt{\frac{E}{M_t}} \mathbf{hs} + n, \tag{3.3}$$

where y is the received signal,
$\mathbf{h} = [h_1 \dots h_{M_t}]$ is the channel transfer function vector,
$\mathbf{s} = [s_1 \dots s_{M_t}]^T$ is the transmitted symbol vector,
n is the noise at the receiver;

MIMO channel:

$$\mathbf{y} = \sqrt{\frac{E}{M_t}} \mathbf{Hs} + \mathbf{n}, \tag{3.4}$$

where $\mathbf{y} = [y_1 \dots y_{M_r}]^T$ is the received signal vector,
$\mathbf{H} = \begin{bmatrix} h_{1,1} & \dots & h_{1,M_t} \\ . & & . \\ . & & . \\ . & & . \\ h_{M_r,1} & \dots & h_{M_r,M_t} \end{bmatrix}$ is the channel transfer function matrix,
$\mathbf{s} = [s_1 \dots s_{M_t}]^T$ is the transmitted symbol vector,
$\mathbf{n} = [n_1 \dots n_{M_r}]^T$ is the noise vector at the receiver.

If not stated otherwise the channel transfer functions between each transmit/receive antenna pair are independent and identically distributed zero-mean circularly symmetric complex Gaussian random variables with unity variance. They are assumed constant over the time of one channel access, change though for each channel use and are uncorrelated in time. For the realistic application of the model, the following assumptions should be fullfilled [Heath Jr and Paulraj, 2002]:

- the transmission bandwidth is much less than the coherence frequency of the channel (hence fading is frequency-flat),
- the antenna spacing is larger than the coherence distance (hence signals at receive antennas are uncorrelated),
- the frames are separated by at least the coherence time of the channel (hence channel matrix values for each channel use are uncorrelated in time),
- frame length is not longer than the channel coherence time (hence channel matrix is constant during the transmission of a frame), and
- sufficient scattering is present (hence elements of the channel matrix are independent).

The noise at a receiver antenna is modelled as zero mean circularly symmetric complex Gaussian random variable, with variance N_0.

3.3 MIMO Information Theory

Information theory gives expressions for channel capacity that is an important metric for channel characterization. However, channel capacity is only a limit to error-free bitrate that can only be approached in practice by appropriate techniques. In this section, the expressions for channel capacities depending on the number of antennas at the receiver and transmitter side are given.

3.3.1 SISO Channel Capacity

The capacity C_{SISO} of an additive white Gaussian noise (SISO) channel has been defined by Shannon [Shannon, 1948a, Shannon, 1948b]:

$$C_{SISO} = \lim_{T \to \infty} \max_{f(s)} \frac{1}{T} I(s; y), \tag{3.5}$$

where s and y are transmitted and received symbol (random variables) and $f(s)$ is the marginal probability density function (PDF) of s. $I(s; y)$ is the mutual information between s and y, defined as:

$$I(s; y) = H(y) - H(y|s) = H(y) - H(n), \tag{3.6}$$

where $H(y)$ is the differential entropy of y; $H(y|s)$ is the conditional differential entropy of y given the knowledge of s, and is equal to $H(n)$.

The maximum mutual information is obtained by maximizing $H(y)$, and that is the case when y has zero-mean Gaussian distribution, which means that s also has zero-mean Gaussian distribution. This leads to the following expression for the capacity of the additive white Gaussian noise channel [Proakis, 2001]:

$$C_{SISO} = \log_2 \left(1 + \frac{E}{N_0} \right). \tag{3.7}$$

3.3.2 MIMO Channel Capacity

The capacity of the MIMO channel has been defined in [Foschini, 1996, Telatar, 1999] as:

$$C_{MIMO} = \max_{f(\mathbf{s})} I(\mathbf{s}; \mathbf{y}), \tag{3.8}$$

where, in contrast to Equ. (3.5), $\mathbf{s}$ and $\mathbf{y}$ are transmitted symbol and received symbol vectors. The mutual information $I(\mathbf{s}; \mathbf{y})$ can be reduced to:

$$I(\mathbf{s}; \mathbf{y}) = \log_2 \det \left(\mathbf{I}_{\mathbf{M_r}} + \frac{E}{M_t N_0} \mathbf{H} \mathbf{R}_{\mathbf{ss}} \mathbf{H}^H \right), \tag{3.9}$$

where $R_{ss} = \mathtt{E}\{\mathbf{s}\mathbf{s}^H\}$ is the covariance matrix of $\mathbf{s}$. Using this equation, the formula for the MIMO channel capacity becomes:

$$C_{MIMO} = \max_{\mathtt{Tr}(\mathbf{R_{ss}})=M_t} \log_2 \det \left(\mathbf{I_{M_r}} + \frac{E}{M_t N_0} \mathbf{H R_{ss} H}^H \right) \tag{3.10}$$

If the channel is completely unknown at the transmitter - *uninformed transmitter*, the symbols of the vector $\mathbf{s}$ may be chosen to be independent and equi-powered, i.e. $\mathbf{R_{ss}} = \mathbf{I_{M_t}}$. Then, the capacity reduces to:

$$C_{MIMO} = \log_2 \det \left(\mathbf{I_{M_r}} + \frac{E}{M_t N_0} \mathbf{H H}^H \right). \tag{3.11}$$

If the channel matrix $\mathbf{H}$ is an orthogonal square matrix with the dimension $M_r = M_t = M$, i.e. it applies:

$$\mathbf{H H}^H = \mathbf{H}^H \mathbf{H}, \tag{3.12}$$

and the elements of matrix $\mathbf{H}$ satisfy $|\mathbf{H}_{i,j}|^2 = 1$, i.e. squared Frobenius norm [Golub and Loan, 1989] of $\mathbf{H}$ satisfies:

$$\|\mathbf{H}\|_F^2 = \sum_{i=1}^{M} \sum_{j=1}^{M} |h_{i,j}|^2 = M^2 \tag{3.13}$$

the expression for the channel capacity has the following form:

$$C_{MIMO} = M \log_2 \left(1 + \frac{E}{N_0} \right), \tag{3.14}$$

thus the capacity of an orthogonal MIMO channel is M times the capacity of the SISO channel.

The MIMO channel capacity when the channel is known at the transmitter - *informed transmitter* is at least the MIMO channel capacity when there is no channel knowledge at the transmitter. This capacity can be obtained by allocating different power levels for spatial subchannels, applying the water-filling algorithm [Cover and Thomas, 1991, Paulray et al., 2003, Larsson and Stoica, 2003].

3.3.3 SIMO and MISO Channel Capacity

The capacities of SIMO and MISO channels can be treated as special cases of the MIMO channel. For a SIMO channel, with normalized channel vector $\mathbf{h}$, $\|\mathbf{h}\|_F^2 = M_r$, it applies:

$$C_{SIMO} = \log_2\left(1 + \frac{E}{N_0}\|\mathbf{h}\|_F^2\right) \tag{3.15}$$

$$= \log_2\left(1 + M_r\frac{E}{N_0}\right), \tag{3.16}$$

thus SIMO channel offers only logarithmic increase in capacity.

As for the MISO channel, the capacity differs depending on the presence of the channel knowledge at the transmitter. In case of uninformed transmitter, the power is equally allocated to all spatial substreams, and the capacity is given by the following expression:

$$C_{MISO} = \log_2\left(1 + \frac{E}{M_t N_0}\|\mathbf{h}\|_F^2\right). \tag{3.17}$$

For the normalized channel vector $\mathbf{h}$, $\|\mathbf{h}\|_F^2 = M_t$, there is no improvement in capacity over a SISO channel. However, for the informed transmitter, all the power can be directed into the single - best spatial subchannel, hence the according capacity is given by:

$$C_{MISO} = \log_2\left(1 + \frac{E}{N_0}\|\mathbf{h}\|_F^2\right) \tag{3.18}$$

$$= \log_2\left(1 + M_t\frac{E}{N_0}\right), \tag{3.19}$$

and it is equal to the capacity of the SIMO channel when the number of receive antennas is the same as the number of transmit antennas of the MISO channel [Paulray et al., 2003].

3.3.4 Ergodic and Outage Capacity

The previous expressions for channel capacities apply for the case of a deterministic channel realization. However, in practical systems, the channel is changes randomly over time. For the purpose of temporal channel capacity characterization, ergodic and outage capacity are used.

The ergodic capacity $\overline{C}_{MIMO}$ of a MIMO channel in case of uninformed transmitter is the average capacity over different realizations of the channel matrix $\mathbf{H}$ for the given distribution of $\mathbf{H}$ [Larsson and Stoica, 2003]:

$$\overline{C}_{MIMO} = \mathtt{E}\left\{\log_2 \det\left(\mathbf{I}_{\mathbf{M_r}} + \frac{E}{M_t N_0}\mathbf{H}\mathbf{H}^H\right)\right\}. \tag{3.20}$$

In case of informed transmitter, the ensemble averaging is done over capacities achieved by water-filling algorithm.

Ergodic capacity gives the mean channel capacity for a certain distribution of channel matrix $\mathbf{H}$. Outage capacity further characterizes the distribution of the random channel capacity. The $q\%$ outage capacity $C_{out,q}$ is defined as the information rate that is guaranteed for $(100-q)\%$ of channel realizations [Ozarow et al., 1994, Biglieri et al., 1998]:

$$P(C \leq C_{out,q}) = q\%. \tag{3.21}$$

3.4 MIMO Channel Modeling

The most commonly used MIMO channel model assumes the independent identically distributed zero-mean circularly symmetric complex Gaussian random variable with unity variance as elements of the channel transfer matrix $\mathbf{H}$. Practical channels may in practice deviate from this idealized case, due to e.g. spatially correlated fading or presence of a LoS component leading to Ricean fading.

Generally, there are two approaches in channel modeling: antenna specific and antenna generic. In the first one, besides propagation characteristics, the antenna geometry is also included in the model, whereas the other channel model can be used with an arbitrary antenna configuration.

Other classification recognizes deterministic and stochastic channel models. Deterministic channel models are either ray tracing based, or are a collection of recorded impulse responses. Stochastic models can be geometrically based, parametric, or correlation based.

In geometrically based models, the received signal is calculated based on the positions of the scatterers that are located at some (model dependent) positions in the vicinity of the transmitter and receiver, e.g. geometrically based circular model [Ertel et al., 1998].

Parametric stochastic channel models are site generic channel models, such as IEEE 802.11n [IEEE, 2004b], 3GPP Spatial Channel Model (SCM) [3GPP, 2007] and COST 273 MIMO channel model [1]. The resulting channel in different scenarios is obtained by summing up individual paths and their subpaths. The relevant parameters include angle spread at transmitting and receiving station and power-delay distribution. The parameters take different values depending on the scenario and the type of station (base or mobile station), i.e its location.

Correlation based models are not physical models; they imply that the elements of $\mathbf{H}$ are correlated. That can be mathematically described by the following equation:

$$\mathrm{vec}(\mathbf{H}) = \mathbf{R}^{1/2}\mathrm{vec}(\mathbf{H}_w), \tag{3.22}$$

where $\mathrm{vec}(\mathbf{H})$ is an operator that stacks the elements of $\mathbf{H}$ columnwise, and $\mathbf{H}_w$ is spatially white MIMO channel (with independent elements). Matrix R is the $M_tM_r \times M_tM_r$ covariance matrix defined as:

$$R = \mathtt{E}\left[\mathrm{vec}(\mathbf{H})\mathrm{vec}(\mathbf{H})^H\right]. \tag{3.23}$$

This model can capture any correlation effects between transmitter and receiver.

However, due to complexity reasons, Kronecker model is the more often used. Kronecker model assumes separability of transmit and receive antenna correlation:

$$\mathbf{H} = \mathbf{R}_r^{1/2}\mathbf{H}_w\mathbf{R}_t^{1/2}, \tag{3.24}$$

where $\mathbf{R}_r$ is $M_r \times M_r$ receive correlation matrix, and $\mathbf{R}_t$ is the transmit correlation matrix [Paulray et al., 2003].

[1] http://www.lx.it.pt/cost273/

3.5 Receiver and Transmitter Algorithms

The choice of the MIMO scheme to apply in the system is a complex decision. Besides the limitations imposed by the system requirements, transceiver complexity level and its cost range, the channel propagation characteristics, and the design of the rest of the system play an important role. Some of the factors that have to be taken into account are the following:

- channel knowledge:
  - open loop or close loop communication, feedback rate in close loop systems
  - reliability of CSI, and robustness of algorithms to potential CSI mismatches,
- deployment environment: picocell, macrocell, etc.
- fading correlation seen by the antenna elements on both transmit and receive antennas,
- dispersion of the channel in time and frequency,
- application scenario.

In this section, an overview of transmitter and receiver algorithms for STC, is given. In addition, descriptions of some beamforming algorithms are given for the sake of completeness.

3.5.1 Spatial Diversity (SDIV)

In the presence of multiple antennas, it is possible to exploit the spatial diversity of the channel. Spatial diversity, as time or frequency diversity, provides a receiver with multiple copies of the transmitted symbol and it is a method for mitigating fading over wireless channels. However, in contrast to time and frequency diversity, exploiting spatial diversity does not require additional time or bandwidth. In addition to diversity gain, spatial diversity also provides array gain that is the increase of average SNR. These benefits come for the cost of increased transmitter and receiver complexity. Receive and transmit diversity schemes are described in the following.

Receive Diversity

In order to exploit receive diversity gain over a SIMO link, the perfect channel knowledge at the receiver is needed. In order to maximize the received SNR, the receiver performs Maximum Ratio Combining (MRC) [Proakis, 2001, Paulray et al., 2003]:

$$\begin{aligned} z &= \sqrt{E}\mathbf{h}^H\mathbf{h}s + \mathbf{h}^H\mathbf{n} \\ &= \sqrt{E}\|\mathbf{h}\|_F^2 s + \mathbf{h}^H\mathbf{n}, \end{aligned} \tag{3.25}$$

where z is the receiver output. The post-processing SNR η at the receiver is given by:

$$\eta = \|\mathbf{h}\|_F^2 \frac{E}{N_0}. \tag{3.26}$$

In addition to the diversity order of the system equal to the number of antennas at the receiver M_r, the average SNR at the receiver is enhanced by a factor of M_r compared to the standard SISO link due to the array gain (array gain is $10\log_{10} M_r$) [Paulray et al., 2003]:

$$\overline{\eta} = \mathbf{E}\{\eta\} = M_r \frac{E}{N_0}. \tag{3.27}$$

Despite these benefits, deploying multiple antennas at the receiver is limited by the terminal size, complexity and cost. In the next section, spatial diversity is exploited on the other side of the communication link by applying multiple antennas at the transmitter.

Transmit Diversity

Exploiting transmit diversity requires preprocessing at the transmitter. Without any preprocessing at the transmitter, the symbol would be transmitted over multiple antennas over a MISO channel:

$$y = \sqrt{\frac{E}{M_t}} \left(\sum_{i=1}^{M_t} h_i \right) s + n \tag{3.28}$$

Since $\frac{1}{\sqrt{M_t}} \sum_{i=1}^{M_t} h_i$ is a scaled sum of complex Gaussian variables with unit variance, it is itself a complex Gaussian variable with unit variance [Larson and Shubert, 1979], this technique does not provide diversity gain [Paulray et al., 2003].

Assuming the perfect channel knowledge at the transmitter, the transmitter can do preprocessing of the symbol prior to its transmission with the weight vector $\mathbf{w}$, hence the received signal can be modelled by the following equation:

$$y = \sqrt{\frac{E}{M_t}}\mathbf{hw}s + n. \tag{3.29}$$

The weight vector, normalized to satisfy $\|\mathbf{w}\|_F^2 = M_t$, that maximizes the received SNR is given in [Titus, 1999]:

$$\mathbf{w} = \sqrt{M_t}\frac{\mathbf{h}^H}{\sqrt{\|\mathbf{h}\|_F^2}}. \tag{3.30}$$

This scheme is called transmit-MRC. Hence, the received signal has the following form:

$$y = \sqrt{\frac{E}{M_t}}\left(\sum_{i=1}^{M_t} h_i w_i\right) s + n, \tag{3.31}$$

and the SNR of the received signal is:

$$\eta = \|\mathbf{h}\|_F^2 \frac{E}{N_0}, \tag{3.32}$$

and it is equal to the corresponding SNR in the receive diversity scheme. This scheme is called transmit MRC [Paulray et al., 2003]. It should be noted here that in the transmit diversity schemes presented the perfect channel knowledge is required at the transmitter, while in the previously presented receive diversity scheme the channel knowledge is required at the receiver. With these assumptions, it is possible to achieve the same diversity order and the same array gain as in the receive diversity scheme, for $M_t = M_r$.

Alamouti Coding

Even when the channel is not known at the transmitter, it is possible to exploit the transmit diversity. In this case it is necessary to code across both space and time to achieve diversity [Larsson and Stoica, 2003].

Alamouti coding, introduced in [Alamouti, 1998], is a transmit diversity scheme that applies two transmit and one receive antennas, and does not require the channel knowledge at the transmitter. This scheme attracted a lot of attention due to its simplicity.

Two complex symbols s_1 and s_2 are transmitted simultaneously during two time intervals, by the following rules:

- during the first interval, s_1 is transmitted using the first antenna, and s_2 is transmitted using the second one;
- during the second interval complex conjugate simbols are transmitted: $-s_2^*$ using the first antenna, and s_1^* using the second one.

The channel transfer function for each antenna pair is assumed to be constant during the transmission. The received signals in the first and in the second interval have the following form:

$$y_1 = \sqrt{\frac{E}{2}} h_1 s_1 + \sqrt{\frac{E}{2}} h_2 s_2 + n_1 \tag{3.33}$$

$$y_2 = -\sqrt{\frac{E}{2}} h_1 s_2^* + \sqrt{\frac{E}{2}} h_2 s_1^* + n_2. \tag{3.34}$$

The receiver forms a rearranged signal vector $\mathbf{y}$:

$$\mathbf{y} = \begin{bmatrix} y_1 \\ y_2^* \end{bmatrix} = \sqrt{\frac{E}{2}} \begin{bmatrix} h_1 & h_2 \\ h_2^* & -h_1^* \end{bmatrix} \begin{bmatrix} s_1 \\ s_2 \end{bmatrix} + \begin{bmatrix} n_1 \\ n_2^* \end{bmatrix} \tag{3.35}$$

$$= \sqrt{\frac{E}{2}} \mathbf{H_{eff}} \mathbf{s} + \mathbf{n}, \tag{3.36}$$

where $\mathbf{H_{eff}} = \begin{bmatrix} h_1 & h_2 \\ h_2^* & -h_1^* \end{bmatrix}$, $\mathbf{s} = \begin{bmatrix} s_1 \\ s_2 \end{bmatrix}$ and $\mathbf{n} = \begin{bmatrix} n_1 \\ n_2^* \end{bmatrix}$. Postprocessing the signal with ${\mathbf{H_{eff}}}^H$ results in:

$$\mathbf{z} = {\mathbf{H_{eff}}}^H \mathbf{y} = \sqrt{\frac{E}{2}} \|\mathbf{h}\|_F^2 \mathbf{s} + {\mathbf{H_{eff}}}^H \mathbf{n}, \tag{3.37}$$

and the received SNR η per symbol is given by:

$$\eta = \frac{\|\mathbf{h}\|_F^2}{2}\frac{E}{N_0}. \tag{3.38}$$

Hence, the Alamouti scheme does not allow for array gain; however, it extracts a diversity order 2 (full diversity). In Section 3.5.2, Alamouti scheme will be mentioned in the context of OSTBC.

3.5.2 Space-Time Coding (STC)

Space-Time Block Coding (STBC)

STBC is a way of mapping a set of n_s complex symbols $\{s_1, \ldots, s_{n_s}\}$ onto a matrix $\mathbf{X} = [x_1 \cdots x_N]$ of dimension $M_t \times N$:

$$\{s_1, \ldots, s_{n_s}\} \mapsto \mathbf{X}, \tag{3.39}$$

where the columns of matrix $\mathbf{X}$ are transmitted consecutively, each entry using one of M_t transmit antennas [Larsson and Stoica, 2003].

Linear STBC

In a special class of STBC schemes, *linear STBC*, the mapping is linear in symbols $\{s_1, \ldots, s_{n_s}\}$:

$$\mathbf{X} = \sum_{n=1}^{n_s} \left(\mathcal{R}e(s_n)\mathbf{A_n} + i\,\mathcal{I}m(s_n)\mathbf{B_n}\right), \tag{3.40}$$

where symbols $\mathbf{A_n}$ and $\mathbf{B_n}$, $n = 1 \cdots n_s$, stand for sets of fixed matrices [Larsson and Stoica, 2003]. Linear STBC schemes are simple to implement, and provide good performance gains. They make only a small subclass of all the possible mappings $\{s_1, \ldots, s_{n_s}\} \mapsto \mathbf{X}$ (*nonlinear STBC*).

Orthogonal STBC

An important subclass of linear STBC is OSTBC. It has the following unitary property:

$$\mathbf{X}\mathbf{X}^H = \sum_{n_1}^{n_s} |s_n|^2 \cdot \mathbf{I}, \tag{3.41}$$

and achieves $M_t M_r$ diversity order.

OSTBC were originally presented in [Tarokh et al., 1999a], as a response to Alamouti coding, with motivation to achieve orthogonal design of STBC schemes with more transmit antennas. ST codes for real constellations can be designed for any number of transmit antennas, and they can achieve the code rate 1. As for complex constellations, the maximum code rate can be achieved with the scheme with two antennas, and that is the case for the already presented Alamouti scheme [Tarokh et al., 1999a].

The importance of OSTBC schemes lays in decoupling the Space-Time (ST) channel into $2n_s$ independent and real scalar Additive White Gaussian Noise (AWGN) channels [Proakis, 2001], or equivalently n_s complex AWGN channels [Larsson and Stoica, 2003].

Spatial Multiplexing (SMUX)

SMUX is a scheme where M_t independent symbols are transmitted per symbol period, increasing the throughput in this way with the factor of M_t; at the same time, it does not achieve transmit diversity.

Although it is not STC strictly speaking, formally it can be treated as a linear STBC scheme by setting $N = 1$, $n_s = M_t$, and $\{\mathbf{A}_n, \mathbf{B}_n\}$ to the n^{th} column of $M_t \times M_t$ identity matrix.

With *horizontal encoding*, data stream is first demultiplexed into M_t separate streams. Each stream is then independently encoded and transmitted using one antenna. This scheme captures at most M_r diversity order. With *vertical encoding*, data stream is first encoded, and afterwards demultiplexed into M_t streams and transmitted over M_t antennas. This type of encoding provides at least M_r diversity order; however it has a drawback of the joint reception, that can be too complex.

Variations of these two basic encoding types are possible, which can exploit diversity order of $M_t M_r$ (e.g. D-BLAST [Foschini, 1996]).

Space-Time Trellis Coding (STTC)

STTC [Tarokh et al., 1998, Tarokh et al., 1999b] are an extension of conventional trellis codes to multiple-antenna systems. In an STTC scheme, a stream of data is encoded via M_t convolutional encoders (or via one convolutional encoder with M_t outputs) to obtain M_t streams $x_1, \ldots, x_{M_t}$ that are then transmitted via the M_t transmit antennas. These codes may be designed to extract diversity gain and coding gain. They are effective means of capturing diversity. However, the computational complexity for decoding STTC increases exponentially with the number of states in the trellis diagram [Paulray et al., 2003].

3.5.3 Receiver Algorithms

This chapter gives an overview of the SMUX receiver algorithms. Besides noise, the problem faced by a SMUX receiver is the presence of Multi-Stream Interference (MSI).

Maximum Likelihood (ML) Receiver

ML is the optimal receiver in the absence of channel coding. It performs vector decoding. Assuming equally likely transmit symbols, the ML receiver chooses the vector $\mathbf{s}$ that solves [Paulray et al., 2003]:

$$\hat{\mathbf{s}} = \arg\min_{s} \left\| \mathbf{y} - \sqrt{\frac{E}{M_t}} \mathbf{H}\mathbf{s} \right\|, \tag{3.42}$$

where the search is performed over all candidate vector symbols $\mathbf{s}$. This leads to the exponential algorithm complexity with the exponent M_t. However, methods to solve this problem by posing it as an integer least-square problem, such as sphere decoding [Fincke and Pohst, 1985] and Kannan algorithm [Kannan, 1983], significantly reduce the complexity.

Linear receivers are preferred due to their low complexity. They are analyzed further in this chapter in detail, and considered throughput this work.

Zero Forcing (ZF) Receiver

ZF receiver uses the filter matrix $\mathbf{G_{ZF}}$:

$$\mathbf{G_{ZF}} = \sqrt{\frac{M_t}{E}}\mathbf{H}^\dagger, \tag{3.43}$$

where $\mathbf{H}^\dagger$ stands for pseudo-inverse [Golub and Loan, 1989] of matrix $\mathbf{H}$, to separate the received signal into the originally transmitted streams. It is assumed that the matrix $\mathbf{H}$ has full column rank, and that $M_r \geq M_t$. The output of the receiver is given by:

$$\mathbf{z} = \mathbf{s} + \sqrt{\frac{M_t}{E}}\mathbf{H}^\dagger\mathbf{n}. \tag{3.44}$$

The filter matrix nulls MSI, and transforms the matrix channel into M_t parallel scalar channels.

The post-processing SNR η_k on the stream k is given by:

$$\eta_k = \frac{E}{M_t N_0}\frac{1}{[(\mathbf{H}^H\mathbf{H})^{-1}]_{k,k}}, \tag{3.45}$$

where $\left[(\mathbf{H}^H\mathbf{H})^{-1}\right]_{k,k}$ stands for the element in the k^{th} row and k^{th} column of the matrix $\left[(\mathbf{H}^H\mathbf{H})^{-1}\right]$.

η_k is a random variable, and it has been proven [Winters et al., 1994, Gore et al., 2002] that it follows a Chi-squared distribution with $M_r - M_t + 1$ degrees of freedom with the following PDF:

$$f(x) = \begin{cases} \frac{M_t N_0}{E(M_r - M_t)!} e^{-\frac{M_t N_0}{E}x}\left(\frac{M_t N_0}{E}x\right)^{M_r - M_t} & \text{, if} \quad x \geq 0 \\ 0 & \text{, if} \quad x < 0 \end{cases} \tag{3.46}$$

The ergodic performance of the ZF receiver for log-normal shadowing was investigated in [Park et al., 2007].

The ZF algorithm decomposes the channel into M_t parallel channels, spatial subchannels, each with array gain and diversity gain proportional to $M_r - M_t + 1$ [Paulray et al., 2003]. It has the benefit of its low (linear) complexity, but due to the noise amplification, it has poor performance in the low SNR region.

Minimum Mean Square Error (MMSE)

While the ZF receiver completely nulls MSI, and doing so amplifies the noise, the MMSE receiver minimizes the total error. The applied filter matrix has the following form [Paulray et al., 2003]:

$$\mathbf{G_{MMSE}} = \arg\min_{\mathbf{G}} \mathtt{E}\{\|\mathbf{Gy} - \mathbf{s}\|\}, \tag{3.47}$$

where $\mathtt{E}$ stands for the expectation. Using the orthogonality principle, $\mathbf{G_{MMSE}}$ can be derived:

$$\mathbf{G_{MMSE}} = \sqrt{\frac{M_t}{E}} \left(\mathbf{H}^H \mathbf{H} + \frac{M_t N_0}{E} \mathbf{I_{M_t}} \right)^{-1} \mathbf{H}^H. \tag{3.48}$$

The post-processing SNR η_k on the stream k is given by:

$$\eta_k = \frac{1}{\left[\left(\frac{E}{M_t N_0} \mathbf{H}^H \mathbf{H} + \mathbf{I_{M_t}} \right)^{-1} \right]_{k,k}} - 1. \tag{3.49}$$

Al low SNR, the MMSE receiver outperforms the ZF receiver. At high SNR, the performance of the MMSE converges to that of the ZF receiver, also extracting $M_r - M_t + 1$ order diversity.

Successive Cancellation (SUC) Receivers

The main idea of SUC techniques is successive layers decoding and their substraction from the received signal. In the basic form, the layers are not ordered. With the ordered SUC receiver, the stream with the highest remaining signal-to-Interference-plus-Noise Ratio (SINR) is always chosen for the detection.

Although it promisses better diversity order then pure linear receivers, the SUC generally suffers from the error propagation; however, the ordered version has significantly better performance.

In [Michalke et al., 2006] the comparison of performance of different receiver algorithms for a number of application scenarios is given, and it is shown that linear receivers allow achieving very good performance (within only 1-2 dB) compared to the advanced detection strategies.

3.5.4 Beamforming and SDMA

If the transmitter has the knowledge of the MISO channel $\mathbf{h}$ to its own user, the transmit MRC or matched beamforming described in Section 3.5.1 can be applied to maximize the SNR at the receiver. However applying beamforming techniques in combination with SDMA offers additional performance gains.

SDMA [Farsakh and Nossek, 1994, Piolini and Rolando, 1999] is a multiple access scheme where conventional channel (frequency, time, code, or their combination) can be shared among spatially separated users. Usually, in cellular environments, the base station is equipped with multiple antennas, while the other stations are not required to have multiple antennas. The base station can, applying an appropriate beamforming algorithm, open multiple data pipes with users that have sufficient spatial separation, as illustrated in Figure 3.3. This increases the throughput linearly with the number of open pipes. Besides the algorithms to generate the adaptive antenna pattern, a big challenge of SDMA is dynamic resource scheduling in centralized architectures [Koutsopoulos and Tassiulas, 2002, Shad et al., 2001] and MAC algorithms in decentrally organized systems - directional MAC protocols [Nasipuri et al., 2000, Ko et al., 2000], including directional busy tone MAC protocol [Tobagi and Kleinrock, 1975, Huang et al., 2002].

Applying transmit ZF, or null-steering beamformer produces nulls in up to $M_t - 1$ directions, thus generating no co-channel interference to other users. However, the weights estimated by this scheme do not maximize the output SNR at the intended user, particularly when the intended user is close to one of the other users. The optimal beamformer [Godara, 1997a, Godara, 1997b] trades the signal power delivered to the intended user for interference generated to the other users.

However, due to concentrated power in directions of intended users, in multicell scenarios this may also produce increased interference (compared to omnidirectional radiation) in case that the cell on the first interference ring is in the same direction.

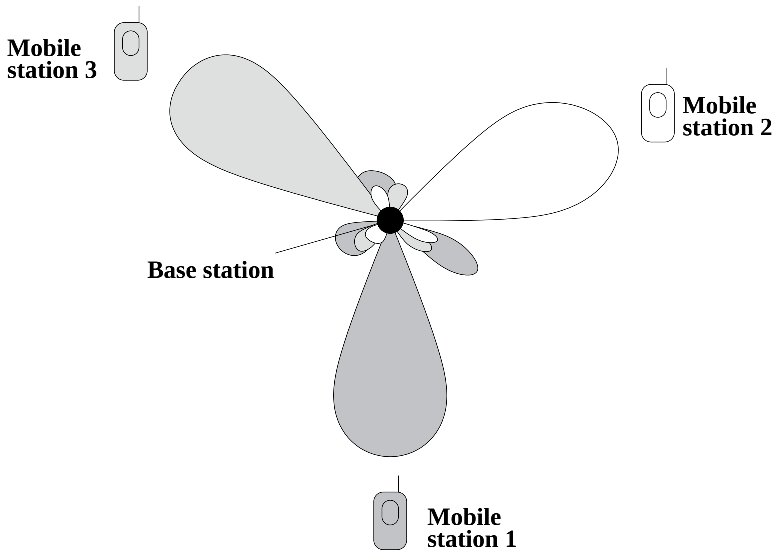

Figure 3.3: SDMA: base station forms an individual antenna pattern that steers a beam in direction of the intended mobile station, minimizing the interference produced to other two users

CHAPTER 4

IEEE 802.11

Contents

IEEE 802.11 belongs to the IEEE 802 family of standards for Local Area Networks (LANs), Personal Area Networks (PANs) and Metropolitan Local Area Networks (MANs), together with 802.3 [IEEE, 2005] (Ethernet), 802.15.1 (Bluetooth), 802.16 (WiMAX), etc. The main motivation for the work in this direction was the need for wireless Ethernet in the areas where providing wired connectivity was not easy or possible at all. This chapter contains an overview of IEEE 802.11 standards, with special attention payed to the (future) IEEE 802.11n standard.

4.1 Overview of IEEE 802.11-2007

In the focus of 802.11 are Carrier Sense Multiple Access with Collision Avoidance (CSMA/CA) based WLAN standards. Since founding in 1990, the IEEE standardization body has specified IEEE 802.11-1999 (the successor of IEEE 802.11-1997), that was published in 1999 and reaffirmed in 2003 [IEEE, 2003]. The standard has been followed by amendments to the existing MAC and PHY functions.

In 2007, IEEE 802.11-1999 standard has been merged with several amendments to IEEE Std. 802.11-2007 [IEEE, 2007c]. This revision specifies technical corrections and clarifications to IEEE Std 802.11 for WLANs as well as enhancements to the existing MAC and PHY functions. Such enhancements include improved data link security, codified vendor-specific extensions to the protocol, and incorporated interpretation requests. It incorporates Amendments 1 through 8 (802.11a, b, d, e, g, h, i, j) including a corrigendum. An overview of the included amendments is given in Table 4.1.

Table 4.1: Description of amendments to IEEE 802.11-1999 included in IEEE 802.11-2007

Amendment	Description
IEEE 802.11a	PHY for the 5 GHz UNII bands, $6 - 54$ Mb/s
IEEE 802.11b	PHY for the 2.4 GHz ISM band, 5.5 and 11 Mb/s
IEEE 802.11d	Specification for operation in different regulatory domains
IEEE 802.11e	Enhancements for QoS
IEEE 802.11g	PHY for the 2.4 GHz ISM band, $6 - 54$ Mb/s
IEEE 802.11h	Spectrum and power management enhancement to 802.11a
IEEE 802.11i	Security enhancements
IEEE 802.11j	Enhancement to 802.11a for operation in $4.9 - 5.0$ GHz in Japan

In Figure 4.1 the relation of 802.11 to International Organization for Standardization (ISO)-Open Systems Interconnection (OSI) protocol stack is given [Walke, 1999]. Same as the other IEEE 802 standards, IEEE 802.11 focuses on the PHY and Data Link Layer (DLL). As the Logical Link Control (LLC) IEEE 802.2 is applied.

The major physical components of IEEE 802.11 networks are the following [Gast, 2002]:

- *Distribution system* is a logical component used to forward frames to their destination when several access points are connected to form a large coverage area. The technology used by the distribution system is not specified by the standard. In nearly all commercial products, Ethernet is used as the backbone network technology.
- *Access points* perform many functions, but the most important one is translating the IEEE 802.11 frames to the form understandable to the rest of the network; thus they serve as wireless-to-wired bridges.
- *Wireless medium* is used to transmit frames. The standard and its amendments containt several PHY specifications; they are described in Section 4.1.2.

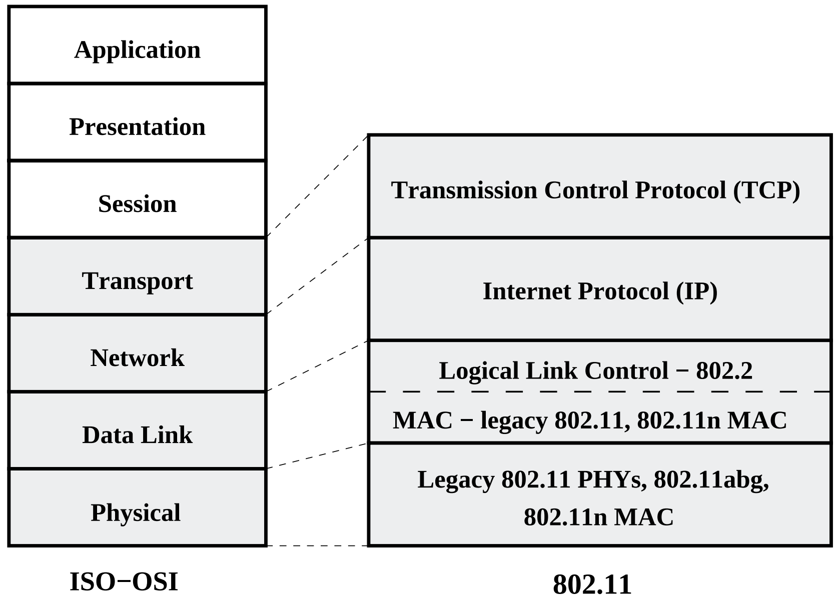

Figure 4.1: ISO OSI and IEEE 802.11 protocol stacks comparison

- *Stations* are the devices with wireless interfaces that are interconnected in the presence of the wireless network. They are usually mobile, battery operated notebooks and handheld devices, but can also be fixed devices such as desktop computers.

The basic building block of an IEEE 802.11 network is the Basic Service Set (BSS). There are several types of IEEE 802.11 networks, concerning its size and structure.

- *Independent networks, Independent Basic Service Set (IBSS)*, or *ad-hoc BSS* - consist only of stations establishing direct connections among each other.
- *Infrastructure BSS* have an access point in addition to the IBSS. Stations communicate with each other via the Access Point (AP).
- *Extended Service Set (ESS)* is an arbitrarily large IEEE 802.11 network achieved by chaining BSSs together with a backbone network.

Station mobility is supported for transmission between two APs within an ESS, and also for transmission from one to another ESS [Gast, 2002, Cooklev, 2004].

4.1.1 Medium Access Control (MAC)

Access to the wireless medium is controlled by coordination functions specified in the standard. CSMA/CA access is provided by the Distributed Coordination Function (DCF). The standard also specifies, although in practice it is not used, the Point Coordination Function (PCF) for the contention free services.

CSMA in IEEE 802.11 DCF uses CA. Colision Detection (CD) that is applied in IEEE 802.3 is not possible due to two main reasons: for CD full duplex connection is required, and second, the assumption that all the station in the network can hear each other may not be true in wireless environment.

Contention-Based Medium Access

The basis of DCF is CSMA/CA, with a random backoff procedure. A station with a data packet to transmit draws a random number between 0 and Contention Window (CW), which determines the duration of the backoff timer in time slots. The CW doubles after a collision, never exceeding its maximum value, and is set back to its minimum value after a successful transfer, indicated by an Acknowledgment (ACK) frame. The bounds of CW and time slot duration are PHY specific.

The medium access procedure is illustrated in Figure 4.2. After detecting the medium free for a time interval equal to Distributed Coordination Function Interframe Space (DIFS), the mobile station counts down the backoff timer until it reaches zero and initiates then its transmission. If during the countdown another station occupies the medium, all stations in backoff interrupt their count down and defer until they detect the medium free for at least DIFS.

The standard includes an optional Request-to-Send (RTS) - Clear-to-Send (CTS) handshake prior to the transmission to alleviate the hidden node problem and reserve the medium for the data transmission. A station with a data packet, after finishing the backoff procedure, first transmits an RTS frame. The stations which receive the RTS frame and are not its intended receivers set their Network Allocation Vector (NAV) timers and defer from the medium in order not to interfere with the transmission. NAV is used for virtual carrier sensing, by forcing stations to defer from the medium for the duration specified in the previously received frame. If the intended receiver of the RTS is idle and thus able to receive data, it responds with a CTS frame, after Short Interframe Space (SIFS). Mobile stations which receive the CTS set their NAV timer as well, and the sender of the RTS can transmit its data packet after SIFS. After receiving the CTS frame, the initiator of the transfer transmits the data packet. If successfully received by the intended receiver, the data packet is acknowledged by an ACK frame after SIFS. If the transmitted data packets are acknowledged before the timeout, they are removed from the data queue at the transmitter; otherwise they are retransmitted.

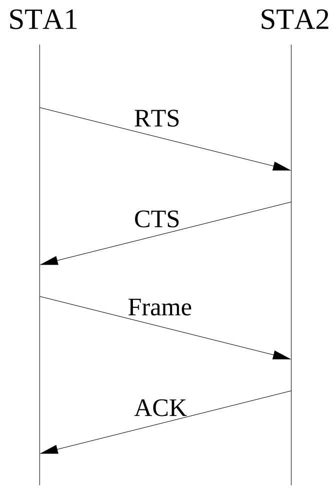

Figure 4.2: IEEE 802.11 DCF medium access

Interframe Spaces (IFSs)

Interframe spacing plays an important role in coordinating the medium access, including the prioritized access. IEEE 802.11 uses four different interframe spaces, whose values are given in PHY specifications:

- The SIFS is the shortest of all the IFSs and it is used for the highest priority transmissions. It is the minimum time that needs to elapse between to successive frame transmissions. It takes into account time needed by devices to switch from the receive mode to the transmit mode and back, MAC and PHY processing delay and RF delay.
- The Point Coordination Function Interframe Space (PIFS) is used by the PCF during the contention free operation, and it is equal to

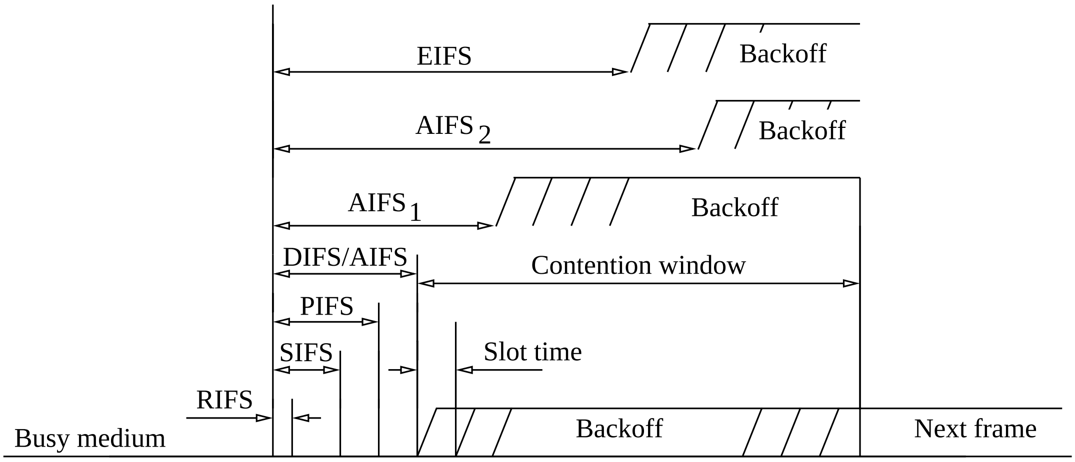

Figure 4.3: Interframe space relationships

the sum of SIFS and one slot time.

- The DIFS is the minimum medium idle time for contention based operation. DIFS duration is equal to the sum of SIFS and two time slots.
- The Extended Interframe Space (EIFS) is the interval used by a station after an error in frame reception. In order to protect the ACK from coliding with a frame from that station, the EIFS has the length of sum of SIFS, DIFS and the time needed to transmit an ACK frame using the lowest mandatory PHY mode.

The relationships between the interframe spaces is illustrated in Figure 4.3. The figure explains the prioritizing of different stations as well as the backoff procedure. Arbitration Interframe Space (AIFS) is an interframe space introduced in IEEE 802.11e, and it will be discussed in Section 4.1.3, and Reduced Interframe Space (RIFS) is the new feature of IEEE 802.11n, described in Section 4.2.

4.1.2 PHY Specifications

The initial version of IEEE 802.11 included three PHY specifications:

- Frequency-Hopping Spread-Spectrum (FHSS),
- Direct-Sequence Spread-Spectrum (DSSS), and
- Infrared (IR) PHY.

They support data rates 1 Mb/s and 2 Mb/s.

Three PHY related amendments followed:

- 802.11b - High Rate / Direct Sequence Spread Spectrum (HR/DSSS) at 2.4 GHz,
- 802.11a - OFDM at 5 GHz, and
- 802.11g - OFDM at 2.4 GHz

PHY is divided into two sublayers: the higher one - Physical Layer Convergence Procedure (PLCP) and the lower one - Physical Medium Dependent (PMD) sublayer. The Protocol Data Unit (PDU) for all PHYs consists of a preamble and a header followed my MAC data. Preamble is used for detection and synchronization, while header contains the information such as data rate and length.

IEEE 802.11a

The 802.11a [IEEE, 2007c] specifies the OFDM based PHY in 5 GHz band. Operating channels in 802.11a are 20 MHz wide, with several bandwidths and their corresponding allowed power specified for different regulatory regions. Each channel consists of 52 subcarriers, out of which 48 are used for data transmission, and the other 4 are pilot subcarriers. OFDM symbol duration is 4 μs, with guard time with cyclic prefix 800 ns long.

Table 4.2: MCS in IEEE 802.11a

PHY data rate	Coding rate	Modulation	Data bits per symbol
6 Mb/s	1/2	BPSK	0.5
9 Mb/s	3/4	BPSK	0.75
12 Mb/s	1/2	QPSK	1
18 Mb/s	3/4	QPSK	1.5
24 Mb/s	1/2	16 QAM	2
36 Mb/s	3/4	16 QAM	3
48 Mb/s	2/3	64 QAM	4
54 Mb/s	3/4	64 QAM	4.5

Maximum raw data rate is 54 Mb/s, equivalent to about 20 Mb/s net throughput. IEEE 802.11a has its own PLCP, which, among other information contains the data rate. The specified data rates with the corresponding Modulation and Coding Scheme (MCS) are given in Table 4.2. Other IEEE 802.11a parameters related to the MAC functionality are given in Table 4.3.

Table 4.3: MAC parameters in IEEE 802.11a

Parameter	Value
Slot time	9 μs
SIFS	16 μs
PIFS	25 μs
DIFS	34 μs
EIFS	43 μs
Contention window size	15 to 1023

4.1.3 IEEE 802.11e

IEEE 802.11e is an amendment to IEEE 802.11 standard that defines a set of Quality of Service (QoS) enhancements on the MAC layer.

The central enhancement of IEEE 802.11e is the new coordination function, Hybrid Coordination Function (HCF), which combines the functionalities of both DCF and PCF. HCF introduces the concept of Transmission Opportunity (TXOP), and provides the contention free medium access - Hybrid Coordination Function-Controlled Channel Access (HCCA), and contention based medium access mechanism - Enhanced Distributed Coordination Function (EDCF).

IEEE 802.11e also introduces the negotiable acknowledgements (no acknowledgement, no explicite acknowledgement - piggybacked acknowledgment, Block Acknowledgment (BA) or positive acknowledgment), instead of the positive acknowledgments in the original standard.

Further enhancements are traffic prioritization and parameterization. The traffic is sorted by the priority levels associated to the traffic types classified by IEEE 802.1D [IEEE, 2004a] into separate queues (four queues are mandatory). Each queue is assigned different AIFS and CW size in order to accordingly prioritize the traffic. When accessing the channel, contention first takes place among the queues within a station, and afterwards on the very wireless medium.

In the network operating in infrastructure mode after legacy standard, all communication between any two stations goes via the AP. That wastes resources, but also degrades the performance. To deal with this issue, IEEE 802.11e introduces Direct Link Protocol (DLP) that allows direct links between peer stations.

4.2 IEEE 802.11n

With growing demands for the WLAN capacity, there was a need for development of a standard that substantially increases the performance of the existing standards. In September 2003, the IEEE 802.11n Task Group (TGn) was established to compose a high-throughput extension of the current WLAN standard that will increase transmission rate and reduce compulsory overhead. The main goal was to define a new MAC and PHY protocol that provide higher capacity, and at the same time, allow coexistence with widely deployed legacy devices.

IEEE 802.11n [IEEE, 2007a] is an emerging standard that significantly improves the network throughput and range. Its most important feature is the application of MIMO technology. The standard defines extensibility to up to four spatial streams by applying multiple antennas. It promises 100 Mb/s of throughput as measured at the MAC Service Access Point (SAP), or maximum 600 Mb/s PHY layer data rate, and up to twice the range of IEEE 802.11g.

IEEE 802.11n is designed to operate in both the 5 GHz and the 2.4 GHz frequency bands, enabling backward compatibility for IEEE 802.11b/g/a devices. Using channel bonding, IEEE 802.11n can form a double-width 40 MHz channel out of two legacy 20 MHz channels. IEEE 802.11n uses improved OFDM PHY compared to IEEE 802.11a/g, by applying short guard interval of 400 ns instead of 800 ns in legacy standards.

Another important MAC feature that is added is frame aggregation. Frame aggregation enables transmission of several frames together within a single larger frame. This improves transmission efficiency by reducing the relative overhead.

A new interframe space, RIFS, is introduced. It is only $2\,\mu$s long and enables a station to retain control of the wireless channel and burst multiple successive frames by gaining prioritized medium access. It shortens the delay between two frame transmission and increases efficiency as well. Low-Density Parity-Check (LDPC) codes [Gallager, 1963] are also included in the standard.

An IEEE 802.11n device can operate in three modes:

- legacy mode - operating as an IEEE 802.11b/g/a station,
- mixed mode - operating as an IEEE 802.11n device, in the presence of other 802.11b/g/a devices, and
- greenfield mode - operating with all the high speed features of 802.11n, without the need to protect legacy stations.

The highest capacity is achieved in Greenfield mode, where all the high-throughput features are possible to apply.

4.2.1 MIMO Features of IEEE 802.11n

One of the MIMO features of IEEE 802.11 is transmit beamforming. In order for a beamformer to calculate an appropriate steering matrix for transmit spatial processing when transmitting to a specific beamformee, the beamformer needs to have an accurate estimate of the channel that it is transmitting over. There are two methods defined as follows:

- *Implicit feedback* - the beamformer receives long training symbols transmitted by the beamformee, which allow the MIMO channel between the beamformee and beamformer to be estimated. If the channel is reciprocal, the beamformer can use the training symbols that it receives from the beamformee to make a channel estimate suitable for computing the transmit steering matrix. Generally, calibrated radios in MIMO systems can improve reciprocity.
- *Explicit feedback* - the beamformee makes a direct estimate of the channel from training symbols received from the beamformer. The beamformee may prepare CSI or steering feedback based on an observation of these training symbols. The beamformee quantizes the feedback and sends it to the beamformer. The beamformer can use the feedback as the basis for determining transmit steering vectors [IEEE, 2007b].

Antenna selection is also specified in the standard. That is a time-variant mapping of the signals at the RF chains onto a set of antenna elements, when the number of RF chains is smaller than the number of antenna elements at a STA and/or AP. The mapping can be chosen based on instantaneous or averaged channel state information. Antenna selection requires the training of the full size channel associated with all antenna elements, which is obtained by transmitting or receiving sounding frames over all antennas. Antenna selection supports up to eight antennas and up to four RF chains [IEEE, 2007b].

IEEE 802.11n also supports STBC, with up to 4 antennas at both the transmitter and the receiver, supporting in this way up to four spatial streams.

4.2.2 Frame Aggregation

IEEE 802.11n defines two types of frame aggregation: MAC Service Data Unit Aggregation (A-MSDU) and MAC Protocol Data Unit Aggregation (A-MPDU). The maximum aggregated frame length 65535 byte, which compared to 2304 maximum MAC Service Data Unit (MSDU) size in the legacy standard, is a high MAC efficiency improvement.

MSDU Aggregation (A-MSDU)

The A-MSDU frame carries multiple MSDUs with only one MAC header common to all the MSDUs. This improves the efficiency of the MAC layer, particularly in case of short MSDUs.

An A-MSDU is a sequence of A-MSDU subframes as shown in Figure 4.4. Each A-MSDU subframe consists of an A-MSDU subframe header followed by an MSDU and 0-3 octets of padding (except for the last one). The A-MSDU subframe header contains three fields: `Destination Address (DA)`, `Source Address (SA)`, and `Length`, in the same order as in the IEEE 802.3 [IEEE, 2005] frame format.

An A-MSDU only contains MSDUs whose `DA` and `SA` parameter values map to the same receiving and transmitting stations, i.e., all the MSDUs are intended to be received by a single receiver, and necessarily they are all transmitted by the same transmitter. The value of `Traffic`

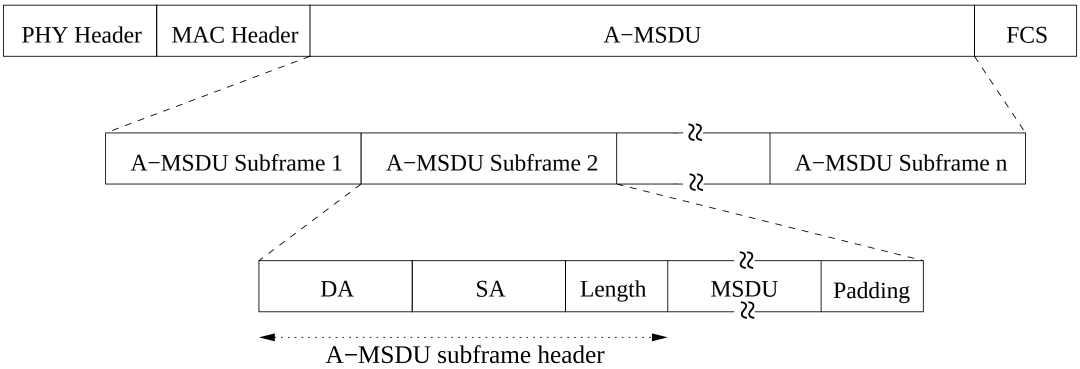

Figure 4.4: Frame aggregation: A-MSDU structure

`Identifier (TID)` present in the `QoS Control` field of the MPDU carrying the A-MSDU indicates the TID for all MSDUs in the A-MSDU, thus only MSDUs with the same TID can be aggregated. On the other side, the lifetime of the contained MSDUs may differ, and the lifetime of the A-MSDU is equal to the maximum of these values.

The major drawback of A-MSDU is manifested under error-prone channels. By compressing all MSDUs into a single MPDU that also has larger size which makes it more error prone, an erroneous reception has a consequence that the entire A-MSDU must be retransmitted.

MPDU Aggregation (A-MPDU)

The concept of A-MPDU aggregation is to join multiple MPDU subframes with a single leading PHY header. In contrast to A-MSDU method, in an A-MPDU frame the individual MSDUs have their own MAC header. Therefore, the constraint for the common TID is not relevant. However, all the MPDUs within an A-MPDU still have to be addressed to the same receiver station.

An A-MPDU consists of a sequence of one or more A-MPDU subframes as shown in Figure 4.5. Each A-MPDU subframe consists of an MPDU delimiter followed by an MPDU and 0-3 octets of padding (except for the last one). The MPDU delimiter is 4 octets in length. The purpose of the MPDU delimiter is to locate the MPDUs within the A-MPDU such that the structure of the A-MPDU can usually be recovered when one or more MPDU delimiters are received with errors.

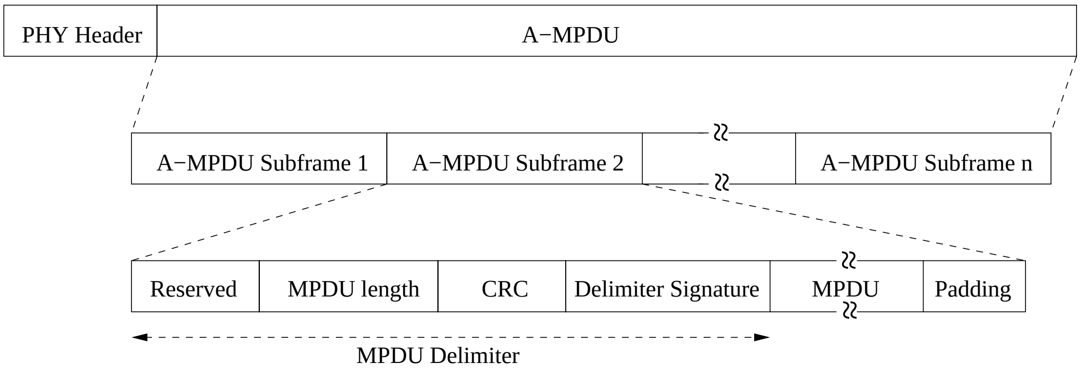

Figure 4.5: Frame aggregation: A-MPDU structure

The maximum length of A-MPDU 65,535 byte; an A-MPDU can consist of maximum 64 subframes, and the subframe size must not exceed 4095 byte. Such large frame size improves the MAC efficiency, and also, in contrast to A-MSDU, does not require the retransmission of all the subframes in case of an error within one frame. Instead, single erroneous A-MPDUs can be identified to be retransmitted. It is also possible to achieve two-level frame aggregation by packing multiple A-MSDUs into an A-MPDU subframe [Skordoulis et al., 2008, Kuppa and Dattatreya, 2006].

Frame aggregation can increase the throughput at the MAC layer under ideal channel conditions. However, the larger the aggregated frame size is, the larger is the probability of erroneous reception. This also means that a station may occupy the medium for a longer period of time. Also, if the minimum A-MPDU/A-MSDU size is defined, the delay of internal frames is increased. Thus, there is a tradeoff between throughput and delay. This issue is well covered in the literature, including the the two level combination of A-MPDU and A-MSDU and the challenges of real working environment [Skordoulis et al., 2008, Lin and Wong, 2006].

CHAPTER 5

System Description

Contents

This chapter contains a description of the system which is analyzed in the remaining of the thesis. An ad-hoc network of possibly multiple antennas stations is assumed. The MAC protocol that is an extension to IEEE 802.11 DCF for MIMO support is in the primary focus. There are two modes of operation of the MAC protocoal, referred to SU-DCF [Mirkovic et al., 2007a] and MU-DCF [Mirkovic et al., 2007c].

5.1 MAC Protocol Description

MU-DCF enhances the IEEE 802.11 DCF with MIMO capability, in particular, SMUX. SU-DCF is a special case of MU-DCF, therefore a description of MU-DCF will be given first, followed by the restrictions that apply in case of SU-DCF.

Prior to data transmissions, in the association procedure, stations share among each other the information about their hardware capabilities.

Similarly as in the IEEE 802.11 DCF, medium access in MU-DCF is based on CSMA/CA with a random backoff procedure and optional four-way handshake. MU-DCF uses extended forms of RTS, CTS, and ACK -

MIMO-RTS (M-RTS), MIMO-CTS (M-CTS) and MIMO-ACK (M-ACK) to support frame exchange in the presence of multiple antennas. The structure of these frames depends on the scheduling policy, and it is analyzed in detail in Section 5.3. Setting the NAV timers is same as in the IEEE 802.11 standard, as well as the usage of IFSs.

All the control frames are transmitted using a scheme that is supported by all the stations, independently of their hardware capabilities, including the stations with only one antenna.

The choice of the scheme used for *data* transmission is a system design issue: random or adaptive antenna selection, transmit or receive diversity or both, etc. Using schemes that increase diversity order (more receive than transmit antennas), will increase the probability of correct reception, whereas pure spatial multiplexing increases the throughput. In case of adaptive scheduling, the MIMO scheme used for the transmission of data packets is selected based on the stations hardware capabilities, QoS demands of the connection, radio propagation conditions, and current status of the network. Choosing the MIMO scheme is the part of the scheduler located at the transmitter that uses the feedback from the receiver as well as the connection parameters as input parameters. This is covered in Chapter 8.

5.1.1 SU- and MU-MIMO Transmissions - SU-DCF and MU-DCF

Whichever scheduling policy the transmitter applies, an important characteristic of the choice of individual packets that build a MIMO frame is their destination address. Thus, SU- and MU-MIMO transmissions can be differentiated - the first term corresponds to the case where all the packets have the common destination address, and the second one to the case where the addresses are not necessarily same.

In ubiquitous networking, a station may communicate with more stations at a time; the first example is an AP in a WLAN, but also other non-infrastructure connections are possible. In MIMO systems, achieving a high network throughput becomes less critical than ensuring a timely delivery for a specific flow. With respect to this characteristic, enabling MU transmissions provides two important advantages:

- under light load, the delay characteristic is improved, and
- under heavy load, the delay jitter is reduced.

With the relaxed rule that a MIMO frame does not have to be constructed from the data packets with a common destination, the transmission could be started earlier. Improving the delay characteristic is especially important for applications such as multimedia streaming, Voice-over-IP (VoIP), tele- and videoconference, interactive gaming, etc. Particularly, applications with light load would benefit from this.

However, MU transmissions have the drawback of introducing additional complexity to the system, including the medium access protocol and frame structure changes. Thus SU is a straight-forward extension of a SISO system, whereas MU-MIMO tries to exploit the additional degree of freedom, that imposes certain challenges. Both approaches are analyzed in this work, from the aspect of both, the performance and complexity. SU-DCF will be used where referring to the protocol when only SU-MIMO transmission is allowed.

5.2 Frame Exchange

Frame exchange during a transmission window has different form in case of SU-DCF and MU-DCF. The two procedures are presented in Figure 5.1 and analyzed in detail in the following sections.

5.2.1 Frame Exchange in SU-DCF

In SU-DCF, the frame exchange presented in Figure 5.1(a) does not substantially differ from the standard DCF frame exchange. Instead of the standard forms of control frames, the corresponding extended ones are applied for MIMO support. Depending on the scheduling algorithm, the transmitter may request the CSI feedback in the M-RTS frame. If requested, the CSI is contained in the following M-CTS frame, and the transmitter uses this information for channel adaptation The following MIMO frame consists of packets that are all addressed to the same receiver, and the correctly received packets are acknowledged in the ACK frame.

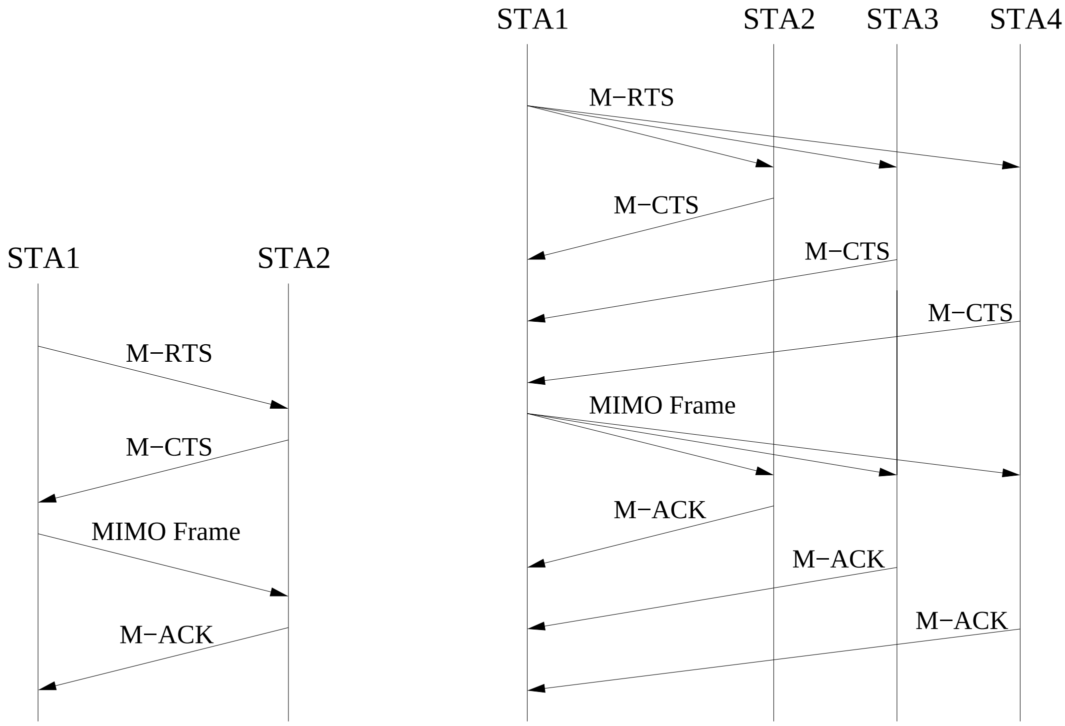

(a) SU-DCF

(b) MU-DCF

Figure 5.1: Transmission of a MIMO frame

5.2.2 Frame Exchange in MU-DCF

Frame exchange following the rules from MU-DCF is presented in Figure 5.1(b). In the procedure, more then two stations are involved; besides the station that is the source of the MIMO frame (`STA1`), multiple other stations are involved as the receivers of the individual packets building the MIMO frame (`STA2, STA3, and STA4`).

In the following, the additional MAC protocol functionality during a transmission cycle in MU-MIMO scenarios are described:

- A transmission is initiated by an M-RTS frame transmission that polls multiple receivers.
- Upon receiving the M-RTS frame, the stations that are present in the receiver list reply with M-CTS frames. The order of replies is implicitly determined by the receivers order in the M-RTS frame.
- Upon receiving the M-CTS frame(s), the transmitter compiles the collected information, creates a MIMO frame and transmits it.

- Each station that receives the MIMO frame, checks if there is a packet that is addressed to itself. If there is at least one such packet correctly received, the station generates an M-ACK that contains the information about the correctly received packets. The order of M-ACK frames is implicitly determined by the order of data packets of the MIMO frame.
- When the transmitter receives the M-ACK frame(s), it removes the acknowledged data packets from the queue and, if necessary, initiates another medium access procedure for the next transmission. Unacknowledged packets are retransmitted.

It is worth noting that if stations are polled in the M-RTS frames, it does not necessarily mean that data packets will be transmitted to those stations within the next MIMO frame (e.g. if their channel is in the bad state). Moreover, a station that is not addressed in the M-RTS frame can also be a receiver of a data packet in the transmitted MIMO frame. This decision is made by the transmitter that does the final scheduling after receiving the M-CTS replies.

The essential features of MU-DCF are:

- Simultaneous transmission of multiple data packets that do not necessarily have a common destination - MU-MIMO.
- Alleviating the hidden station problem in MU case using M-RTS and M-CTS frames as replies to M-RTS.
- M-ACK for selective acknowledging of correctly received data packets.
- Coexistence and interoperability of stations with different number of antennas, including backward compatibility with single antenna stations.

The illustarted frame exchange in MU-DCF in Figure 5.1(b) shows that after M-RTS frame transmission, and MIMO frame transmission, several M-CTS and M-ACK frames are successively transmitted in time. Instead of transmitting multiple M-CTS and M-ACK frames using TDMA, OFDMA can be used. In that case, the set of data subcarriers is split into subsets and each subset is allocated to one station to transmit its M-CTS/M-ACK frame. This approach reduces the signaling overhead; the benefits of using OFDMA signaling are discussed more in detail in Sections 7.1.3 and 8.5. Using OFDMA in "uplink" requires an accurate synchronization among the transmitting stations [van de Beek et al., 1999].

5.3 Extended Control Frame Structure

The control frames in SU-DCF and MU-DCF are extended for better support of MIMO transmissions and they are described more in detail in this section. Basic structure of the standard control frames is remained, namely `Frame Control`, `Duration` and `Frame Check Sequence (FCS)` fields.

M-RTS and M-CTS

In Figure 5.2 the structure of M-RTS frame is illustrated. M-RTS frame in the SU case (Figure 5.2(a)) has the same structure as the standard RTS frame. It contains the field `Receiver Address`, as well its own address in the field `Transmitter Address`. In MU-DCF, M-RTS has multiple `Receiver Address` field to gain the ability to poll multiple receivers.

M-RTS also includes in the preamble the training sequence for each transmit antenna for the channel estimation (in PHY).

2 byte	2 byte	6 byte	6 byte	4 byte
Frame Control	Duration	Receiver Address	Transmitter Address	FCS

(a) M-RTS in SU-DCF (this is the standard RTS frame)

2 byte	2 byte	n x 6 byte	6 byte	4 byte
Frame Control	Duration	n x Receiver Addresses	Transmitter Address	FCS

(b) M-RTS in MU-DCF

Figure 5.2: M-RTS frame structure

The M-CTS frame does not differ in case of SU-DCF and MU-DCF. However, there are still two versions of the frame. The basic M-CTS (Figure 5.3(a)) has the same structure as the standard CTS frame. Only the receiver address of the frame is needed, since the station that transmitted M-RTS can identify the station that transmitted the M-CTS frame by the used resources: time in case of TDMA signaling, or subcarriers in case of OFDMA signaling.

In case that channel adaptive scheduling is applied in the system, the M-CTS contains the CSI feedback. The length of that field depends on the number of antennas, applied scheduling and MIMO scheme that determine the type of CSI needed.

2 byte	2 byte	6 byte	4 byte
Frame Control	Duration	Receiver Address	FCS

(a) Basic M-CTS (this is the standard CTS and ACK frames)

2 byte	2 byte	6 byte		4 byte
Frame Control	Duration	Receiver Address	Channel State Information	FCS

(b) M-CTS with CSI feedback

Figure 5.3: M-CTS frame structure

The transmitter collects the CSI from the polled stations and makes the decision about which MIMO scheme should be used and which packets are scheduled for the next transmission, taking into account, additionally, the QoS requirements of each connection.

M-ACK and ARQ

The standard ACK frame has the same structure as the standard CTS frame presented in Figure 5.3(a). In addition to these fields, M-ACK presented in Figure 5.4 contains a new field for selective acknowledgments. It can be a bitmap, but also a field with encoded information.

Data transmission can be followed by several M-ACK frames, depending on the number of distinct receivers of the transmitted MIMO frame. When the transmitter receives an M-ACK frame, it reads the information about the outcome of the previous data transmission, and removes the correctly received packets from the queue. If an expected M-ACK frame is not received, after a timeout data will be retransmitted.

Thus, in contrast to IEEE 802.11 DCF that applies the plain positive acknowledging, in MU-DCF and SU-DCF selective acknowledging is the

2 byte	2 byte	6 byte		4 byte
Frame Control	Duration	Receiver Address	ARQ Bitmap	FCS

Figure 5.4: M-ACK frame structure

ARQ mechanism applied.

5.4 MIMO Frame Size

As MU-DCF and SU-DCF have been described, each antenna is always active and transmits a single packet. The main performance gain of MU-DCF is the increased system capacity. If trying to keep high channel efficiency (by using all the available spatial streams), stations must wait to have enough packets to transmit over all available spatial channels. That may increase delay under light load: the packet that arrives first into the queue waits in the queue for a time duration that for some applications (such as VoIP) might be too long, and it could be dropped at the transmitter instead of transmitting it.

By allowing the transmitter to initiate the transmission earlier, before the MIMO frame is filled, applications with low data rate, but very strict delay requirements, such as VoIP, or interactive gaming become feasible. This approach would produce another problem: under heavy load, channel utilization and total system capacity would decrease, and the stations with heavy load may suffer. In case of many stations with low load and only a few of them with high load, the stations with high load will not have enough chance to access the channel, because the users with light load would be occupying it all the time, possibly with low channel utilization.

Fragmenting packets to transmit fragments over different spatial streams is another option to reduce waiting time in buffers. However, applications with strict delay requirements, typically, have very short packets, thus the reduction of the transmission window by fragmentation will be small and the efficiency will not change much.

Therefore, a mechanism is needed to delay the transmission of packets:

- as much as possible, to fill the MIMO frame and thereby increase the channels utilization, and also decrease the number of channel

access events, and
- not too long, to avoid packets running into delay timeout.

Building MIMO frames can also be seen as a way of packet aggregation that has been extensively covered in the literature. The optimum packet size in IEEE 802.11 DCF in ideal and error-prone channel conditions under a saturated traffic model to maximizes throughput has been investigated in [Yin et al., 2004]. The authors found that longer packets are preferred by better channels, and the optimal packet length does not change with the number of contending nodes.

In [Ci and Sharif, 2005], variable packet size and variable data rate schemes for goodput enhancement is proposed. Two optimal packet size predictors are proposed: a goodput regulator to maintain the committed goodput for non-greedy applications and an optimal packet size predictor for maximizing goodput for greedy applications. A data rate drafting scheme and develop a variable size and variable rate (VSVR) scheme for further goodput improvement are also proposed. With extensive simulation results it is shown that the proposed algorithm can double the channel goodput.

The impact of frame aggregation in IEEE 802.11n networks has also been analyzed in [Lin and Wong, 2006]. Larger frames decrease the relative overhead, but increase the delay for other stations, and in case of frame error, retransmissions might cost a lot of the capacity. The authors propose an optimal frame size adaptation algorithm for error-prone channels. However, they do not account for the QoS requirements of particular applications.

The decision whether a station should wait for more frames to be generated or should immediately start a transmission could be made by modifying a backoff algorithm that would take the following parameters into account:

- predicted own offered load,
- the traffic load to the network,
- success rate of previous frame transmission,
- experienced waiting time, frame lifetime and their relation, etc.

Algorithms like these are out of the scope of this work. In the remaining of this work, if not stated differently, it is assumed that the number of transmitted frames is the same as the number of active transmit antennas.

5.5 MU-DCF, SU-DCF and IEEE 802.11n

When it comes to MIMO capable WLANs, one thinks of IEEE 802.11n. The main difference of MU-DCF compared to the IEEE 802.11n is the capability of MU-MIMO transmissions. It should be noted that in the comparison of MU-DCF with IEEE 802.11n presented later, in order to provide fair comparison, not all the options of the IEEE 802.11n are activated (such as Block Acknowledgment (BA), link adaptation, 40 MHz channel bandwidth etc.). The same options would improve the performance of MU-DCF in the same manner as well.

Therefore, the performance of SU-DCF that supports only SU-MIMO transmission, can be seen as a reference corresponding also IEEE 802.11n.

5.6 Evaluation Tools

The remaining of the thesis presents the performance analysis of the described systems on link and system levels.

For system level performance evaluation, besides mathematical models and Monte Carlo simulations, the simulator MACNET2 is used. MACNET2 is an event driven simulation tool developed at the Chair of Communication Networks, RWTH Aachen, for the performance evaluation of HiperLAN/2 and IEEE 802.11 MAC protocols. A more detailed description is given in Appendix A.

CHAPTER 6

Physical Layer Analysis

Contents

In this chapter a physical layer analysis of SU-/MU-DCF is given. An analysis given in [Mirkovic et al., 2006] has been extended to second order statistics, and besides the ZF receiver, the MMSE algorithm is also investigated. The primary concern of the analysis is the PHY performance, i.e. gain obtained by different MIMO schemes compared to the SISO system, post-processing SNR distributions as well as the achievable bitrates.

6.1 Post-Processing SNR Analysis

In this section, post-processing SNR is analyzed in detail. For the selected set of antenna configurations:

- 1×1 antenna,
- 1×4 antenna,
- 2×4 antenna, with ZF receiver and with MMSE receiver, and
- 4×4 antenna, with ZF receiver and with MMSE receiver,

the average values of post-processing SNR are analyzed, and the impact of additional antennas is studied. Finally, for fixed antenna configurations the order statistics of post-processing SNR is evaluated.

6.1.1 Average Post-Processing SNR Analysis

Throughput this chapter, the signal models, channel models and propagation conditions introduced in Section 3.2.1 are used. The receiver has the perfect channel knowledge. It is assumed that the total transmit power is constant for all the schemes, irrelevant of the number of antennas. Each antenna is transmitting with an equal fraction of the avaliable power. The total average SNR is equal to the link budget divided by the noise power at the receiver.

In case of 1×1 antenna system, the MMSE receiver is applied; its performance is the same as that of the ZF receiver, and they both after detection give the ML receiver performance. In case of one transmit and more receive antennas, the MRC receiver is applied (both, MMSE and ZF receivers reduce to MRC in case of one transmit antenna).

Impact of Additional Antennas on Average Post-Processing SNR

Multiple antennas at the receiver are a necessary prerequisite for spatial multiplexing - at least as many as transmit antennas are needed. Additional ones can be used to exploit the array and diversity gain. In this section the following analysis is presented: signals from i transmit antennas are received with i receive antennas, and it's performance is compared with the post-processing SNR extracted by $M_r = i+1, i+2, ...$ antennas (with $i = 1, 2, 3$, and $M_r \leq 4$).

In Figure 6.1 the 1×1 antenna link is compared to receive diversity schemes with MRC receiver with 2, 3 and 4 antennas. For single antenna link, the average post-processing SNR is equal to the input SNR. Since there is no inter-stream interference, the gain is constant for both low and high SNR region, and takes values 3 dB, 4.8 dB, and 6 dB for 2, 3 and 4 antennas at the receiver, which is in accordance to formula $10 \log_{10} M_r$ (Section 3.5.1).

In Figures 6.2 and 6.3 the results of comparison of 2×2 and 3×3 links, for both ZF (dashed line) and MMSE receivers (solid line) are presented. It can be noticed that the average post-processing SNR in case of the same number of receive and transmit antennas is lower then the average input SNR, since the transmit power per antenna is only a fraction of the total transmit power, and array gain is $10 * \log_{10}(M_r - M_t + 1) = 0$. Adding

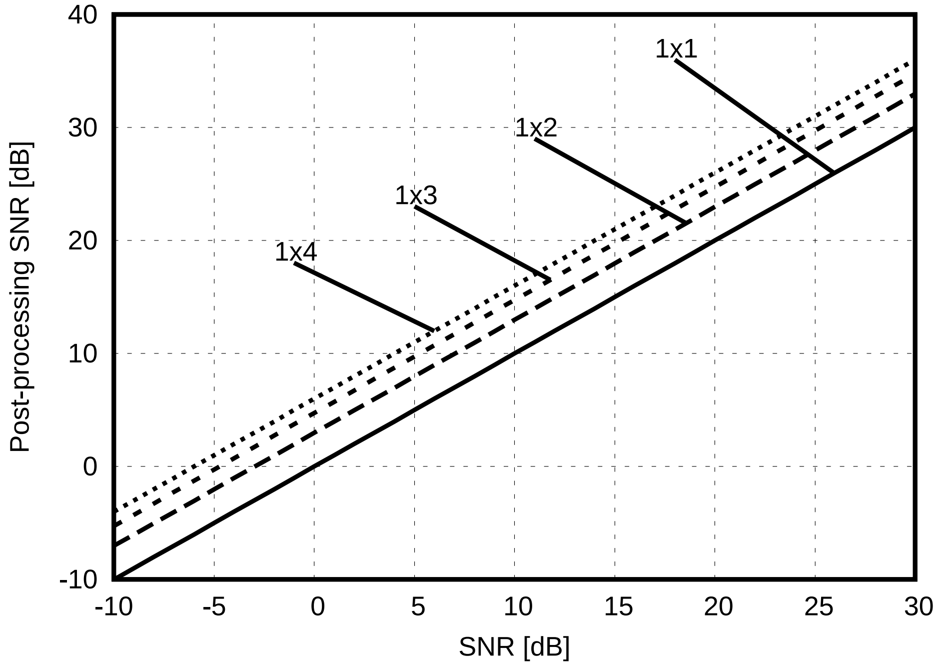

Figure 6.1: Average post-processing SNR for **one spatial stream** with 1, 2, 3 and 4 antennas at the receiver

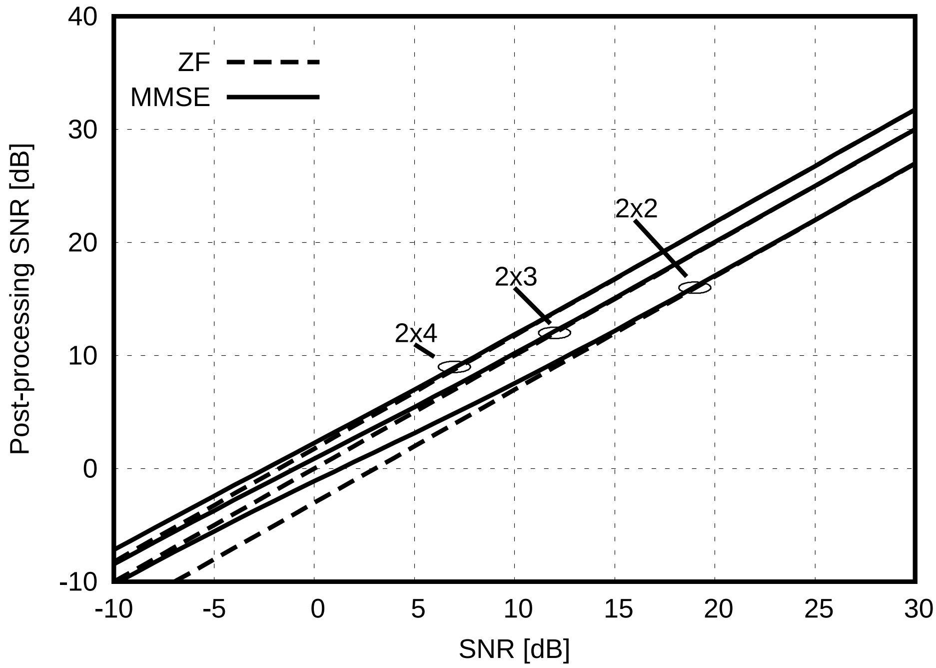

Figure 6.2: Average post-processing SNR for **two spatial streams** with 2, 3 and 4 antennas at the ZF and MMSE receiver

more antennas at the receiver side again improves the performance, for both MMSE and ZF receivers.

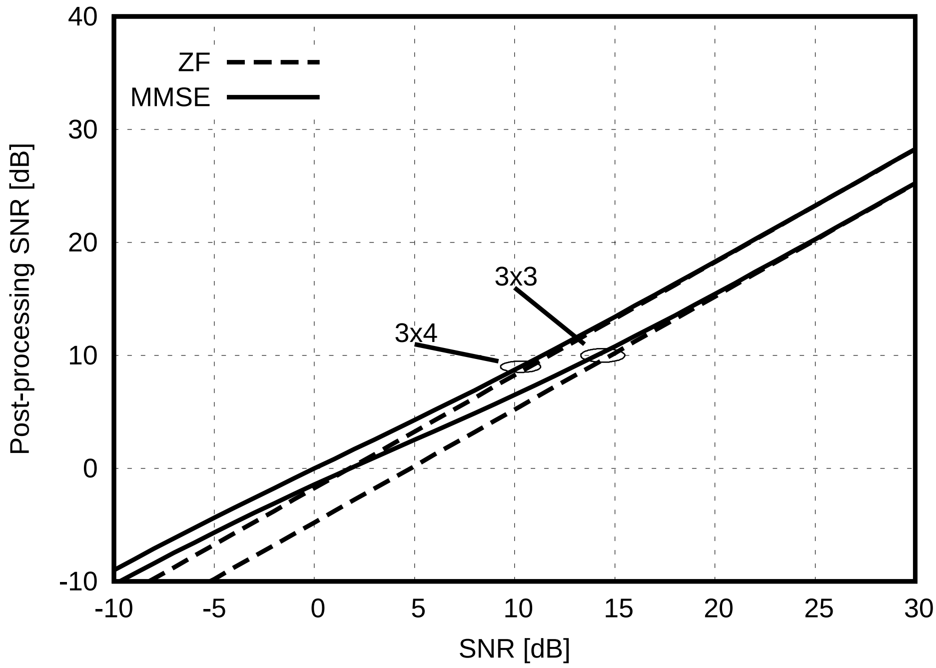

Figure 6.3: Average post-processing SNR for **three spatial streams** with 3 and 4 antennas at the ZF and MMSE receiver

Another observation that can be made is the difference in performance of the two receivers, which is decreasing with the number of antennas and input SNR. As a consequence, additional antenna at the receiver side gives more benefits to the ZF receiver, although MMSE receiver outperforms it.

In the analyzed three figures (6.1, 6.2 and 6.3), it has been shown that due to the lower power per transmit antenna, when more of them are present, but also due to the multiple stream interference, the post-processing SNR reduces with the number of transmit antennas (which corresponds to the number of streams) and grows with the number of receive antennas. Diversity schemes perform better in the sense of post-processing SNR level, but multiplexing schemes perform better in terms of multiplexing gain, since multiple data pipes are open between the transmitter and the receiver. An analysis that takes into account this aspect is given in Section 6.2.

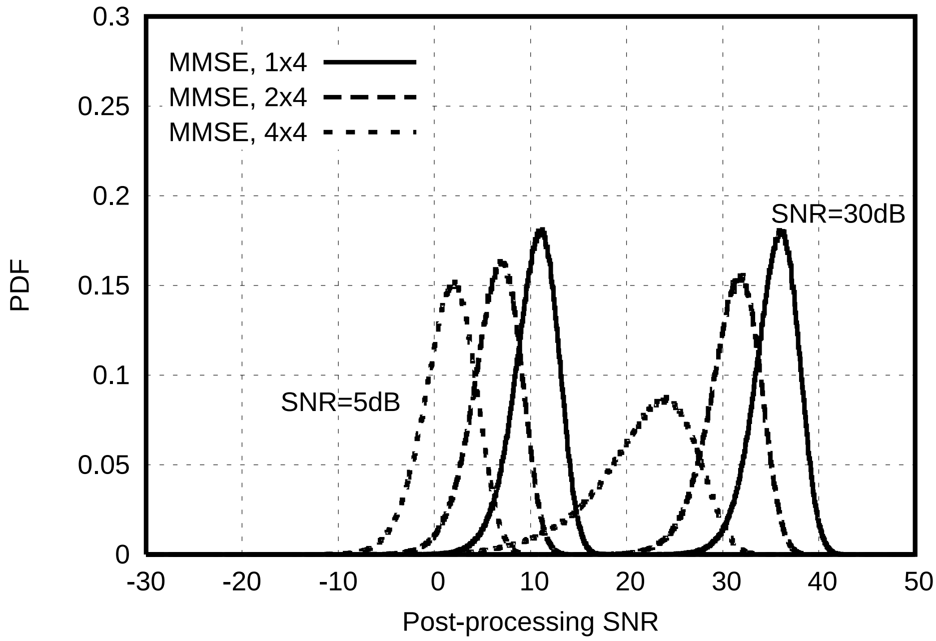

Figure 6.4: PDF of post-processing SNR for 5 dB and 30 dB input SNR with MMSE receiver

6.1.2 Distribution of Post-Processing SNR

In Figure 6.4 distribution of post-processing SNR with the MMSE receiver is illustrated for low SNR region at 5 dB and high SNR region at 30 dB with different number of spatial streams. It can be seen that the post-processing SNR has the lowest variance in case of one spatial stream, and it gradually increases with additional antenna. Also, the post-processing SNR in low SNR region with more spatial streams has lower variance than in high SNR region. That is the characteristic of the MMSE receiver; ZF has the same performance independently of SNR.

Since post-processing SNR is a random variable, it is interesting to see for a given channel realization, what is the standard deviation of the corresponding post-processing SNR values, calculated from:

$$\sigma = \sqrt{\frac{1}{M_t}\sum_{i=1}^{M_t}(\eta_k - \overline{\eta})^2}, \qquad \overline{\eta} = \frac{1}{M_t}\sum_{i=1}^{M_t}\eta_k \tag{6.1}$$

where η_k is the post-processing SNR on stream k. It should be emphasized that this is not the standard deviation of post-processing SNR on a stream over multiple channel realizations, but it is a measure of deviation among post-processing SNRs for a fixed channel realization.

Figure 6.5 shows the standard deviation in case of 2×4 and 4×4 antenna configurations with the MMSE receiver at 5 dB and 30 dB SNR. Standard deviation declines when the number of spatial streams is reduced. It can also be seen that with 4 transmit antennas the standard deviation is higher at higher SNR level; this is a property of the MMSE receiver. The ZF receiver performance is SNR independent. With only two active antennas the difference of performance at 5 and 30 dB is minor. Median value with 4 spatial streams at 5 dB SNR is 2 dB and 2.5 dB at 30 dB SNR, whereas with 2×4 is about 1 dB for both SNR levels. The performance of the ZF receiver coincides with the performance of the MMSE receiver at 30 dB.

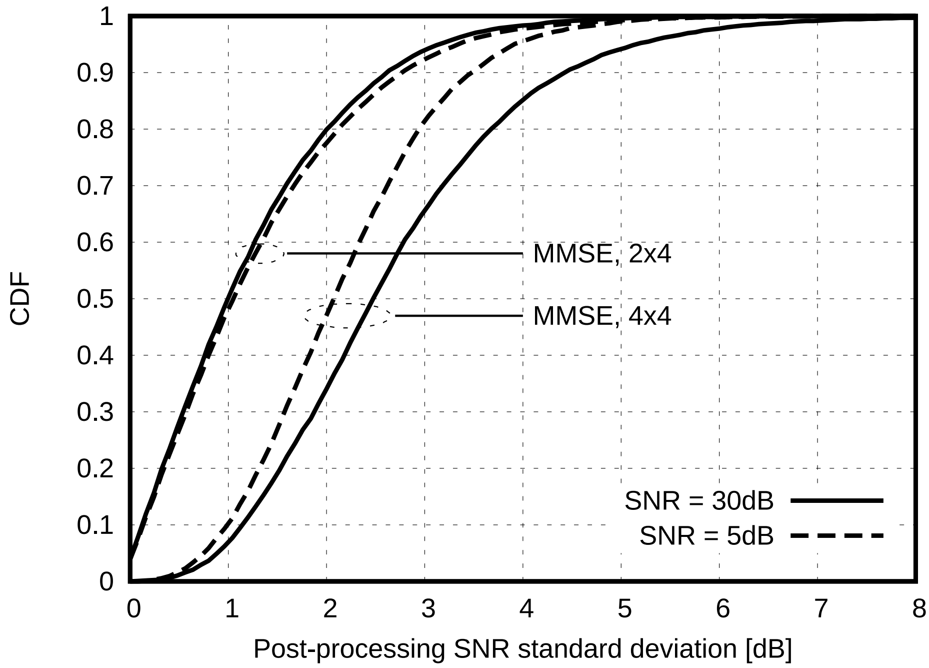

Figure 6.5: CDF of post-processing SNR standard deviation

6.1.3 Post-Processing SNR Order Statistics

In this section, the distribution of post-processing SNR order statistics is analyzed. Since ZF and MMSE receive algorithms give differing performance in the high and low SNR region, the analysis has been performed for two average SNR levels: 5 dB and 30 dB.

After applying the receiver algorithm, the post-processing SNR values are sorted in the array $\{\text{ppSNR}_{(1)}, ..., \text{ppSNR}_{(M_t)}\}$ so that for each $i, j, i < j$ it applies: $\text{ppSNR}_{(i)} \leq \text{ppSNR}_{(j)}$, and their PDF was measured.

Over the 1×1 and 1×4 antenna links there is only one spatial stream, hence there is only one post-processing SNR to evaluate; PDF of post-processing SNR in these two cases is plotted in Figure 6.6.

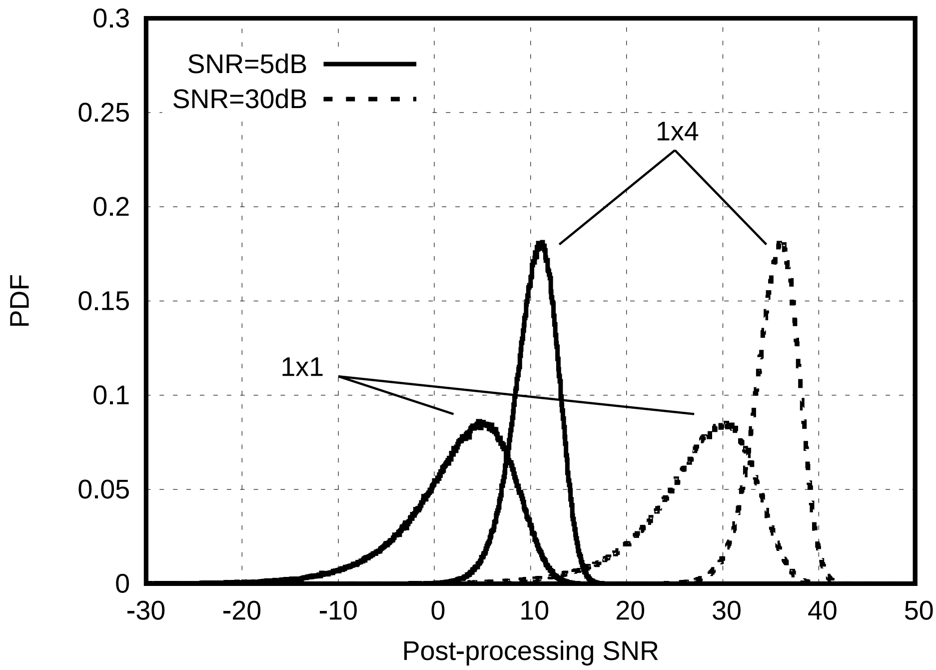

Figure 6.6: Post-processing SNR distribution over 1×1 and 1×4 antenna link, for 5 dB and 30 dB input SNR

There is a significant difference in performance of the two links. First, the average value of the post-processing SNR over SIMO link (1×4) is higher than for the SISO link (as shown in the previous analysis). Another important observation can be made, and that is that the variance of the post-processing SNR is smaller, due to the presence of diversity. This can be interpreted as the lower uncertainty of the received signal, which appears not to depend on the SNR level.

In Figures 6.7 and 6.8 the results are presented for 4×4 antenna link with ZF and MMSE receiver. ZF has the same performance independently of the SNR level, also equal to the performance of MMSE in high SNR region. On the other hand, in low SNR region, MMSE does not amplify noise like ZF, and therefore the post-processing SNR order statistics

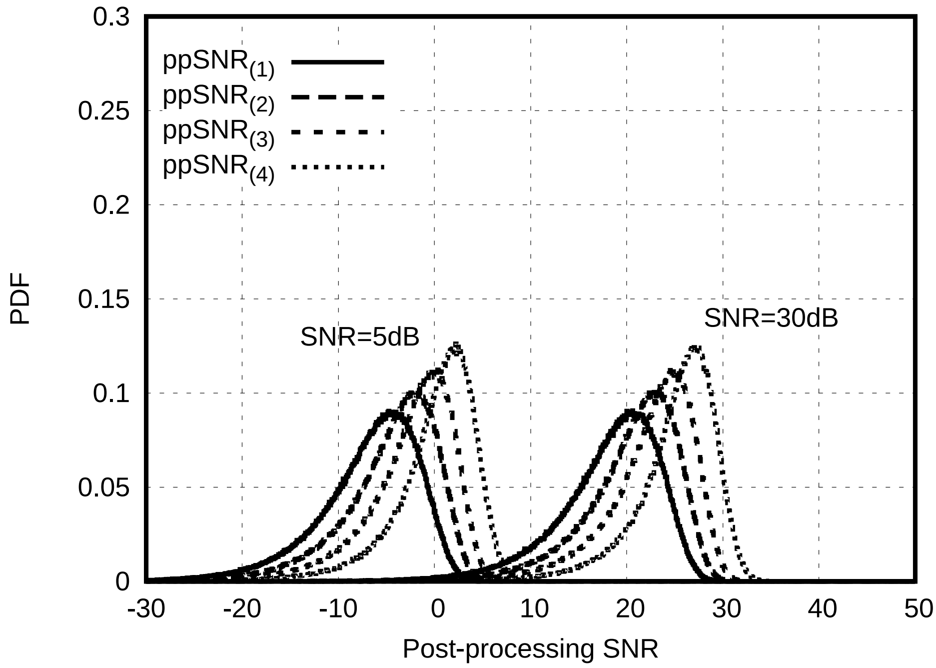

Figure 6.7: Post-processing SNR order distribution with ZF receiver over 4×4 antenna link, for 5 dB and 30 dB input SNR

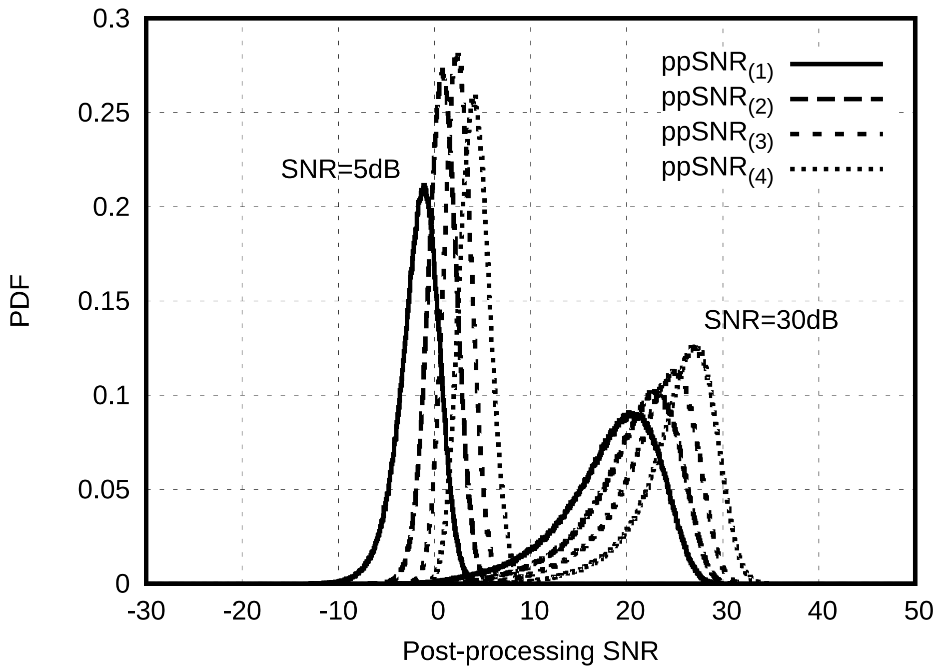

Figure 6.8: Post-processing SNR order distribution with MMSE receiver over 4×4 antenna link, for 5 dB and 30 dB input SNR

achieve higher average value and, in addition, lower variance.

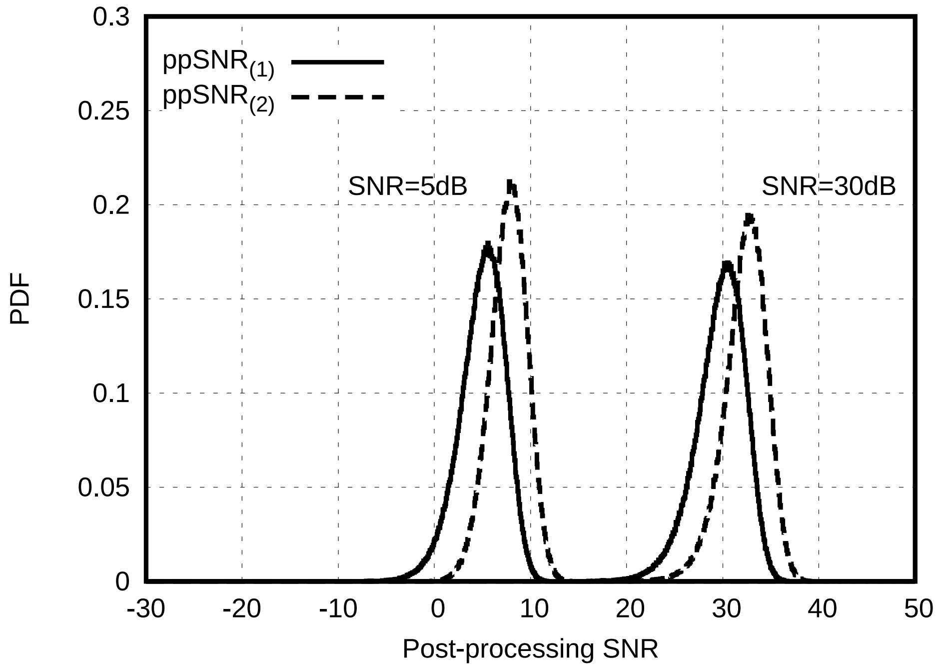

Figure 6.9: Post-processing SNR order distribution with MMSE receiver over 2×4 antenna link, for 5 dB and 30 dB input SNR

In Figure 6.9 the post-processing SNR order distributions for the MMSE receiver over 2×4 antenna link are plotted. The diversity order in this case is 3. The MMSE receiver performs similarly in low and high SNR region, and corresponds to that of the ZF receiver. The difference in performance of MMSE and ZF illustrated for the 4×4 antenna link in Figures 6.7 and 6.8 is significantly reduced with the presence of spatial diversity.

6.2 Gross Bitrate Analysis

The hitherto analysis in this chapter was focused on the achievable post-processing SNR with different antenna configurations. In the following analysis, the focus is on the achievable gross bitrate that this post-processing SNR can be translated to. In other words, it will include the multiplexing gain that can be exploited on the link level.

Multiple antennas can be flexibly used to exploit array, diversity and multiplexing gain. By opening multiple data pipes referred to as spatial streams, the link throughput can be increased. Very important is also the ability to effectively increase the receive SNR (post-processing SNR), which can be then translated into increased network coverage; or to decrease Packet Error Rate (PER), since a high PER may cause many retransmissions extending packet delay on higher layers. Using less spatial streams than available can effectively lead to increased throughput on higher layers, although the bitrate on the PHY may decrease.

In the following gross bitrate analysis, perfect channel state information at both receiver (for correct reception) and transmitter (for the perfect link adaptation) is assumed.

Achievable gross bitrate for the schemes analyzed in Section 6.1 at 5 dB and 30 dB SNR are plotted in Figure 6.10. The transmitter applies a perfect link adaptation, choosing among BPSK, QPSK, 16-QAM and 64-QAM so that Bit Error Rate (BER) is lower than 10^{-3} for the particular channel realization and post-processing SNR. The modulation is chosen for each stream, independently. In the first case, 5 dB SNR, the highest bitrate can be achieved using one spatial stream with 4 receive antennas (1×4). Since the SNR is low, diversity is necessary to increase the post-processing SNR. Somewhat worse performance is achieved with two spatial streams, while with 4 spatial streams and four receive antennas, as well as over a single antenna link, the gross bitrate is almost zero. It can also be seen that the superior performance of the MMSE receiver with regard to post-processing SNR is also reflected by the achievable gross bitrate.

Unlike gross bitrate at 5 dB, at 30 dB SNR gross bitrate is proportional to the number of available spatial streams. Since the minimum SNR for the highest modulation, corresponding to 72 Mb/s is well below 30 dB, in most cases it is chosen by the link adaptation algorithm, thus with four spatial streams gross bitrate is $4 \cdot 72\,\text{Mb/s} = 288\,\text{Mb/s}$. It should also be noted that the difference between ZF and MMSE receiver algorithms is negligible.

In Figure 6.11 gross bitrate analysis is extended to the SNR values from 0 dB to 40 dB. The figure illustrates that the diversity is necessary to improve the link quality in the low SNR region, and at the same time it does not bring much benefit when the channel is already good, in the high SNR region.

When applying multiplexing in the high SNR region, the throughput is

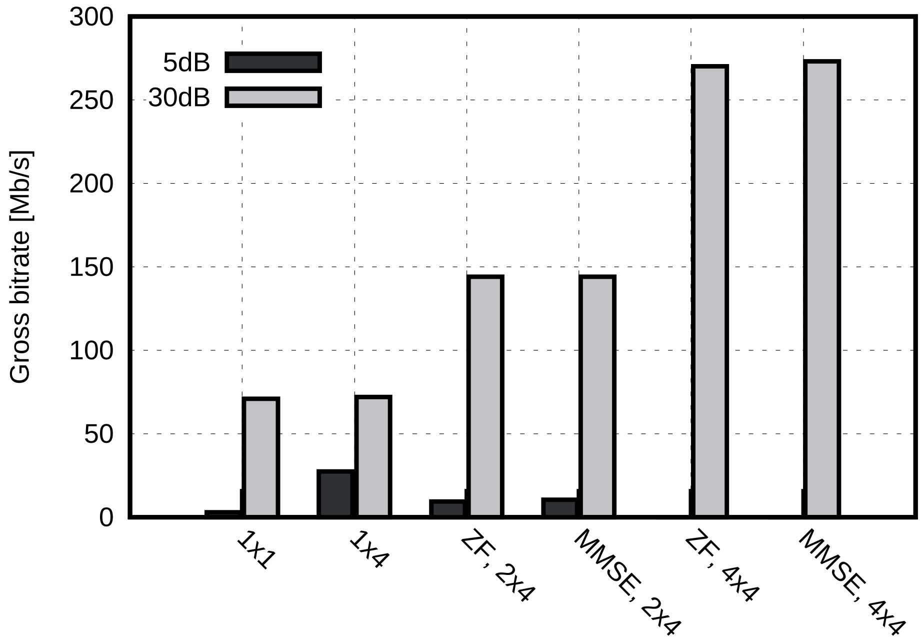

Figure 6.10: Gross bitrate achievable over different MIMO links at 5 dB and 30 dB SNR

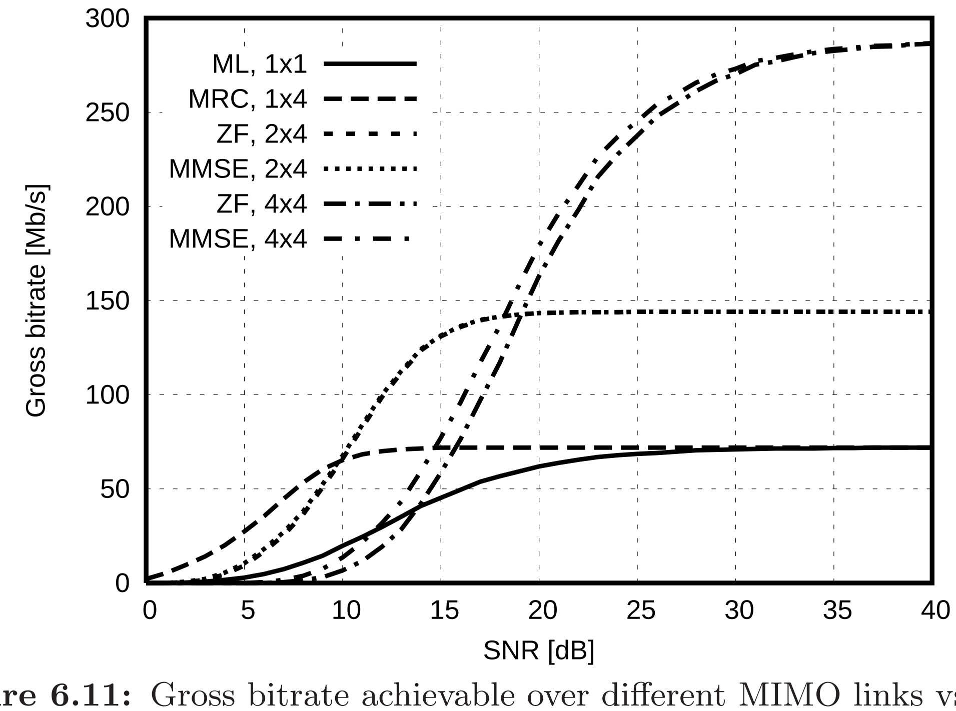

Figure 6.11: Gross bitrate achievable over different MIMO links vs. SNR

directly proportional to the number of spatial streams. On the other hand, it decreases the bitrate when the SNR is low: although having double, or four times more spatial subchannels available (in this example), the BER raises so much that the bitrate on individual spatial subchannels has to be significantly reduced, or no transmission is possible at all.

The shape of the curves in Figure 6.11 looks very similar to the bitrate of different PHY modes vs. SNR level to determine the switching points for a link adaptation algorithm. Similarly, from this figure the switching points between different antenna configurations can be directly read.

This figure also indicates that the spatial dimension also has to be taken into account when doing MIMO link adaptation. This topic is the focus of Section 8.

It is worth noting that the used resources and complexity of these schemes are diverse: as for resources - it is not meant bandwidth or transmit power only, but also antennas, RF units, battery capacity (power spent for signal processing should not be underestimated), and the receiver algorithm complexity. These are also parameters that influence the system design.

CHAPTER 7

System Level Analysis with Uninformed Transmitter

Contents

In this chapter system level performance of MU-/SU-DCF is analyzed, in particular saturation throughput, fair medium access provision and delay characteristic. Special attention is payed to the difference in performance of SU and MU transmission policies. Also, the impact of the traffic characteristic on the system level performace is studied.

Throughout this chapter, a 4×4 antenna configuration is assumed. The transmitter does not have the channel informations, hence channel adaptation is not applied and MIMO scheme as well as the PHY mode are fixed. The purpose of this evaluation is to estimate the behavior, characteristics and performance limits without taking into account the effect of radio propagation; afterwards, in Chapter 8, the impact of an error prone channel is studied. Parts of this chapter have been published in [Mirkovic and Walke, 2008b].

7.1 MIMO Frame Structure

As introduced in Chapter 5, MIMO frame refers to a set of data packets that are simultaneously transmitted over multiple antennas. The number of ACK frames that are following data transmission depends on the number of distinct receivers of the MIMO frame d. If only SU transmission is allowed, the number of distinct receivers is one, and the frame exchange has always the same structure. If MU transmissions are allowed, then the frame exchange has an unsteady structure. The number of distinct receivers d of a MIMO frame depends on the number of established connections, but also on the traffic type.

7.1.1 Load Generators

In this analysis load generators with the following packet interarrival time distributions are analyzed:

- constant packet interarrival time,
- exponential distribution of packet interarrival time, with the following PDF:
$$f_{\exp,X}(x,\lambda) = \begin{cases} \lambda e^{-\lambda x} & \text{, if} \quad x \geq 0 \\ 0 & \text{, if} \quad x < 0 \end{cases}, \tag{7.1}$$
  where λ is the rate parameter;
- hyper-exponential distribution with Coefficient of Variation (CoV) $cv = 2$ and 5.

Hyper-exponentially distributed variable X has the following PDF:

$$f_{\text{hyper-exp},X} = \sum_{i=1}^{n} p_i f_{\exp,Y_i}(y,\lambda_i), \tag{7.2}$$

where Y_i is an exponentially distributed random variable with rate λ_i, and p_i is the probability that X will take the form of the exponential distribution i. In this work, two-phase hyper-exponential distributions are applied, with parameters (rate parameters λ_0 and λ_1, and the probabilities

p_0 and p_1) obtained using the following equations [Law and Kelton, 2000]:

$$p_1 = \frac{1}{2}\left[1 + \sqrt{\frac{cv^2 - 1}{cv^2 + 1}}\right], \tag{7.3}$$

$$p_0 = 1 - p_1, \tag{7.4}$$

$$\lambda_0 = 2p_0\lambda_b, \tag{7.5}$$

$$\lambda_1 = 2p_1\lambda_b, \tag{7.6}$$

where λ_b is the scaling rate parameter that can be used to change the rate of the hyper-exponential distribution.

For this analysis only the order of packets in the presence of multiple connections is relevant, and not the absolute rate, hence the scaling rate parameter λ_b can be set to any value. With $\lambda_b = 1$, the parameters take following values:

$$cv = 2: \qquad p_0 = 0.112702, \qquad p_1 = 0.887298,$$

$$\lambda_0 = 0.225403, \qquad \lambda_1 = 1.7746; \tag{7.7}$$

$$cv = 5: \qquad p_0 = 0.0196155, \qquad p_1 = 0.980384,$$

$$\lambda_0 = 0.0392311, \qquad \lambda_1 = 1.96077. \tag{7.8}$$

7.1.2 Distinct Receivers of a MIMO Frame

An AP that establishes a number of (downlink) connections to its stations is observed. All the connections are characterized by the same packet size and packet interarrival time distribution. It is assumed that all generated packets from all the connections have the same priority, and therefore they are transmitted following global FIFO order.

In Figure 7.1 the number of distinct receivers d of a MIMO frame of size 4 is plotted vs. number of established connections for different traffic types, characterized by different distributions of packet interarrival time.

Constant Packet Interarrival Time

In case of constant packet interarrival time, the MIMO frame structure is deterministic and repeats in cycles, because the packets from different

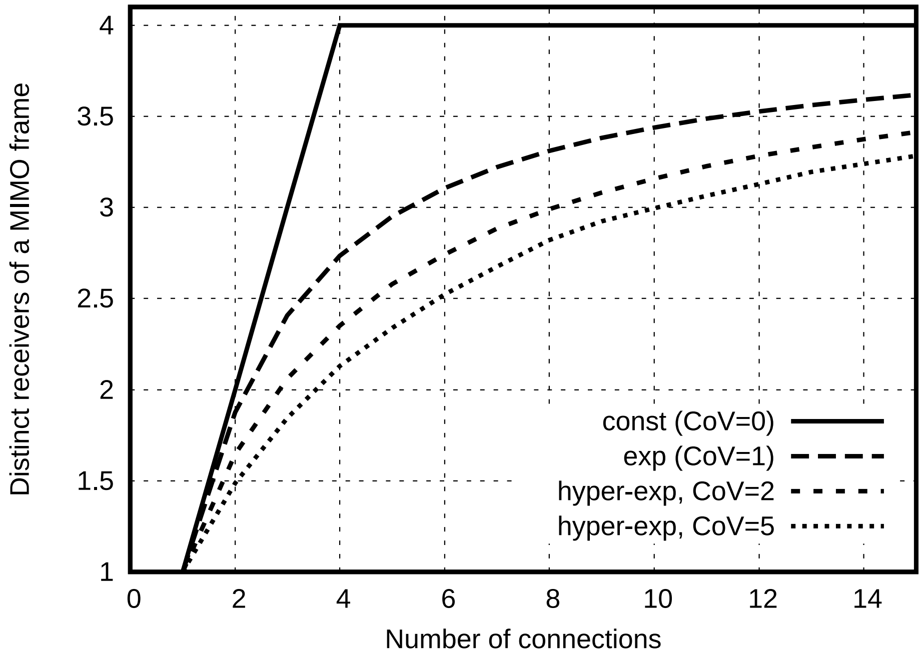

Figure 7.1: Number of distinct receivers of a MIMO frame of size 4 for different traffic types

sources always appear in the same order in the data queue. When the number of connections is less than 4, some receivers will be addressed more then once within a MIMO frame. As soon as the number of connection becomes greater or equal 4, the AP will operate in pure MU mode. Mathematically formulated, the number of different receivers d takes the following value:

$$\mathtt{E}[d] = \min(n-1, 4) = \min(m, 4), \tag{7.9}$$

where $\mathtt{E}[\cdot]$ stands for expectation, n is the number of stations in the system, and $m = n - 1$ is the number of established connections.

Poisson Load - Exponential Distribution of Packet Interarrival Time

In case of Poisson load, since the packet interarrival time is a random variable with exponential distribution, the order of packets in the queue is not deterministic. The traffic is more bursty, thus also with a large number of connections the probability of pure MU operation is not 1. Therefore, the probabilities of different MIMO frame structures have to be considered.

The probability of the event that the MIMO frame contains packets for i distinct receivers is given by the following equations:

$$P_{(d=1)} = \binom{m}{1} \frac{4!/4!}{m^4}; \tag{7.10}$$

$$P_{(d=2)} = \binom{m}{2} \frac{4!/1!\cdot 3! + 4!/2!\cdot 2! + 4!/3!\cdot 1!}{m^4}; \tag{7.11}$$

$$P_{(d=3)} = \binom{m}{3} \frac{4!/1!\cdot 1!\cdot 2! + 4!/1!\cdot 2!\cdot 1! + 4!/2!\cdot 1!\cdot 1!}{m^4}; \tag{7.12}$$

$$P_{(d=4)} = \binom{m}{4} \frac{4!/1!\cdot 1!\cdot 1!\cdot 1!}{m^4}; \tag{7.13}$$

$$P_{(d>4)} = 0. \tag{7.14}$$

The binomial coefficients in previous equations account for the number of different ways to select d different receivers out of $m = n-1$ possible ones. Given the number of connection m, the probability that the Head-of-Line (HoL) is addressed to a specific receiver is $\frac{1}{m}$, owing to the memoryless property of the exponential distribution. Therefore the division by factor m^4.

All the permutations should be counted (numerators), but taking into account that the permutations of packets differ only if the particular receivers differ, independently of the frame sequence number; the denominators of the "small" fractions in numerators account for this effect.

With the convention that $\binom{n}{k} = 0$, if $n < k$, the above formulas apply for $m < 4$ as well.

Using the probability mass function $P_{(d)}$, the average number of distinct receivers is calculated with the following formula:

$$\mathtt{E}[d] = \sum_{i=1}^{4} i P_{(d=i)}. \tag{7.15}$$

The average number of distinct receivers $\mathtt{E}[d]$ when assuming Poisson load has been plotted in Figure 7.1. Independently of the number of connections, the average number of distinct receivers in case of Poisson load is always smaller than that of constant packet interarrival time, but asymptotically approaches that value. Although the traffic is bursty, d increases with the number of stations, since in that case the probability that the bursts happen simultaneously and get mixed in the data queue grows.

Hyper-Exponential Distribution of Packet Interarrival Time

The number of distinct receivers of a MIMO frame for the traffic with hyper-exponential distribution of interarrival time has been obtained by simulation. Data packets from a number of connections are generated with the packet interarrival time distribution parameters given by Equ. (7.7) and (7.8). The packets are put into a global FIFO queue and combined into MIMO frames.

The average number of distinct receivers is further reduced, since d decreases as the CoV grows. Therefore d has the highest value with constant packet interarrival time, decreases under Poisson load ($cv = 1$), and decreases even more under load with hyperexponentially distributed interarrival times.

As the traffic becomes more bursty, the AP is more likely to operate in SU mode. This reduces the duration of the transmission window because the signaling overhead is smaller (particularly if TDMA is used for signaling), but it may also deteriorate the delay characteristic, as shown in the following sections of this chapter.

7.1.3 Overhead estimation

In the description of MU-DCF frame exchange in Section 5.2.2, it was noted that, compared to SU-DCF, MU-DCF experiences higher overhead, that increases with the number of stations involved in the MIMO frame transfer. Using OFDMA instead of TDMA for simultaneous transmission of control frames is a means for decreasing this overhead. In this section the overhead evaluation of these two approaches is done.

The overhead is illustrated on an example with a transmitting station with 4 connections. For each connection, 4 packets are generated at the same time and put into the data queue. All the stations have 4 antennas, and 4×4 multiplexing is applied. The time needed to transmit these packets without taking backoff duration into account is the following:

- SU approach – each MIMO frame consists of the packets for one receiver only:

$$\begin{aligned} T_{\mathrm{SU}} = 4 \cdot (T_{\mathrm{DIFS}} + T_{\mathrm{M\text{-}RTS}_1} + T_{\mathrm{SIFS}} + T_{\mathrm{M\text{-}CTS}} + \\ T_{\mathrm{SIFS}} + T_{\mathrm{Data}} + T_{\mathrm{SIFS}} + T_{\mathrm{M\text{-}ACK}}) \end{aligned} \tag{7.16}$$

- MU approach – each MIMO frame consists of one packet for each receiver:

$$\begin{aligned} T_{\mathrm{MU}} = 4 \cdot (T_{\mathrm{DIFS}} + T_{\mathrm{M\text{-}RTS}_4} + 4 \cdot (T_{\mathrm{SIFS}} + T_{\mathrm{M\text{-}CTS}}) + \\ T_{\mathrm{SIFS}} + T_{\mathrm{Data}} + 4 \cdot (T_{\mathrm{SIFS}} + T_{\mathrm{M\text{-}ACK}})) \end{aligned} \tag{7.17}$$

The transmission clearly lasts longer in the MU case than in SU case. However, unlike with MU, with SU the average delay a station experiences depends on the position of the station's packets in the queue: the station that is last to receive its packets, experiences the longest delay. For some stations such long delay might not be acceptable; particularly if between these transmissions other stations of the network occupy the channel. With MU transmission all the stations experience the same average delay.

In the previous analysis, it was assumed that at the frame start all the four packets addressed to the four stations were already generated. When that is not the case, in SU case the transmitter has to wait at least as long as in MU case for enough packets to be generated for the defined MIMO frame length. Particularly in case of applications with low offered load and high delay sensitivity, this waiting time may easily exceed the packet lifetime. Otherwise, sending immediately what is present in the queue in the SU mode might often mean transmitting a single spatial stream, which effectively means increasing the overhead. Last but not least, in case of light load, MU transmission will improve the delay characteristic.

Since most of the overhead introduced by the MU signaling comes from SIFS durations between each two consecutive frames and from preambles, using OFDMA to transmit M-CTS and M-ACK frames instead of using Time Division Multiple Access (TDMA) might be beneficial, since then

SIFS for different stations before accessing the channel runs in parallel, and at the same time the duration of the control frames is not increased linearly. In MIMO systems it is also possible to apply spatially multiplexing, but since no channel knowledge at the transmitter is assumed in this Chapter it would require some blind multiuser detection; however for control frames a robust channel is very important. Another option would be acquiring the channel knowledge, but that might take more resources than transmitting M-CTS and M-ACK frames themselves using TDMA.

In an OFDM system (which is assumed in this work), using OFDMA to transmit M-CTS and M-ACK frames would require good synchronization among stations and it would bring smallest increase of system complexity (compared to other multiple access schemes such as Code Division Multiple Access (CDMA) or Multi-Carrier Code Division Multiple Access (MC-CDMA) that would have similar effect on the protocol performance).

By using $\lfloor N_s/m \rfloor$ subcarriersto form a subchannel, where N_s is the number of available subcarriers in OFDMA, M-CTS and M-ACK are less than m times longer compared to the case of using all the available subcarriers. The reason is that these frames do not carry much information, and their major part is the preamble on PHY layer. Duration of M-CTS (without the CSI field) is illustrated in Figure 7.2 for different PHY modes when the number of parallel stations is 1, 4 and 10. It can be seen that particularly with higher PHY modes the described effect applies: e.g. at 6 Mb/s M-CTS frame lasts 44 μs when transmitted by a station using the whole channel, and 244 μs when transmitted with 9 other stations in parallel; at 54 Mb/s these durations are 24 μs and 48 μs respectively.

Times $T^{\text{TDMA}}_{\text{M-CTS},m}$ and $T^{\text{OFDMA}}_{\text{M-CTS},m}$ needed to transmit m M-CTS frames in TDMA and in OFDMA is given by the following expressions:

$$T^{\text{TDMA}}_{\text{M-CTS}_m} = m \cdot \left(T_{\text{M-CTS}_1} + T_{\text{SIFS}}\right), \tag{7.18}$$

$$T^{\text{OFDMA}}_{\text{M-CTS}_m} = T_{\text{M-CTS}_m} + T_{\text{SIFS}}, \tag{7.19}$$

where $T_{\text{M-CTS}_m}$ is the time needed to transmit an M-CTS frame using $\lfloor 1/m \rfloor$. With each additional station the overhead is introduced not only by the duration of the M-CTS frame, but also by the duration of SIFS.

In Figure 7.3 overhead introduced with TDMA and OFDMA signaling

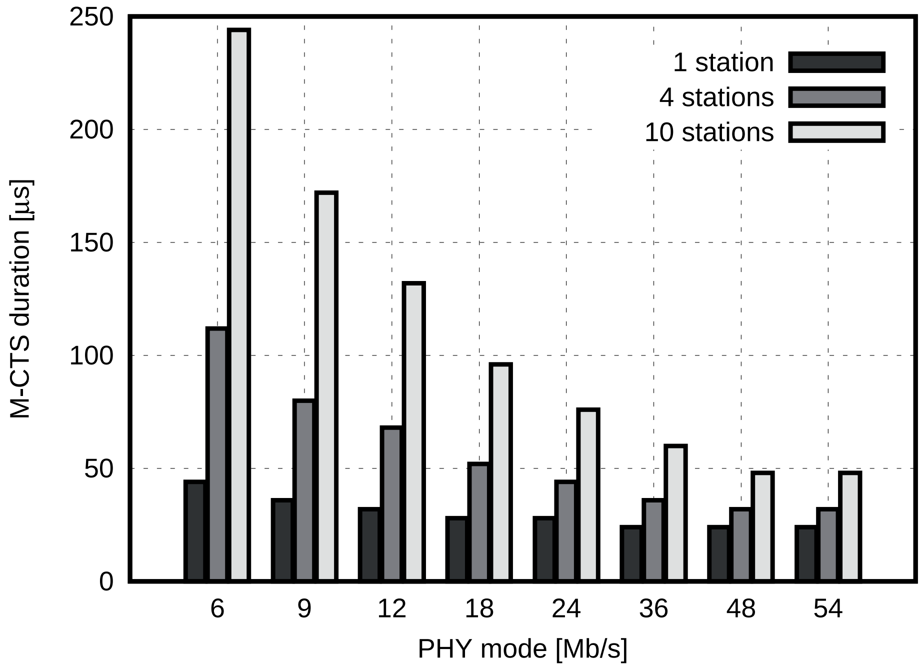

Figure 7.2: Duration of M-CTS frame at different PHY modes with one station occupying the whole channel, and sharing it with another 3 and 9 stations

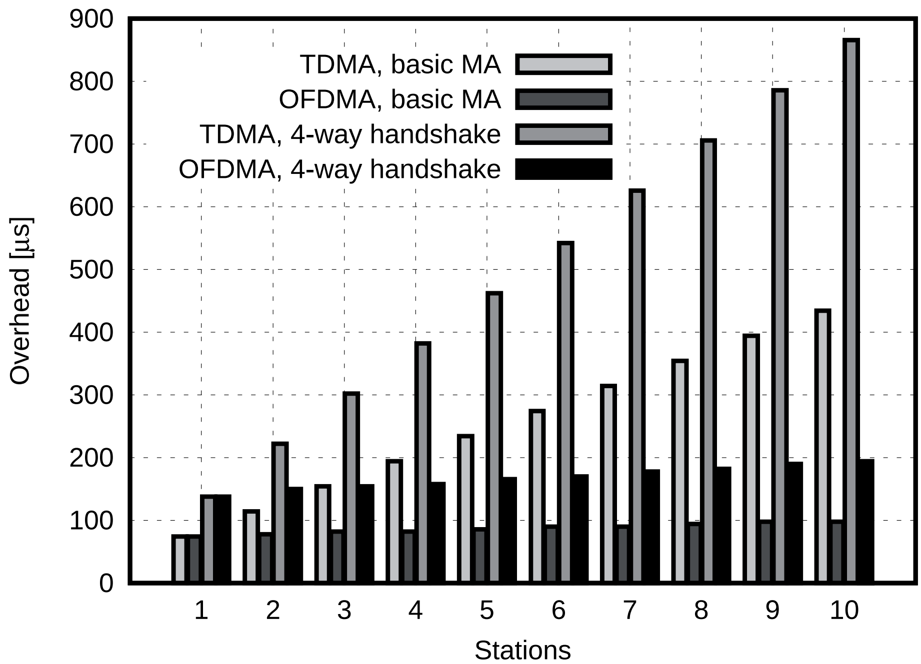

Figure 7.3: Overhead produced by TDMA and OFDMA based signaling

is presented in case of basic medium access and when using M-RTS/M-CTS. It takes into account the control frames duration, as well as the necessary IFSs, but not the backoff interval. M-CTS does not include the CSI feedback, while M-ACK includes 2 byte for selective acknowledgment bitmap.

The figure illustrates faster growth of the overhead in case of TDMA signaling – from 74 μs with 1 station to 434 μs with 10 stations (with basic medium access). When applying OFDMA signaling the overhead changes from 74 μs to 98 μs respectively. This makes TDMA practically unusable for this type of transferring data packets, at least when the number of multiusers is high, since it limits the network capacity, as shown in the next section. However, OFDMA also has a drawback of increased system complexity, in particular achieving the synchronization among stations.

7.2 Throughput Study

IEEE 802.11 networks tend to become unstable as the offered load grows: the carried load follows the growing offered load up to the maximum throughput, and afterwards declines, because of increasing number of collisions, which consequently impacts the average duration of the exponential backoff procedure. This behavior has been widely investigated, see e.g. [Ziouva and Antonakopoulos, 2002, Bianchi, 1998]. In [Bianchi, 2000] Bianchi proposed a simple and accurate model based on two-dimensional Markov chains for performance analysis of IEEE 802.11 networks in saturation. An alternative derivation together with the correction of the model was presented in [Bianchi and Tinnirello, 2005].

This section has the following structure: in the first part, the main results of the analysis published in [Bianchi and Tinnirello, 2005] are presented, since they are used for the analysis of the MIMO supporting version of the system, SU-DCF and MU-DCF, as presented in the second part of this section.

7.2.1 Throughput Analysis of IEEE 802.11 DCF in Saturation

Throughout the analysis, ideal channel conditions are assumed: i.e. erroneous frame receptions happen only as a consequence of collision of multiple frames, and not because of low SNR. A fixed number of stations

n is assumed, whose data queues are never empty. All the stations can hear each other, thus hidden and exposed station problems do not occur.

A discrete integer time scale is adopted, where t and $t+1$ correspond to the beginning of two consecutive time slots. The backoff time counter $b(t)$ is decremented at the beginning of each time slot. These virtual time slots do not correspond to slot durations defined by standard. Also, the adopted time scale does not correspond to the real time. Since the backoff time counter is stopped when the channel is sensed busy, the time slot of the discrete time scale used can cover the duration of several consecutive transmissions, and contains an additional idle backoff slot at the end of a transmission or collision.

The key approximation that enables the modeling is the assumption of constant and independent collision probability p of a packet transmitted by each station, regardless of the number of retransmissions already suffered. This assumption becomes more accurate for a large number of stations in the network [Bianchi and Tinnirello, 2005].

The following notation is adopted:

- $CW_0 = CW_{\min} - 1$, where $CW_{\min}$ is the minimum contention window size,
- $i = 1 \cdots R$ is a backoff stage, which is a number of retransmission suffered by HoL packet,
- $CW_i = \min(2^i \cdot (CW_0 + 1) - 1, CW_{\max})$, $i = 1 \cdots R$,
- b_0, b_1, etc. are random variables drawn from intervals $(0, CW_0)$, $(1, CW_1)$, etc.

Probability of Transmission τ

If `TX` is the event that a station is transmitting a frame during a time slot, and `s=i` the event that the station is found in backoff stage i, $i = 0 \cdots R$, according to Bayes theorem, it applies:

$$P(\texttt{TX})\frac{P(\texttt{s=i}|\texttt{TX})}{P(\texttt{TX}|\texttt{s=i})} = P(\texttt{s=i}),\ i = 0 \cdots R. \tag{7.20}$$

Summing the previous expression for $i = 0 \cdots R$, it follows:

$$P(\texttt{TX}) \sum_{i=0}^{R} \frac{P(\texttt{s=i}|\texttt{TX})}{P(\texttt{TX}|\texttt{s=i})} = \sum_{i=0}^{R} P(\texttt{s=i}) = 1. \tag{7.21}$$

Therefore, τ can be expressed as a function of $P(\texttt{s=i}|\texttt{TX})$ and $P(\texttt{TX}|\texttt{s=i})$:

$$\tau = P(\texttt{TX}) = \frac{1}{\sum_{i=0}^{R} \frac{P(\texttt{s=i}|\texttt{TX})}{P(\texttt{TX}|\texttt{s=i})}}. \tag{7.22}$$

In the following, the conditional probabilities $P(\texttt{s=i}|\texttt{TX})$ and $P(\texttt{TX}|\texttt{s=i})$ are derived.

- The conditional probability $P(\texttt{s=i}|\texttt{TX})$ is the probability that the station that is transmitting is found in stage i. This probability is the steady-state distribution of a discrete time Markov chain $s(k)$ that describes the evolution of the backoff stage during the stations transmission instants k. Non-null one-step transition probabilities of this Markov chain are:

$$P(s(k+1) = i|s(k) = i-1) = p, \qquad i = 1 \cdots R, \tag{7.23}$$

$$P(s(k+1) = 0|s(k) = i) = 1-p, \qquad i = 0 \cdots R-1, \tag{7.24}$$

$$P(s(k+1) = 0|s(k) = R) = 1, \tag{7.25}$$

  where p is the constant and independent collision probability of a packet transmitted by each station. It immediately follows:

$$P(\texttt{s=i}|\texttt{TX}) = \frac{(1-p)p^i}{1-p^{R+1}}, \qquad i = 0 \cdots R. \tag{7.26}$$

- The conditional transmission probability $P(\texttt{TX}|\texttt{s=i})$ is the probability that a station transmits in backoff stage i. It can be computed by dividing the average number of slots spent for other's transmissions in a transmission cycle (with the adopted time scale exactly 1 slot), with the average number of slots spent by the station during the whole cycle:

$$P(\texttt{TX}|\texttt{s=i}) = \frac{1}{1+\texttt{E}[b_i]}, \qquad\qquad i = 0\cdots R, \tag{7.27}$$

where $\texttt{E}[b_i]$ is the average backoff counter in the backoff stage i.

Applying these results, the formula for τ is as follows:

$$\begin{aligned}\tau &= \frac{1}{\sum_{i=0}^{R} \frac{1-p}{1-p^{R+1}} p^i (1+\texttt{E}[b_i])} \\ &= \frac{1}{1+\frac{1-p}{1-p^{R+1}}\sum_{i=0}^{R} p^i \texttt{E}[b_i]}.\end{aligned} \tag{7.28}$$

Conditional Collision Probability p

The conditional collision probability p can be expressed as the probability that at least one of the $n-1$ remaining stations transmits. At steady state, each remaining station transmits a packet with probability τ, thus it applies:

$$p = 1-(1-\tau)^{n-1}. \tag{7.29}$$

Equ. (7.28) and (7.29) form a system of equations with the two unknowns τ and p that can be solved by numerical methods.

Saturation Throughput

The saturation throughput S is calculated as the fraction of time the channel is used to successfully transmit payload bits:

$$S = \frac{\text{payload}}{\text{slot duration}}. \tag{7.30}$$

Since all the stations contend for the channel and transmit with the probability τ, the probability P_{tr} that there is at least one transmission in the considered slot time is given by:

$$P_{tr} = 1 - (1 - \tau)^n. \tag{7.31}$$

The probability that a transmission occurring on the channel is successful is given by the probability that exactly one station transmits on the channel, if at least one station transmits:

$$P_s = \frac{n\tau(1 - \tau)^{n-1}}{P_{tr}}. \tag{7.32}$$

Using these results, the saturation throughput can be expressed as:

$$S = \frac{P_s P_{tr} \mathtt{E}[P]'}{(1 - P_{tr})\sigma + P_{tr} P_s T_s' + P_{tr}(1 - P_s)T_c'}, \tag{7.33}$$

where σ is the backoff slot duration. $\mathtt{E}[P]'$ is the average amount of payload bits transmitted in a transmission slot, and T_s' and T_c' are the average durations of successful transmission slot and collision slot:

$$\mathtt{E}[P]' = \mathtt{E}[P] + \sum_{i=1}^{\infty} B_0^i \mathtt{E}[P] = \frac{\mathtt{E}[P]}{1 - B_0}, \tag{7.34}$$

$$T_s' = T_s + \sum_{i=1}^{\infty} B_0^i T_s + \sigma = \frac{T_s}{1 - B_0} + \sigma, \tag{7.35}$$

$$T_c' = T_c + \sigma. \tag{7.36}$$

In the previous expressions $\mathtt{E}[P]$ is the average payload size, and T_s and T_c are given with the following formulas:

$$T_s = T_{\mathrm{Data}} + T_{\mathrm{SIFS}} + T_{\mathrm{ACK}} + T_{\mathrm{DIFS}} \tag{7.37}$$

$$T_c = T_{\mathrm{Data}}^* + T_{\mathrm{EIFS}}, \tag{7.38}$$

for basic medium access (* stands for the longest packet involved in the collision), whereas for the four-way channel access the following applies:

$$T_s = T_{\mathrm{RTS}} + T_{\mathrm{SIFS}} + T_{\mathrm{CTS}} + T_{\mathrm{SIFS}} \\ + T_{\mathrm{Data}} + T_{\mathrm{SIFS}} + T_{\mathrm{ACK}} + T_{\mathrm{DIFS}} \quad (7.39)$$

$$T_c = T_{\mathrm{RTS}} + T_{\mathrm{EIFS}}. \quad (7.40)$$

7.2.2 Throughput Analysis of SU-DCF and MU-DCF in Saturation

In this section comparative analysis of the saturation throughput for the following systems is presented:

- standard IEEE 802.11 DCF (SISO),
- SU-DCF (SU-MIMO), and
- MU-DCF (MU-MIMO), with both TDMA and OFDMA based signaling.

Both basic medium access and four-way handshake are considered. The influence of traffic characteristic is considered by examining network performance for constant packet interarrival time and for offered load with exponential and hyper-exponential distribution of packet interarrival time at stations, with varying CoV.

The following two scenarios, presented in Figure 7.4 are studied, both having the number of stations n as a parameter:

1. AP scenario is presented in Figure 7.4(a) for $n = 6$. Only one station in the network, `STA0`, is transmitting, and it has $m = n - 1 = 5$ unidirectional (downlink) connections with all the other stations in the network. This scenario is used to study the saturation throughput of different MIMO transmission strategies, without taking into account the impact of the medium access procedure.
2. Mesh scenario, presented in Figure 7.4(b) is a fully interconnected mesh: each station establishes connections with all the other stations in the network. In the throughput study, the effects of the medium access procedure on the protocols can be seen.

In both scenarios all the stations can hear each other, thus hidden and exposed station problem do not occur.

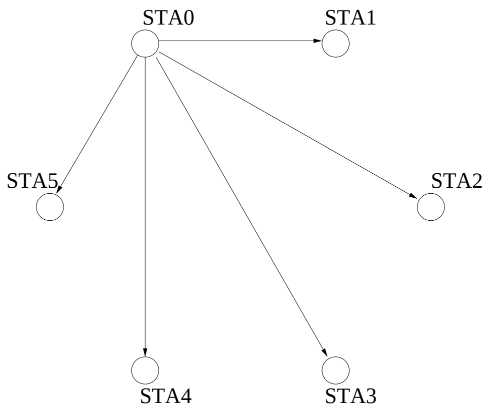

(a) AP scenario

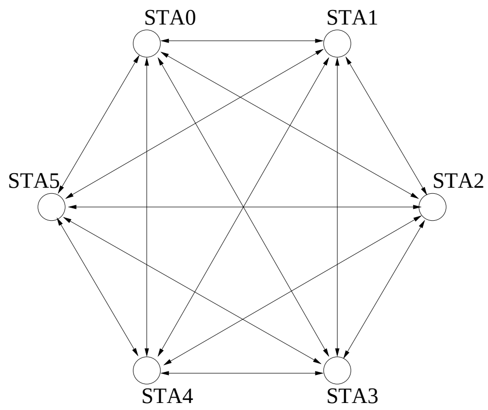

(b) Mesh scenario

Figure 7.4: Analyzed scenarios for the saturation throughput study

In all the cases, all the connections have the same constant data packet size (1024 byte), the same intensity of the offered load, as well as the same distribution of packet interarrival time at stations. Stations' data queues are at all times nonempty, more specific, in the data queue there is at least one packet in DCF, at least four packets for the receiver whose packet is the HoL in SU-DCF, and in MU-DCF at least four packets, independently of their destination.

It is assumed that the channel is not error prone, i.e. erroneous frame receptions happen only as a consequence of collision of multiple frames. Thus, erroneous receptions can happen only in mesh cenario. The discrete integer time scale is adopted as described in [Bianchi and Tinnirello, 2005], which is used as a starting point for the analysis.

AP Scenario

As already mentioned, AP scenario presents a set of $m = n - 1$ downlink connections of an AP, denoted by `STA0`. In Figure 7.5, the saturation throughput at `STA0` vs. the number of stations n in AP scenario is presented.

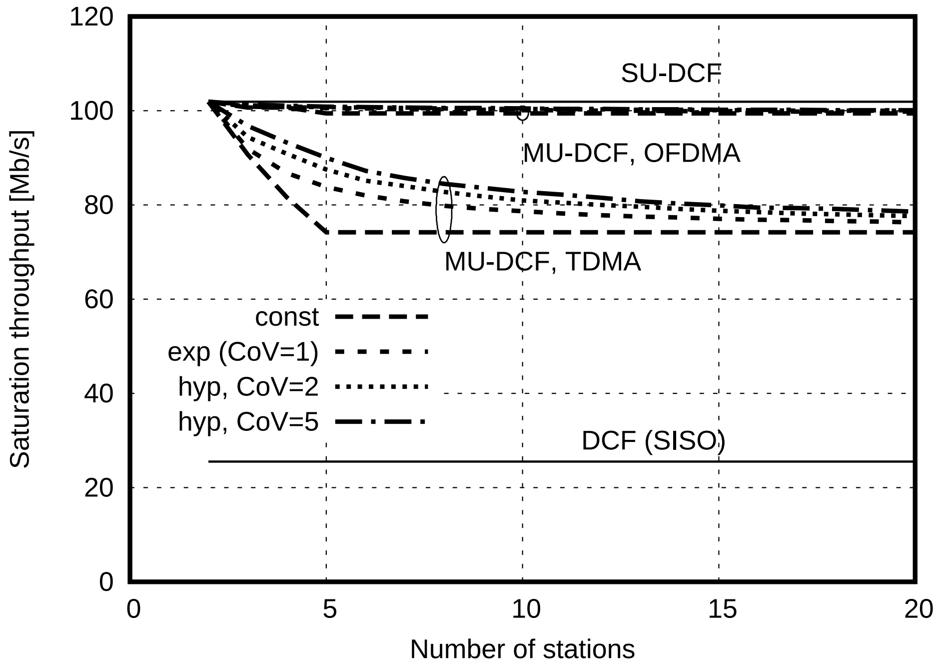

Figure 7.5: Saturation throughput: AP scenario with basic medium access

IEEE 802.11 DCF

In DCF system, the saturation throughput $S_{\mathrm{AP}}^{\mathrm{DCF}}$ can be easily calculated as the ratio of the average data packet length and the duration of the transmission window T_s^{DCF} increased by the average duration of the backoff countdown. The notation from [Bianchi and Tinnirello, 2005, Bianchi, 2000] has been adopted, hence s in subscript stands for successful transmission and c in subscript denotes a collision:

$$S_{\mathrm{AP}}^{\mathrm{DCF}} = \frac{\mathtt{E}[P]}{\frac{\mathrm{CW_{min}}}{2}\sigma + T_s^{\mathrm{DCF}}} \tag{7.41}$$

$$T_s^{\mathrm{DCF}} = T_{\mathrm{DIFS}} + \mathtt{E}\left[T_{\mathrm{data}}\right] + T_{\mathrm{SIFS}} + T_{\mathrm{ACK}} \tag{7.42}$$

In the previous equations P stands for the data packet length, $\mathrm{CW_{min}}$ is the starting - minimum CW size, and σ is the slot duration. For the PHY parameters and data packet length, the saturation throughput takes the following value:

$$S_{\mathrm{AP}}^{\mathrm{DCF}} = 25.48\,{}^{Mbit}/_{s} \tag{7.43}$$

SU-DCF

In SU-DCF system, assuming a separate FIFO queue for each connection, the transmitting station takes 4 packets from the data queue whose HoL has the longest delay and puts them into a MIMO frame. Four data streams are transmitted simultaneously, and the duration of the transmission window depends on the time needed for the longest packet out of four to be transmitted:

$$S_{\mathrm{AP}}^{\mathrm{SU}} = \frac{4 \cdot \mathtt{E}[P]}{\frac{\mathrm{CW}_{\min}}{2}\sigma + T_s^{\mathrm{SU}}} \tag{7.44}$$

$$T_s^{\mathrm{SU}} = T_{\mathrm{DIFS}} + \mathtt{E}\left[max_4\{T_{\mathrm{data}}\}\right] + T_{\mathrm{SIFS}} + T_{\mathrm{M\text{-}ACK}} \tag{7.45}$$

In the analyzed example, the data packet length is assumed constant (1024 byte), and the saturation throughput has the following value:

$$T_s^{\mathrm{SU}} = 101.92\, {}^{Mbit}\!/_{s}. \tag{7.46}$$

For the two cases analyzed up to now, the throughput neither depends on the number of stations, nor on the traffic type (which determines the order of packets in the data queue), since the transmission window has fixed structure, and therefore has constant duration; this is not the case with MU-DCF, analyzed in the following.

MU-DCF

Duration of a transmission window in MU-DCF depends on how many distinct receivers are addressed in the transmitted MIMO frame. Assuming that the MIMO frames are generated from the data queue obeying the FIFO order, the number of distinct receivers depends on the number of stations in the network, as well as on the distribution of the packet interarrival time for each connection. In Figure 7.1 the number of distinct receivers vs. number of connections is plotted for different traffic load types. Similarly to the calculation of $\mathtt{E}[d]$, Equ. (7.15) in Section 7.1, the calculation of the expected duration of transmission window can be done:

$$\mathtt{E}\left[T_s^{\mathrm{MU}}\right] = \sum_{i=1}^{4} P_{(d=i)} \cdot T_{s,i}^{\mathrm{MU}} \tag{7.47}$$

where $T_{s,i}^{\mathrm{MU}}$ is the duration of the transmission window when the number of distinct receivers $d = i$. This value depends on the type of signaling (TDMA or OFDMA based):

$$T_{s,i}^{\mathrm{MU_{TDMA}}} = T_{\mathrm{DIFS}} + \mathtt{E}\left[max_4\{T_{\mathrm{data}}\}\right] + i \cdot (T_{\mathrm{SIFS}} + T_{\mathrm{M\text{-}ACK}}), \tag{7.48}$$

$$T_{s,i}^{\mathrm{MU_{OFDMA}}} = T_{\mathrm{DIFS}} + \mathtt{E}\left[max_4\{T_{\mathrm{data}}\}\right] + T_{\mathrm{SIFS}} + T_{\mathrm{M\text{-}ACK}_i}, \tag{7.49}$$

where $T_{\mathrm{M\text{-}ACK}_i}$ is the time needed for i M-ACK frames to be transmitted over the channel in parallel using $\lfloor \frac{N_s}{i} \rfloor$, where N_s is the number of the available subcarriers. Finally, the saturation throughput is given by the following expression:

$$S_{\mathrm{AP}}^{\mathrm{MU}} = \frac{4 \cdot \mathtt{E}[P]}{\frac{\mathrm{CW_{min}}}{2}\sigma + \mathtt{E}\left[T_s^{\mathrm{MU}}\right]} \tag{7.50}$$

From Equ. (7.47) and (7.50) it can be seen that the saturation throughput in MU-DCF is not a constant value, unlike that of DCF and SU-DCF, but it depends on the traffic type, which determines the probability mass function $P_{(d)}$.

In order to evaluate the performance of the protocol with different levels of the traffic burstiness, the traffic sources with constant packet interarrival time, exponential, and hyper-exponential distribution of packet interarrival time at stations are studied. For constant and exponentially distributed packet interarrival time, the results for the probability mass function $P_d(i)$ obtained in Section 7.1 are used. Since hyper-exponential distribution is different from the exponential distribution in that it has a memory, the results for this case have been obtained by simulating the packet arrival time of individual sources, and measuring the probability of different transmission window realizations. Two-phase hyper-exponential distributions have been considered, with CoV 2 and 5.

SU system performance gives the upper bound (Equ. (7.46)), and the

MU-DCF under constant packet interarrival time gives the lower bound for the saturation throughput:

$$S_{\mathrm{AP,\,min}}^{\mathrm{MU_{TDMA}}}(n-1)|n-1 \geq 4 = 74.22\,{}^{Mbit}\!/_{s}, \tag{7.51}$$

in case of TDMA signaling, and

$$S_{\mathrm{AP,\,min}}^{\mathrm{MU_{OFDMA}}}(n-1)|n-1 \geq 4 = 99.45\,{}^{Mbit}\!/_{s}, \tag{7.52}$$

in case of OFDMA signaling; this is also illustrated in Figure 7.5. It is interesting to compare these values with the saturation throughput of the SU-DCF from Equ. (7.46) and note that using TDMA in MU-DCF significantly deteriorates saturation throughput, in contrast to OFDMA based signaling.

Another observation that can be made is that as the number of stations in the network grows, MU systems' saturation throughput decreases. When the traffic becomes more bursty, the number of distinct receivers of MIMO frames is on average smaller, therefore the transmission window duration becomes shorter and the saturation throughput increases. Since the overhead when transmitting different MIMO frames produced by OFDMA signaling has smaller variance than that of TDMA signaling, the level of saturation throughput when applying OFDMA signaling is much less sensitive to the traffic characteristic.

The saturation throughput levels of the analyzed MIMO systems are mutually equal only when there are only two stations in the network, hence only one connection is present then, and this value corresponds to the SU saturation throughput.

Four-Way Handshake

In Figure 7.6 the saturation throughput for the AP scenario is presented when four-way handshake is used for the channel access. Since in AP scenario no collisions are present, RTS/CTS frame exchange just introduces the additional overhead, given by following expressions:

$$\Delta T_s^{\mathrm{DCF}} = T_{\mathrm{RTS}} + T_{\mathrm{SIFS}} + T_{\mathrm{CTS}} + T_{\mathrm{SIFS}}, \tag{7.53}$$

$$\Delta T_s^{\mathrm{SU}} = T_{\mathrm{M\text{-}RTS}_1} + T_{\mathrm{SIFS}} + T_{\mathrm{M\text{-}CTS}} + T_{\mathrm{SIFS}}, \tag{7.54}$$

$$\Delta T_{s,i}^{\mathrm{MU_{TDMA}}} = T_{\mathrm{M\text{-}RTS}_i} + T_{\mathrm{SIFS}} + i \cdot (T_{\mathrm{M\text{-}CTS}} + T_{\mathrm{SIFS}}), \tag{7.55}$$

$$\Delta T_{s,i}^{\mathrm{MU_{OFDMA}}} = T_{\mathrm{M\text{-}RTS}_i} + T_{\mathrm{SIFS}} + T_{\mathrm{M\text{-}CTS}_i} + T_{\mathrm{SIFS}}, \tag{7.56}$$

where $T_{\mathrm{M\text{-}CTS}_i}$ is the time needed for i M-CTS frames to be transmitted over the channel in parallel using OFDMA.

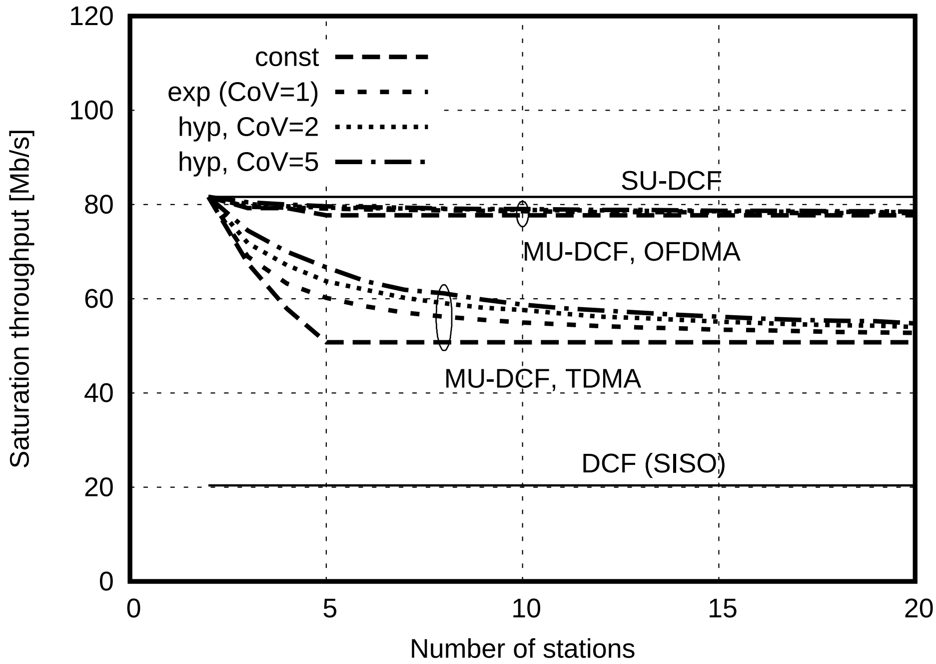

Figure 7.6: Saturation throughput: AP scenario with four-way handshake

The conclusions made for the basic medium access in AP scenario apply for this as well.

Mesh Scenario

Basic Medium Access

For the analysis of the saturation throughput in a fully interconnected network, the model for IEEE 802.11 DCF networks described in Section 7.2.1 has been modified for the calculation of the saturation throughput of the

MIMO systems. The results for the basic medium access are plotted in Figure 7.7.

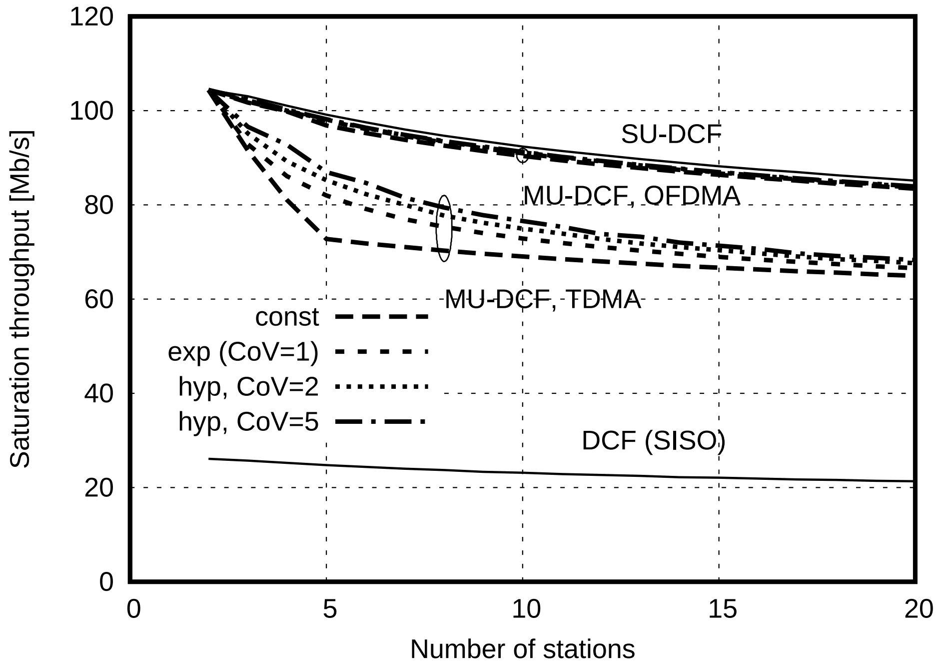

Figure 7.7: Saturation throughput: mesh scenario with basic medium access

The saturation throughput $S_{\text{mesh}}^{\text{DCF}}$ is given by the following expression:

$$S_{\text{mesh}}^{\text{DCF}} = \frac{P_s P_{tr} E\left[P\right]'}{\left(1 - P_{tr}\right)\sigma + P_{tr} P_s T_s'^{\text{DCF}} + P_{tr}\left(1 - P_s\right) T_c'^{\text{DCF}}}, \tag{7.57}$$

where $T_s'^{\text{DCF}}$ and $T_c'^{\text{DCF}}$ are the average durations of successfull transmission slot and collision slot and are equal to T_s' and T_c' given in Equ. (7.35) and (7.36). Due to the changed notation, the expressions are repeated:

$$T_s'^{\text{DCF}} = T_s^{\text{DCF}} + \sum_{i=1}^{\infty} B_0^k T_s^{\text{DCF}} + \sigma = \frac{T_s^{\text{DCF}}}{1 - B_0} + \sigma, \tag{7.58}$$

$$T_c'^{\text{DCF}} = T_c^{\text{DCF}} + \sigma, \tag{7.59}$$

$$T_c^{\text{DCF}} = T_{\text{Data}}^{*} + T_{\text{EIFS}}, \tag{7.60}$$

where T_s^{DCF} is given in Equ. (7.42).

In order to determine the saturation throughput for the MIMO systems, T_s^{SU}, $\mathtt{E}\left[T_s^{\text{MU}_{\text{TDMA}}}\right]$ and $\mathtt{E}\left[T_s^{\text{MU}_{\text{OFDMA}}}\right]$ instead of T_s^{DCF} are applied in

Equ. (7.58). In case of MU systems, the expectation of the respective transmission window durations has to be applied, depending on the traffic type. The duration of the collistion slot in this case is same for all the MIMO systems:

$$T_c'^{\text{SU-DCF}} = T_c'^{\text{MU}_{\text{TDMA}}} = T_c'^{\text{MU}_{\text{OFDMA}}} = T_c^{\text{MIMO}} + \sigma \tag{7.61}$$

$$T_c^{\text{MIMO}} = \mathtt{E}\left[max_4\{T_{\text{data}}\}\right]^* + T_{\text{EIFS}} \tag{7.62}$$

The values corresponding to constant packet interarrival time and Poisson load are calculated, and plotted in Figure 7.7, together with the results for the hyper-exponentially distributed packet interarrival time at stations, obtained by simulation. All the systems suffer from the increased number of collisions as the network size grows. The higher the original saturation throughput when the number of stations is small, the more the system suffers from the collisions resulting from multiple transmissions. The reason is that the time that is lost because of collision (time needed to transmit a data packet) carries a higher fraction of the total transmission window duration. Whilst with 5 stations in the network, the difference between the saturation throughput of SU-DCF and the lower bound for the TDMA based MU-DCF is 30 $^{Mbit}/_{s}$, the difference reduces with 15 stations to about 20 $^{Mbit}/_{s}$ (the difference in the AP scenario is 27 $^{Mbit}/_{s}$).

Four-Way Handshake

In Figure 7.8 saturation throughput of the fully interconnected mesh network with four-way handshake medium access is plotted varying the number of station in the network. The calculation of the saturation throughput is analogous to that of the basic medium access, with differing durations of successful packet transmission and collision.

For the duration of the successful packet transmission, produced overhead for each case has to be considered. They are given in Equ. (7.53)-(7.56). As for the time lost due to collisions, it has the following durations:

$$T_c^{\text{DCF}} = T_{\text{RTS}} + T_{\text{EIFS}}, \tag{7.63}$$

$$T_c^{\text{SU}} = T_{\text{M-RTS}_1} + T_{\text{EIFS}}, \tag{7.64}$$

$$T_{c,i}^{\text{MU}_{\text{TDMA}}} = T_{c,i}^{\text{MU}_{\text{OFDMA}}} = T_{\text{M-RTS}_i} + T_{\text{EIFS}} \tag{7.65}$$

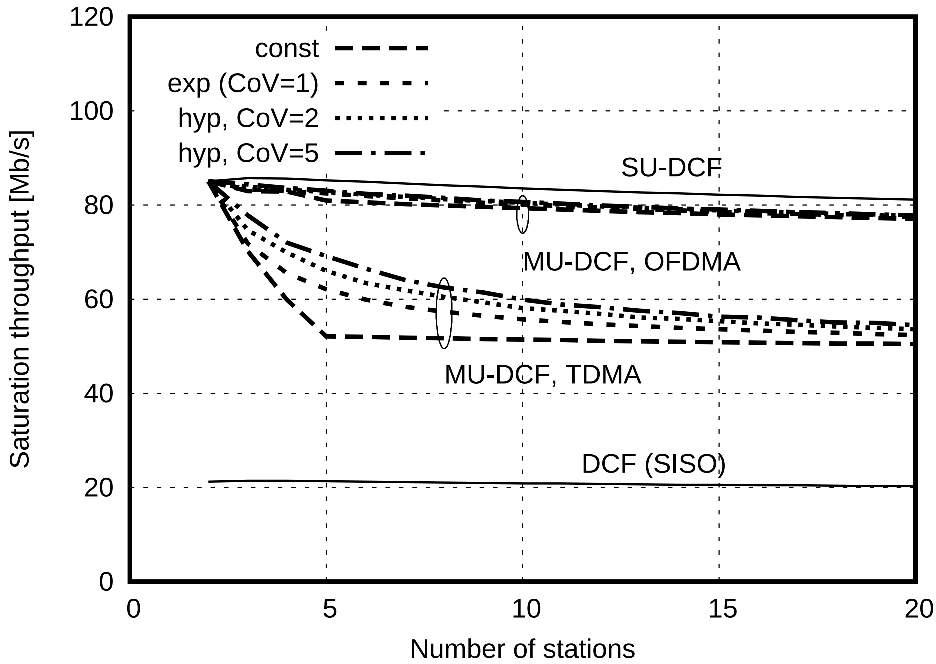

Figure 7.8: Saturation throughput: mesh scenario with four-way handshake

As already known for the IEEE 802.11 DCF, applying four way handshake alleviates the loss of throughput due to collisions. However, when talking about the absolute levels of the saturation throughput, for each system there is a switching point: if the number of stations is small, and therefore the collision probability is low, using M-RTS/M-CTS only presents an overhead. With the growing collision probability using four way handshake becomes more beneficial.

In the previous analysis, both of AP and mesh scenario specific traffic types have been assumed, however the derived formulas apply in general. For an arbitrary load source only the probability mass function P_d will change.

7.3 Fairness Study

In this section, SU and MU transmission strategies are compared from the aspect of fair service provision by means of analytical and Monte-Carlo methods. These results, as well as those in Section 7.4.2, have partially been published in [Mirkovic, 2008].

Providing fairness is a very common problem that occurs in both wireless and wired networks, as well as on different protocol layers. In the context of wireless networks, it is primarily concerned with providing fair bandwidth allocation with MAC. Fairness has a strong impact on other network performance metrics, particularly delay, which is essential for providing QoS to applications such as VoIP, multimedia streaming and Internet gaming. Moreover, poor performance on lower layers propagates to higher layers (e.g. Transmission Control Protocol (TCP)). In multihop networks, the concept of end-to-end fairness applies.

Fairness can be characterized in two different manners:

- *Long-term fairness*: fairness observed over long time periods (corresponding for instance to the transmission of ∼1000 packets).
- *Short-term fairness*: fairness over short time periods (duration of ∼10 packets).

The impact of the transmission strategy on both short-term and long-term fairness is studied.

A MAC layer can be considered as long-term fair if the probability of successful access to the channel observed on a long term converges to $1/N$ for N competing hosts. While most MAC protocols provide long-term fairness, providing short-term fairness is a much bigger challenge [Berger-Sabbatel et al., 2004].

One of the objectives of MAC layer design is high efficiency in resource utilization. MAC layer schedulers based on opportunistic strategies are able to provide it, but at the same time, they can significantly deteriorate performance in terms of fairness, and hence delay distribution. The most commonly used throughput maximizing allocation strategy that also takes into account fairness aspects is the proportionally fair scheduler introduced in [Kelly et al., 1998].

The fairness problem occurs when the number of users becomes larger than the number of resources in the system. If the network capacity is increased (e.g. using MIMO technology), effectively the number of resources is increased, which can help to avoid congestion; however, fairness, particularly short-term fairness, remains an issue.

The problem of dealing with multiple flows in packet switched networks has been traditionally handled by a global First In - First Out (FIFO) policy, as shown in Fig. 7.9(a). In case that all the flows have approximately the same offered load, this method is fair. However, in case that e.g. one flow has substantially smaller throughput, it can experience unacceptably bad performance.

In the solution proposed by J. Nagle in [Nagle, 1987], different flows are not put in the global FIFO queue, but each flow maintains a separate FIFO queue, and this set of queues is served in a Round Robin (RR) fashion, as shown in Fig. 7.9(b). This scheme does not take the packet length into account, thus it may happen that flows with long packets occupy the resources more than the flows with the short ones. A fair queuing Bit-by-Bit Round Robin (BR) algorithm has been proposed in [Demers et al., 1989] to solve this problem. Other schemes with further optimization strategies addressing this issue have also been proposed [McKenney, 1991, Shreedhar and Varghese, 1995].

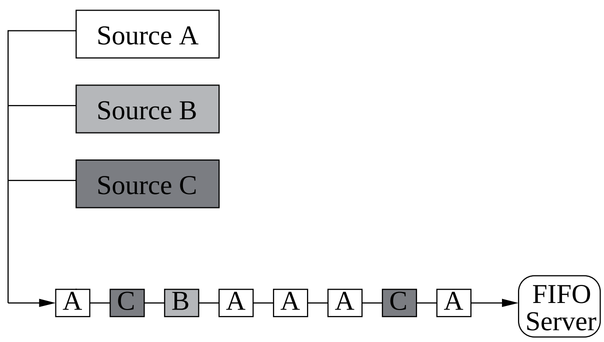

(a) FIFO queuing

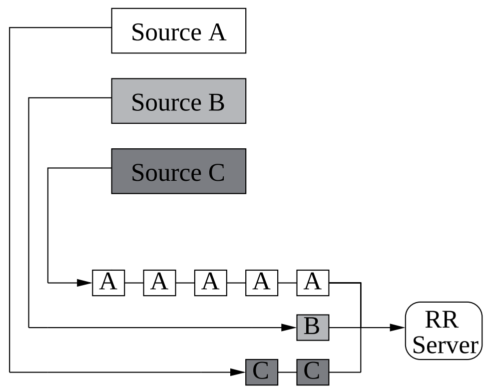

(b) Fair Queuing

Figure 7.9: Queuing multiple flows

In MU-DCF an arbitrary packet can be transmitted over a channel's spatial layer. There are no restrictions regarding a common destination for data packets within a MIMO frame. Let the applications A, B, and C in Fig. 7.9(a) be sources of packets within one station, with different destinations. We consider the case of queue occupancy as shown in Fig. 7.9(a). If the scheduler is working in SU mode, and four packets can be transmitted at a time, the first four packets (for 4×4 scheme) belonging to source A would be scheduled, skipping the packet from the source C. This approach breaks the FIFO rule, which can deteriorate the performance regarding fairness and delay.

If the scheduler is working in MU mode, the first four packets will be scheduled, independently of their destinations, thus obeying the FIFO order. Moreover, a MU scheduler can be configured to maximize the number of different receivers, and operate on the individual FIFO queues like in Figure 7.9(b) to further increase fairness.

Ordering packets in the global queue does not have to be in FIFO fashion; any prioritization of packets, e.g. based on delay or Packet Loss Rate (PLR) requirements, can be used for the initial ordering. The ability of MU transmissions ensures that this order is actually respected.

In this analysis, the scheduler located at an AP of an MU-DCF network is considered in a typical hotspot scenario. The provision of fairness to multiple flows originating from possibly different applications and therefore having possibly different destinations when using SU and MU transmission strategies is investigated. The results demonstrate superior performance of the MU approach in providing fairness, which justifies the increased system complexity.

There are several metrics for fairness evaluation, such as Gini fairness index and Min-max fairness index [Dianati et al., 2005]. In the following analysis, Jain's fairness index proposed in [Jain et al., 1998] is evaluated:

$$f\left(t_1, t_2\right) = \frac{\left(\sum\limits_{i=1}^{m} x_i\right)^2}{m \sum\limits_{i=1}^{m} x_i^2}, \tag{7.66}$$

where $f(t_1, t_2)$ is the fairness index in time interval (t_1, t_2), m is the number of contending stations, and x_i refers to number of resources used by station i within the time interval.

Jain's fairness index takes values from the interval (0, 1], where 1 represents maximum fairness in the system. Minimum value of the fairness index in a system with m users is is $1/m$, indicating the case when only one station occupies all resources during the whole interval (t_1, t_2).

In case of constant load, the packets for different connection always appear in the same order. Therefore, with SU strategy, the first time the fairness index reaches the value 1, which corresponds to the case when each user has been allocated the same amount of resources, happens after the number of intervals equal the number of connections. With MU, assuming 4×4 antenna configuration, this happens 4 times faster.

In Fig. 7.10 the fairness index is plotted, when the number of established connections with load with constant packet interarrival time is 10, 50 and 100. It illustrates previously described behavior in SU-DCF and MU-DCF. The convergence of the fairness index to 1 in MU-DCF is much faster than in SU-DCF, indicating higher ability to provide short-term fairness.

Also, the convergence is slower when more connections are present. In that case it is more critical to enable MU transmissions.

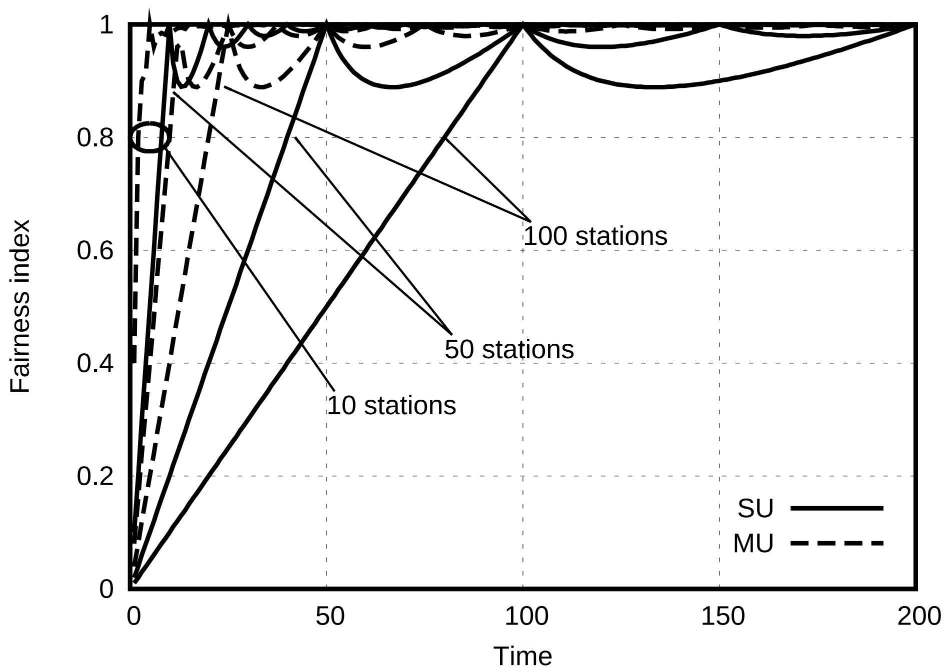

Figure 7.10: Fairness index in AP scenario with constant packet interarrival time

In Figure 7.11 the fairness index is presented for Poisson load, and in Figures 7.12 and 7.13 for the traffic with hyper-exponential distribution of packet interarrival time. It can be seen that the convergence is slower, since the traffic is more bursty, and the system tends to operate with smaller average number of distinct receivers of MIMO frames.

Another interesting effect, particularly strong in Figure 7.13 is that the fairness index is initially high, but afterwords it drops and then it continues converging to value 1. The reason is that in case of bursty traffic,

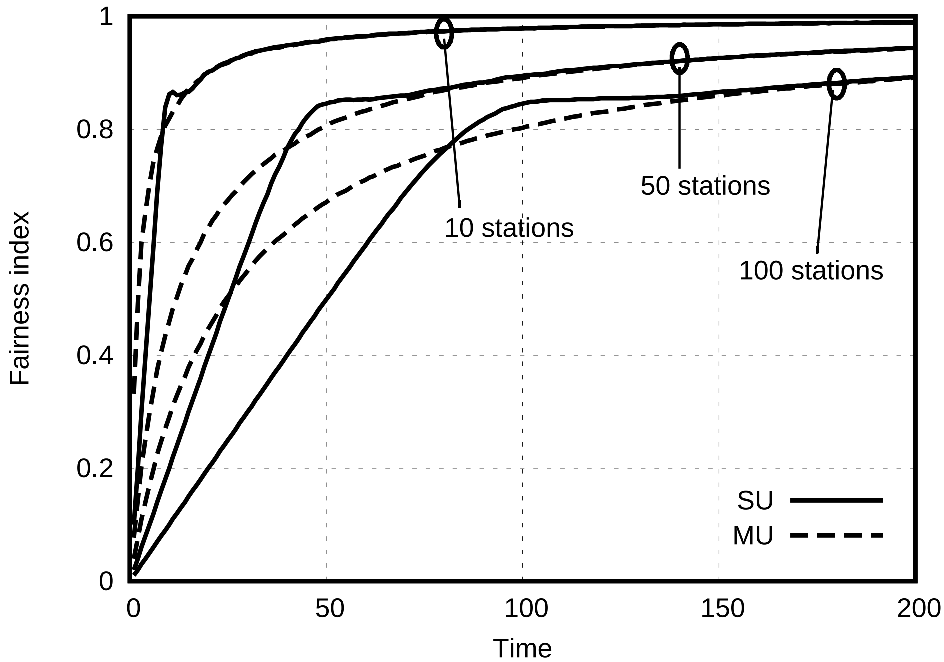

Figure 7.11: Fairness index in AP scenario with offered load with exponential distribution of packet interarrival times

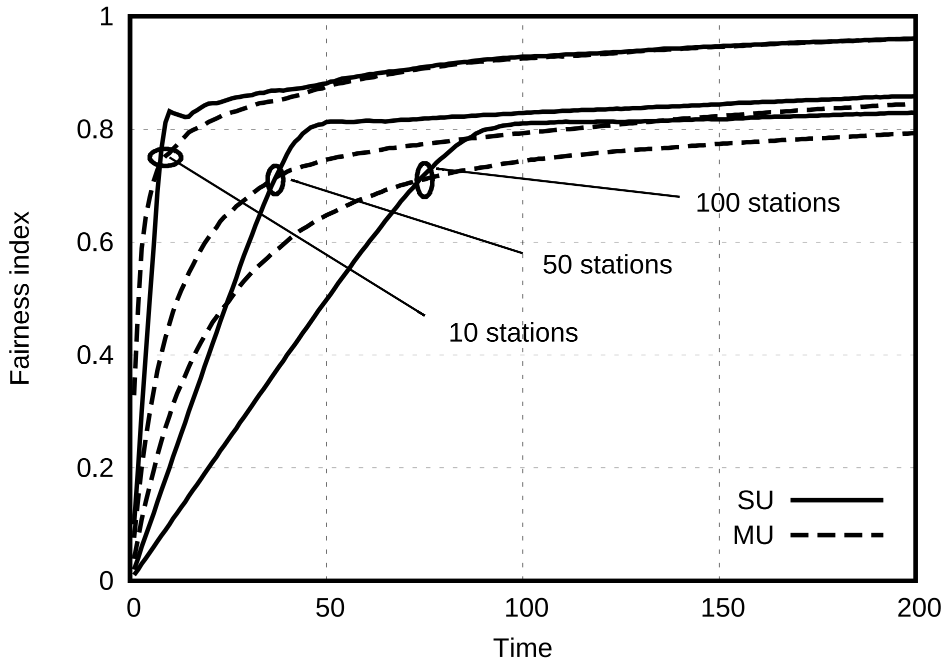

Figure 7.12: Fairness index in AP scenario with offered load with hyper-exponential distribution of packet interarrival times, $cv = 2$

the probability that within the first channel accesses packets for different users are transmitted is high, particularly if the traffic generators are

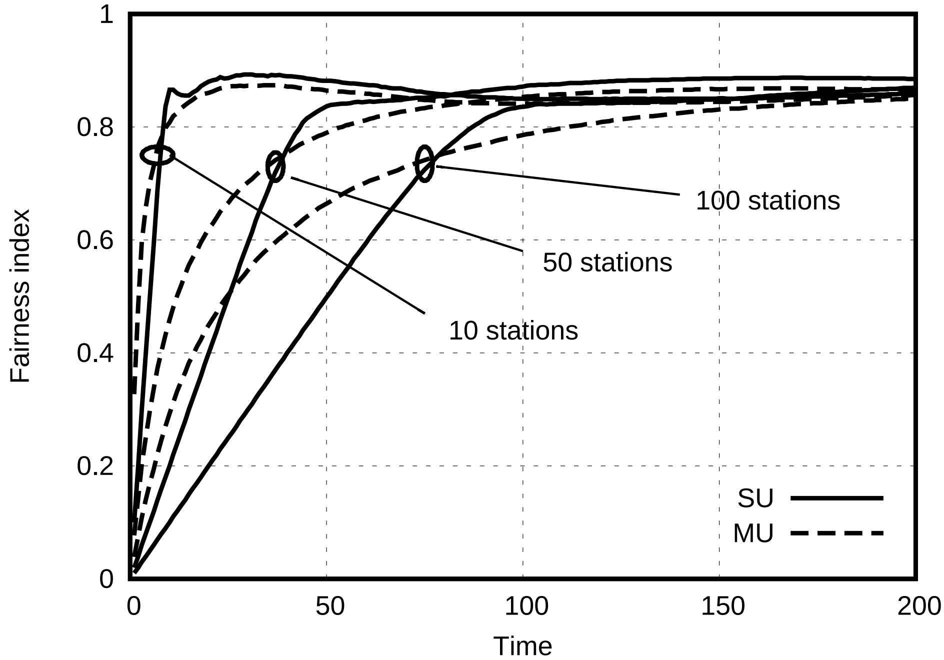

Figure 7.13: Fairness index in AP scenario with offered load with hyper-exponential distribution of packet interarrival times, $cv = 5$

started at the same time, which is the case in these simulations. However, as time elapses, probability of long bursts increases, and they decrease the fairness index.

7.4 Delay Study

In this section the delay produced using SU and MU transmission strategies is compared. Total experienced delay by a packet can be characterized by service time and queue delay, thus they are analyzed separately.

7.4.1 Service Time

If service time is defined as duration between the time the packet becomes HoL and the reception of the coresponding ACK frame, it can be calculated using Little's law:

$$D = \frac{\mathtt{E}\left[N\right]}{S/\mathtt{E}[P]}, \tag{7.67}$$

where $\mathtt{E}[N]$ stands for the expected number of stations that will eventually successfully deliver their HoL packets, and the denominator stands for the delivery rate expressed in packets per second.

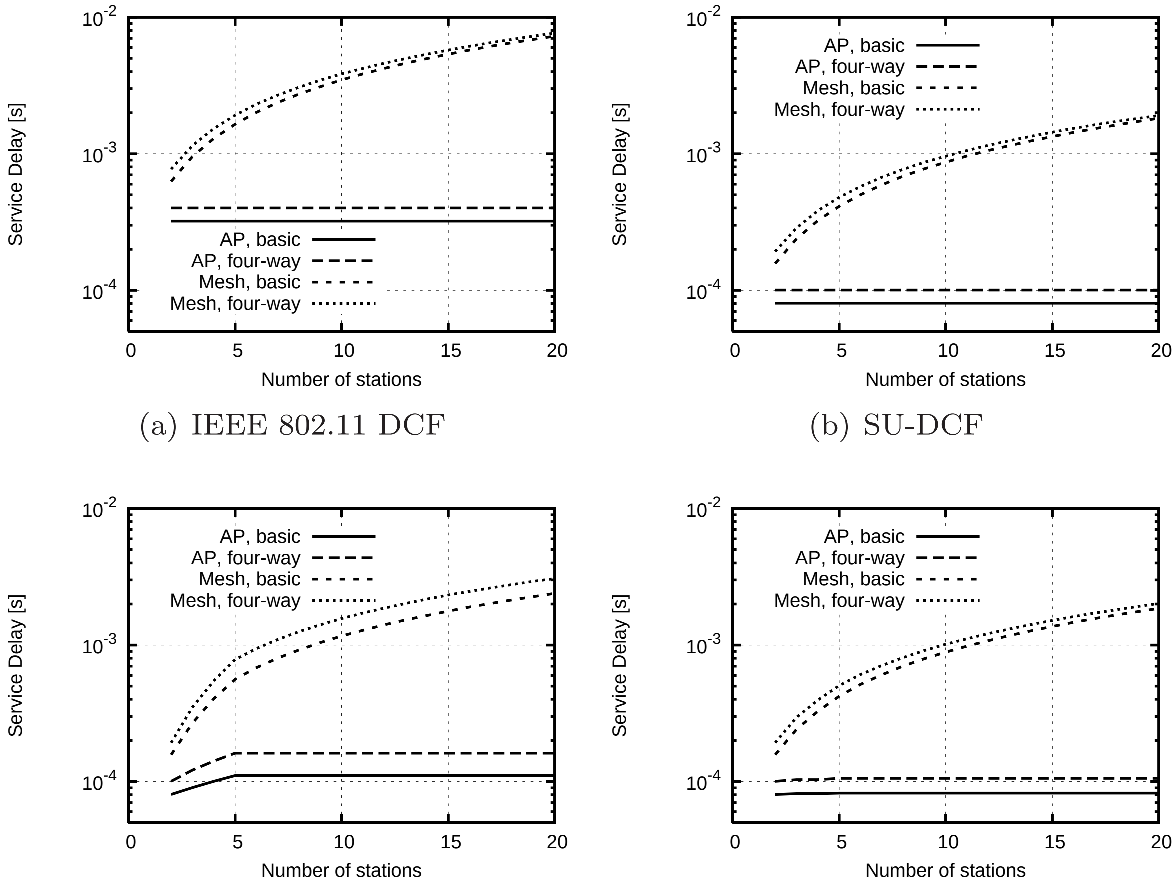

(a) IEEE 802.11 DCF

(b) SU-DCF

(c) MU-DCF with TDMA signaling

(d) MU-DCF with OFDMA signaling

Figure 7.14: Service time in different systems

In Figure 7.14 service delay is presented for different systems, namely standard DCF, SU-DCF, and MU-DCF with TDMA and OFDMA signaling, with connections with load with constant packet interarrival time. In each subfigure, the curves are plotted for the case of AP and mesh scenario, with basic medium access and four-way handshake.

In all the cases, the service time remains the same in case of an AP scenario, since at a time only one station has a packet(s) that is the HoL packet. In mesh scenario service time grows linearly with the number of stations in the network. Thus, in case of only two stations in the network, service time in a mesh is double that of an AP scenario, since in the first case two connections are established, and in the second only one.

The service time in DCF (Figure 7.14(a)) compared to 4×4 SU-MIMO system (Figure 7.14(b)) is exactly 4 times shorter. The reason is that the number of resources is 4 times larger. If the channel is seen as a processing module of a queuing system, then in case of DCF only one processor is present, whereas in case of the MIMO system there are 4 parallel processors.

The service time in cases when MU transmissions are allowed (Figures 7.14(c) and 7.14(d)) is somewhat longer since in then the transmission window lasts longer; however, the difference is not significant. Larger difference, in will be experienced by packets for the queue delay.

7.4.2 Queue Delay Study

In this section, queue delay in SU and MU based system is compared based on event-driven simulation. Only the basic medium access is analyzed, since the protocol overhead is not included in the queue delay analysis; the system with four-way handshake performs similarly.

Case Study I: Fixed Offered Load per Connection

In this case study, the offered load *per connection* is fixed to 1 Mb/s, and the delay distribution depending on the number of connections is analyzed in an AP scenario. The number of connections is varied from 1 to 46, hence the total load varies from 1 Mb/s to 46 Mb/s. Since the total offered load is below the system capacity, the data packet queues do not grow indefinitely.

The simulations are conducted for different traffic types, and the results are presented in Figure 7.15. It depicts the 50^{th}, 75^{th} and 95^{th} percentiles of queue delay.

The queue delay in SU-DCF under constant packet interarrival time does not depend much on the number of stations (Figure 7.15(a)). The AP does not initiate the transmis sion before four packets with the same destination are present in the queue. Thus, on average it should be that one quarter of packets has zero queue delay, the second quarter has queue

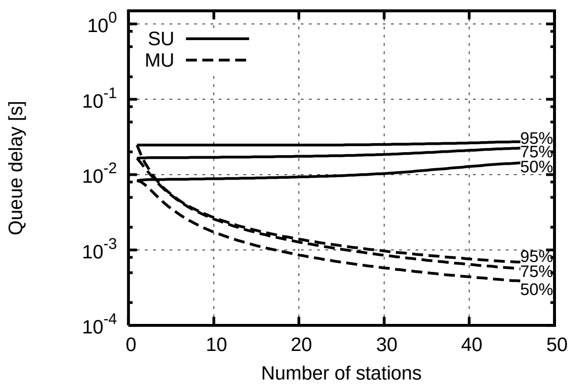

(a) Constant

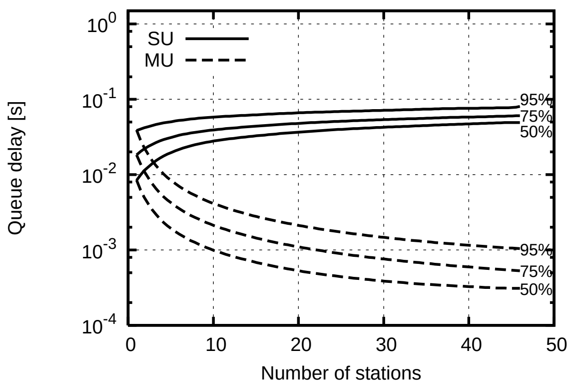

(b) Exponential distribution

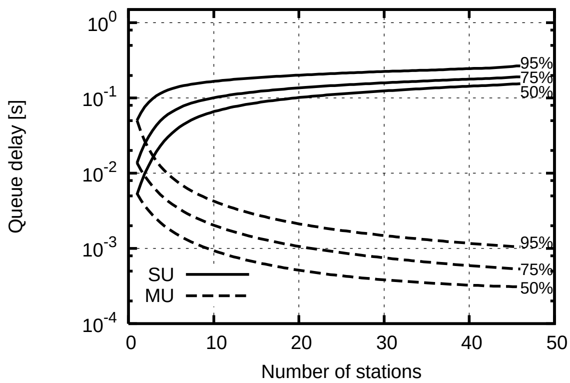

(c) Hyper-exponential distribution, $cv = 2$

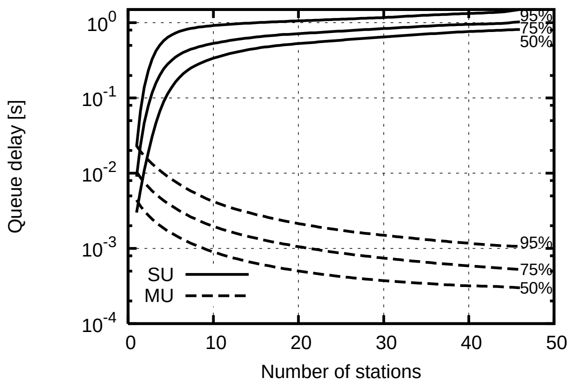

(d) Hyper-exponential distribution, $cv = 5$

Figure 7.15: 50^{th}, 75^{th} and 95^{th} percentiles of queue delay in a scenario with fixed offered load (1 Mb/s) per station with different distribution of packet interarrival-time

delay equal to packet interarrival time, the third quarter two times packet interarrival time, and the last quarter three times packet interarrival time (duration of one packet interarrival time in this case is 0.008192 s). The result presented in the Figure 7.15(a) do not perfectly match that calculation owing to different times where the load generators create the first packet. Therefore it might happen that in the moment when 4 packets for one connection are collected in the queue, the medium is already occupied, and these packets then experience additional delay.

Unlike SU-DCF, MU-DCF starts a transmission as soon as four packets are generated, independently of their destination. Therefore the queue delay is inversely proportional to the number of stations in this case. More-

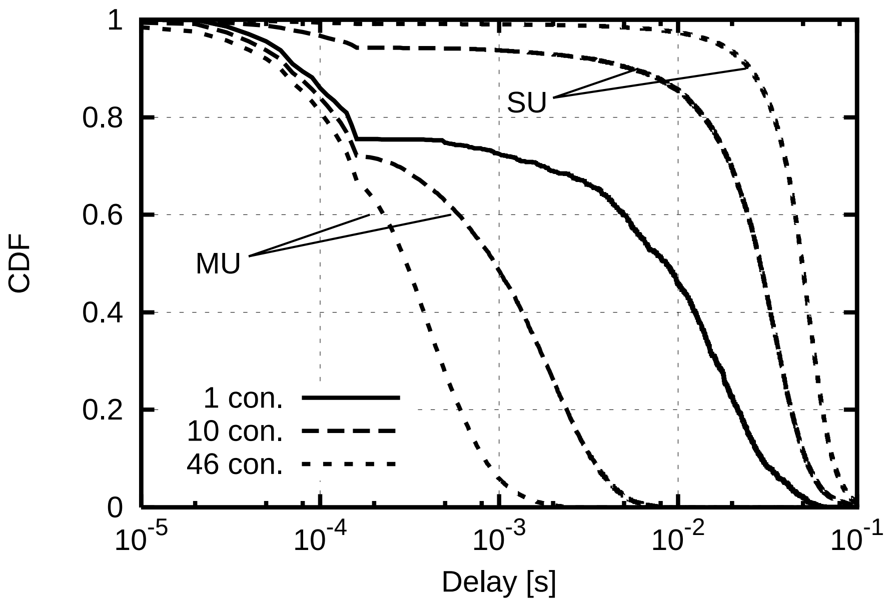

Figure 7.16: CDF of queue delay in the scenario with fixed offered load per connection with Poisson load

over, it can be seen that the variance of delay decreases with a growing number of stations and increases with the CoV of packet interarrival time.

The results for growing CoV, 1, 2 and 5, of packet interarrival time, are presented in Figures 7.15(b), 7.15(c) and 7.15(d) respectively. It can be seen that higher CoV degrades the performance in SU case. The impact of load type is particularly severe when there are more then 4-5 established connection, when the value of the 95$^{\text{th}}$ percentile exceeds 1 s in case of CoV 5.

The performance of the system in MU case is alsodegraded, but not to the same extent. Therefore, under bursty load applying MU transmissions is more beneficial than under constant packet interarrival time.

Figure 7.16 shows the Cumulative Distribution Function (CDF) of queue delay in SU-DCF and MU-DCF with different number of established connections: 1, 10 and 46. If there is only one established connection the two systems perform identically, thus the solid line that corresponds to queue delay CDF in that case in both figures is the same. In SU-DCF with growing number of connections, this CDF is “stretched” above, while in case of MU-DCF it is “stretched” below the reference CDF of queue delay in case of single connection.

An explanation may be required for the behavior of CDF after ~0.75. The reason is that CDF above that value in case of one connection corresponds to one quarter of packets that are the last one generated from the set of packets that build a MIMO frame, and that ultimately initiate the transmission. When there are more connections, in SU-DCF this last missing packet does not always instantly initiate a transmission, because the channel may already be occupied by a transmission to another user. In MU-DCF this effect is still present, but the shape of the curve becomes less sharp due to reduced average queue delay.

Case Study II: Fixed Total Offered Load

In the second case study, the *total* offered load is assumed fixed to 46 Mb/s, and each connection contributes with the same fraction to the total offered load. The delay distribution is studied, depending on the number of connections. In Fig. 7.17, the 50$^{\mathrm{th}}$, 75$^{\mathrm{th}}$ and 95$^{\mathrm{th}}$ percentiles of queue delay are presented, with each subfigure presenting results for different load types.

MU-DCF outperforms SU-DCF in this case, too. Since the destination of a packet is not relevant for creating a MIMO frame applying MU strategy, the queue delay does not depend on the number of stations. On the other hand, the queue delay in SU case grows linearly. The variance grows with both SU and MU strategy.

It can also be noticed that in MU case the 50$^{\mathrm{th}}$ percentile is the highest in case of constant packet interarrival time. The reason is that in case of bursty load the packets that are generated within one burst do not have to wait for a certain number of packets to be present in the queue (they are already there), as in case of constant packet interarrival time. However, for the 95$^{\mathrm{th}}$ percentile the opposite applies, since if some packets wait for the next burst to complete a MIMO frame; this time depends of the CoV of packet interarrival time distribution.

In Figure 7.18 CDF of queue delay in SU-DCF with different traffic types and 46 connections is presented. Similarly as in Figure 7.16, the CDF curve under constant load, has the steps that correspond to each

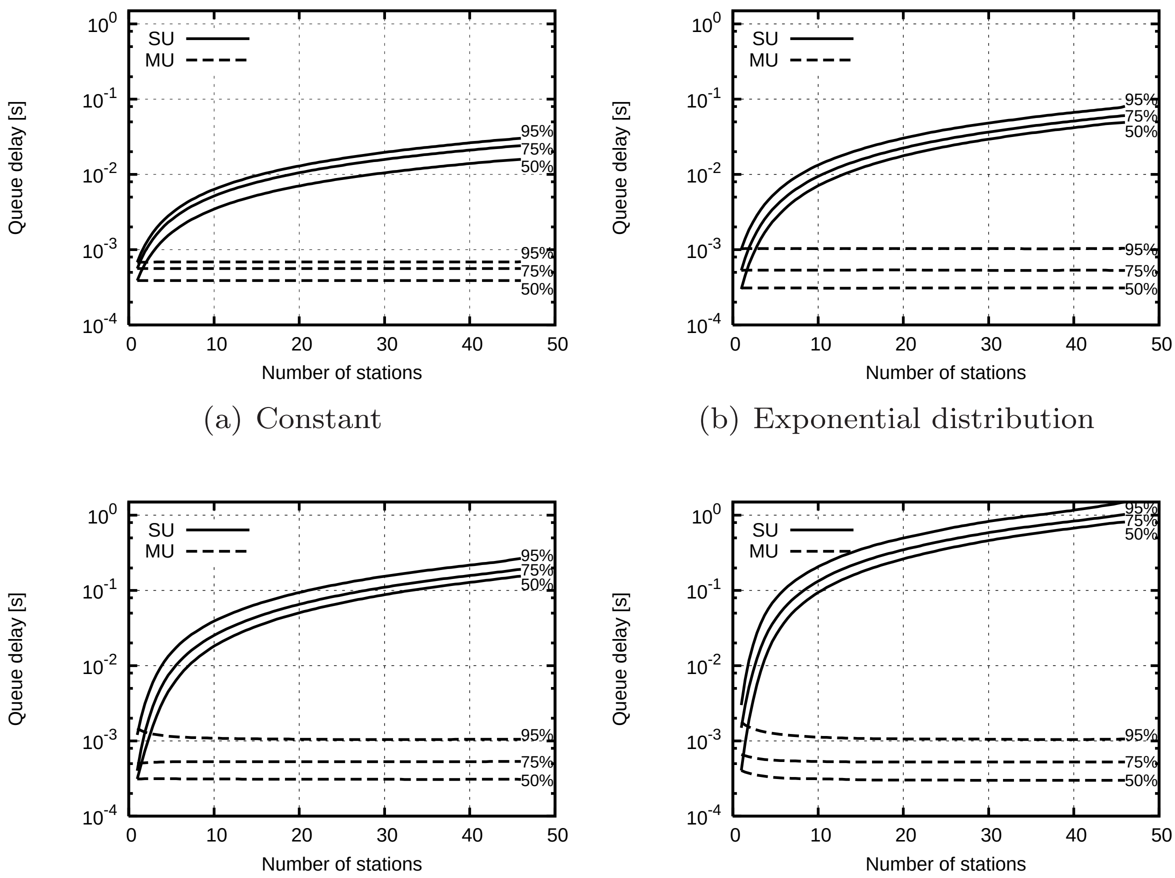

(a) Constant (b) Exponential distribution

(c) Hyper-exponential distribution, $cv = 2$ (d) Hyper-exponential distribution, $cv = 5$

Figure 7.17: 50^{th}, 75^{th} and 95^{th} percentiles of queue delay in a scenario with fixed total offered load (46 Mb/s) with different distribution of packet interarrival-time

generated packet. As the load becomes bursty, they vanish and the curve becomes more smooth. Also since the given curves have approximately same slope on the logarithmic scale, the variance is increased.

It is also interesting to compare SU and MU strategies in case of constant and hyperexponential distribution of packet interarrival times. The corresponding queue delay CDFs are plotted in Figure 7.19 (with 46 connections as well). In case of constant packet interarrival time, median queue delay in MU-DCF is one order of magnitude smaller than in SU-DCF (see Figure 7.19(a)), whereas under bursty load the difference grows to three orders of magnitude (Figure 7.19(b)).

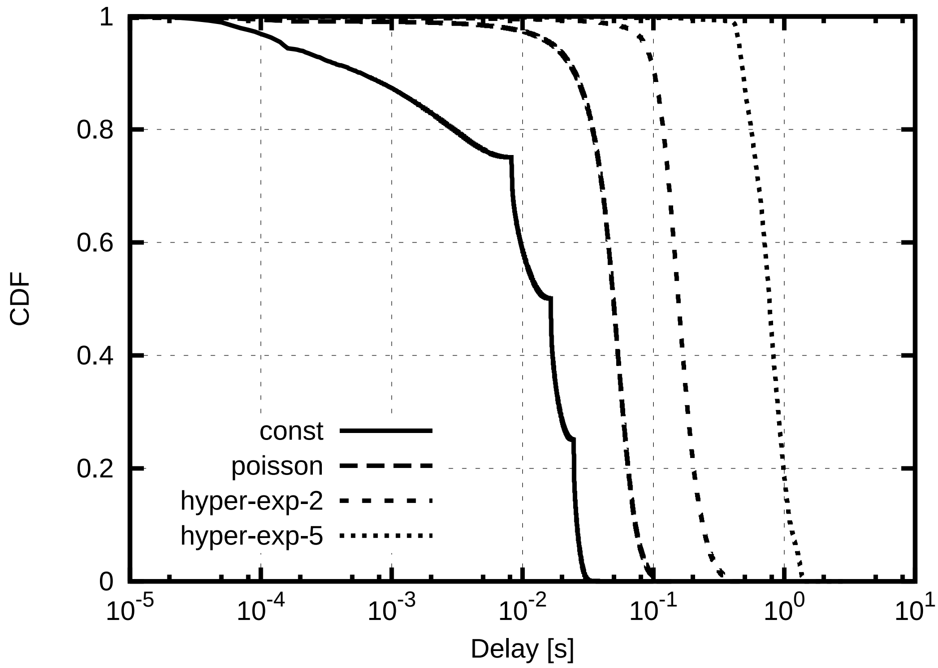

Figure 7.18: CDF of queue delay in SU-DCF depending on traffic type

7.5 Summary

This chapter gives a comprehensive comparison of SU-DCF and MU-DCF. In the first step, using analytical model, saturation throughput has been compared for different traffic types. SU-DCF has higher saturation throughput than MU-DCF due to lower overhead. However, it is inferior in providing short-term fairness and timely packet delivery. Therefore, SU-DCF is preferable in smaller networks, with applications that are not delay-sensitive, and that produce relatively monotonous traffic. In case of real-time applications, MU mode has higher potential for providing timely packet delivery, particularly with higher number of connections.

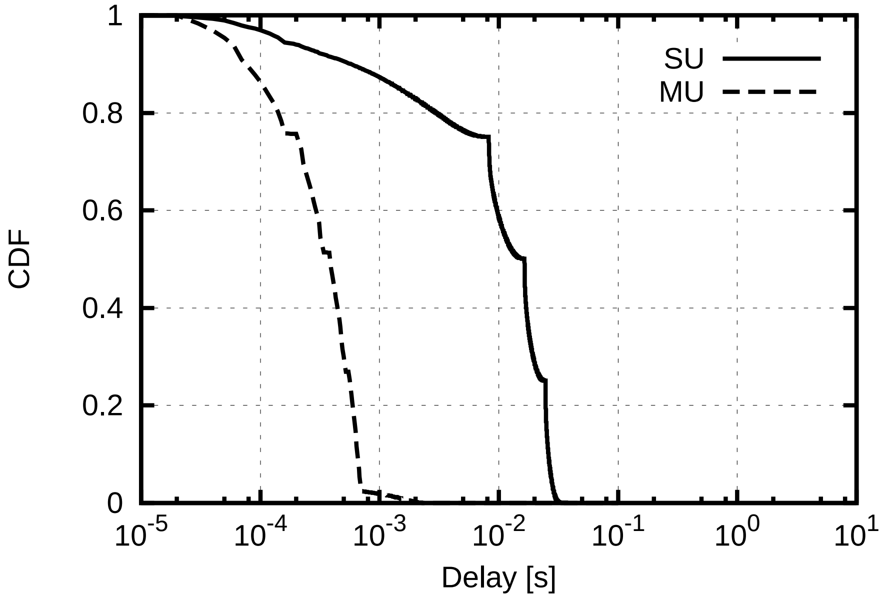

(a) Constant

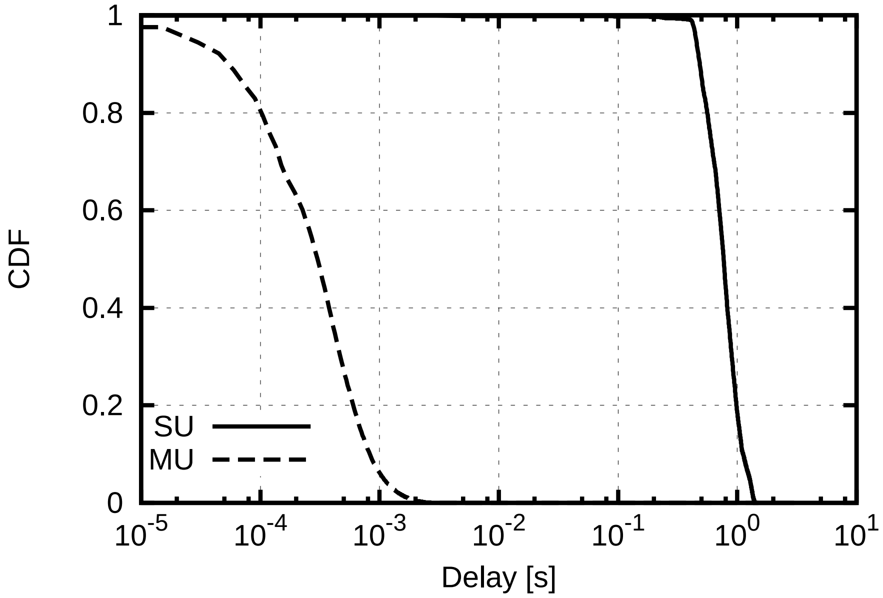

(b) Hyper-exponential distribution, $cv = 5$

Figure 7.19: CDF of queue delay in SU-DCF and MU-DCF with different distributions of packet interarrival time

CHAPTER 8

Channel-Aware Scheduling

Contents

After analysis of SU-DCF and MU-DCF with uninformed transmitter in the previous chapter, this chapter deals with channel-aware scheduling and its impact on link and system level performance.

Special attention in this chapter is payed to the abilities of schedulers to exploit MU diversity and the effect of channel uncertainty on performance of the developed schedulers. The results of this chapter have partly been published in [Mirkovic et al., 2007b], and included in [Mirkovic and Walke, 2008a, Mirkovic et al., 2008].

8.1 Opportunistic Scheduling

The presence of channel state information at the transmitter, as described in Chapter 3.2, can significantly improve MIMO channel capacity. Besides boosting PHY level performance, by appropriate scheduling of transmissions that applies cross-layer optimization, MAC level performace can also be improved. (This does not apply only for MIMO systems, but in general.)

An AP with multiple connections in fading environment is assumed. The basic idea of the opportunistic scheduling algorithms is that the transmissions should take place over links that are in good state. Such scheduling policy, although maximizing the total throughput, has a drawback of potential starvation of stations whose channel is on average not good, as well as unpredictable delays. Besides using the channel quality of different stations to maximize the throughput, the scheduler can also take into account the QoS requirements of particular connections. Thus many methods have been developed to provide fairness and QoS while exploiting the channel knowledge at the transmitter [Kelly et al., 1998, Cao and Li, 2001, Lu et al., 1999, Ng et al., 1998]. QoS requirements can be formulated in many ways; lately, application of utility functions has become popular [Hosein, 2006, Lee et al., 2006].

Antenna selection and different optimization criteria are presented in [Gore et al., 2000, Heath Jr et al., 2001, Heath Jr and Love, 2005]. The authors in [Heath Jr and Love, 2005] also investigate the error rate performance with zero-delay, zero-error feedback, thus not regarding the impact of channel uncertainty. In [Heath Jr and Love, 2005] the authors investigate the error rate performance with zero-delay, zero-error feedback, but without regarding the impact of channel uncertainty and system level aspects, whereas the authors in [Anton-Haro et al., 2006] give a high level overview of cross-layer scheduling for MU-MIMO systems. Depending on the particular MIMO scheme, the PHY level performance, as well as performance of scheduling algorithms highly depend on accuracy of the estimated channel, and that is addressed in the remaining of this chapter.

8.2 CSI Uncertainty

The fundamental condition for applying link adaptation methods and opportunistic scheduling is the presence of some form of channel quality measurement at the transmitter. There are methods where only channel statistics at the transmitter are enough, but for other schemes, such as transmit MRC (see Section 3.5.1), knowledge of transfer functions of channels between each transmit-receive antenna pair is required.

The transmitter can obtain CSI:

(A) by estimating the forward channel and assuming channel reciprocity, or

(B) by requesting channel feedback information from the receiver.

In both cases, there is a certain error between the estimated channel and the channel at the time of the transmission. The duration between the channel estimation and the actual channel usage will impact the accuracy in both cases, whereas in case (A) deviations from channel reciprocity introduce additional error. There are also other impacts, such as measurement error.

Depending on the particular MIMO scheme, the performance on the PHY, as well as the scheduling methods highly depend on the accuracy of the estimated channel. The impact of the channel uncertainty on the channel capacity was investigated in [Yoo et al., 2004]. The authors in [Pohl et al., 2003] investigated the required channel feedback frequency in different systems, pointing out that the coherence time is not the only important parameter, but also others related to system configuration such as number of antennas and MCS used.

In this chapter, following the MAC protocol proposed in Figure 5.1, it is assumed that the CSI at the transmitter is received as a feedback, achieved by M-RTS/M-CTS frame exchange. Particularly in this case applying OFDMA for signaling (to exchange MU-RTS/M-CTS frames) is very beneficial, since it reduces the overhead duration, which is actually the duration between the channel estimation and channel usage. Channel uncertainty is modelled here as the unperfect correlation of estimated and used channel, and it is described in detail in the remaining of this section.

8.2.1 Channel Time Correlation Function

In mobile environment, the channel impulse response changes with time. A widely accepted scattering model to describe the signal received by a moving vehicle was introduced by Clarke [Clarke, 1968]. In this model, the transmitted signal is distorted by three effects:

- a Rayleigh distributed attenuation,
- a phase shift uniformly distributed in the range $[0,2\pi]$ and independent from the attenuation,
- a Doppler frequency offset.

In the case of an uniform distribution of the multipath angle of arrival between 0 and 2π, the Doppler spectrum is U-shaped and it can be proved that the channel time correlation function has the following expression [Sklar, 2001, Jakes, 1974]:

$$R(\Delta t) = J_0(kV\Delta t), \tag{8.1}$$

where $J_0(\cdot)$ is the zero-order Bessel function of the first kind. (This function is also used for coherence time definition in Section 2.3).

The channel time correlation function at 5 GHz carrier frequency is plotted in Figure 8.1 for 5 km/h and 100 km/h terminal speed. As a zero-order Bessel function of the first kind, the channel time correlation function is an oscillatory function, hence not invertible. As the following analysis is based on the performance depending on the value of the channel time correlation function, it will correspond to time T when the function takes the given value for the first time.

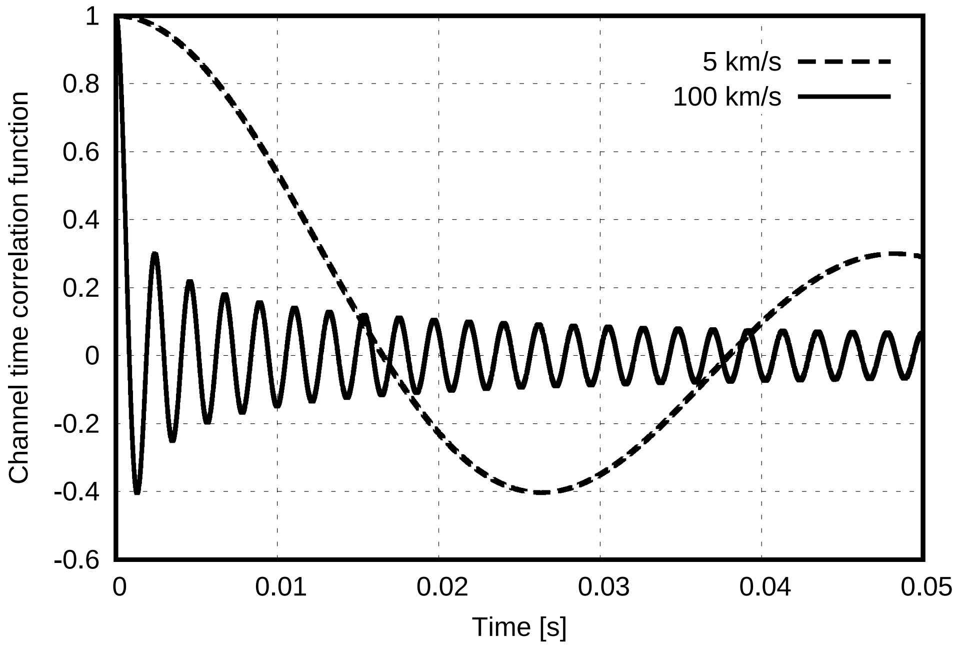

Figure 8.1: Channel time correlation function at 5 GHz carrier frequency for 5 km/h and 100 km/h terminal speed

8.2.2 Post-Processing SNR Time Correlation

In this section, the correlation coefficient between the post-processing SNR values is analyzed depending on the channel time correlation and the SNR level for different antenna configurations.

The estimation of the channel matrix H is performed at $t = 0$, and the transmitter receives the feedback and transmits data at $t = T$. The transmitter has the knowledge of the post-processing SNR values that correspond to the channel matrix $H(0)$, which differ from the ones corresponding to the channel matrix $H(T)$. The time $\Delta t = T$ which elapses determines the correlation level between the channel matrices $H(0)$ and $H(T)$, and inherently between the achievable post-processing SNRs.

In Figure 8.2 the dependency of post-processing SNR correlation coefficient on the channel time correlation and SNR level is illustrated for the 4×4 antenna link with MMSE receiver. The post-processing SNR correlation coefficient grows rather slowly with the channel time correlation level, which increases the importance of accurate channel information for making a good scheduling decision. It can also be seen that the correlation is higher in low SNR region; this is not the case with the ZF receiver that simply inverts the channel matrix.

For a comparative performace analysis of links with different number of antenna streams, in Figure 8.3 the post-processing SNR correlation vs. channel matrix correlation is plotted at 5 dB, 15 dB and 40 dB SNR, for 1×4, 2×4, 3×4 and 4×4 antenna links applying the MMSE receiver.

Several observations can be made: first, the post-processing SNR correlation coefficient over 1×4 antenna link practically does not depend on SNR. 1×4 antenna link achieves the highest post-processing SNR correlation at all input SNR levels, since with diversity the channel can be estimated with higher accuracy. With each additional transmit antenna i.e. spatial stream, the post-processing SNR correlation degrades, so finally the 4×4 antenna link has the poorest performance. Also, the post-processing SNR correlation degrades with the increasing input SNR.

It should be also noted that the asymptotic performance of the MMSE receiver in high SNR region (as shown in Figure 8.3(c) for 40 dB SNR) matches the performance of the ZF receiver.

Post-Processing SNR Correlation with SU-MIMO Transmissions

In the presence of time varying fading, if all the spatial subchannels are used by one receiver it does not make a difference if e.g. the first stream has been estimated as good and the second one as bad, and at the time of

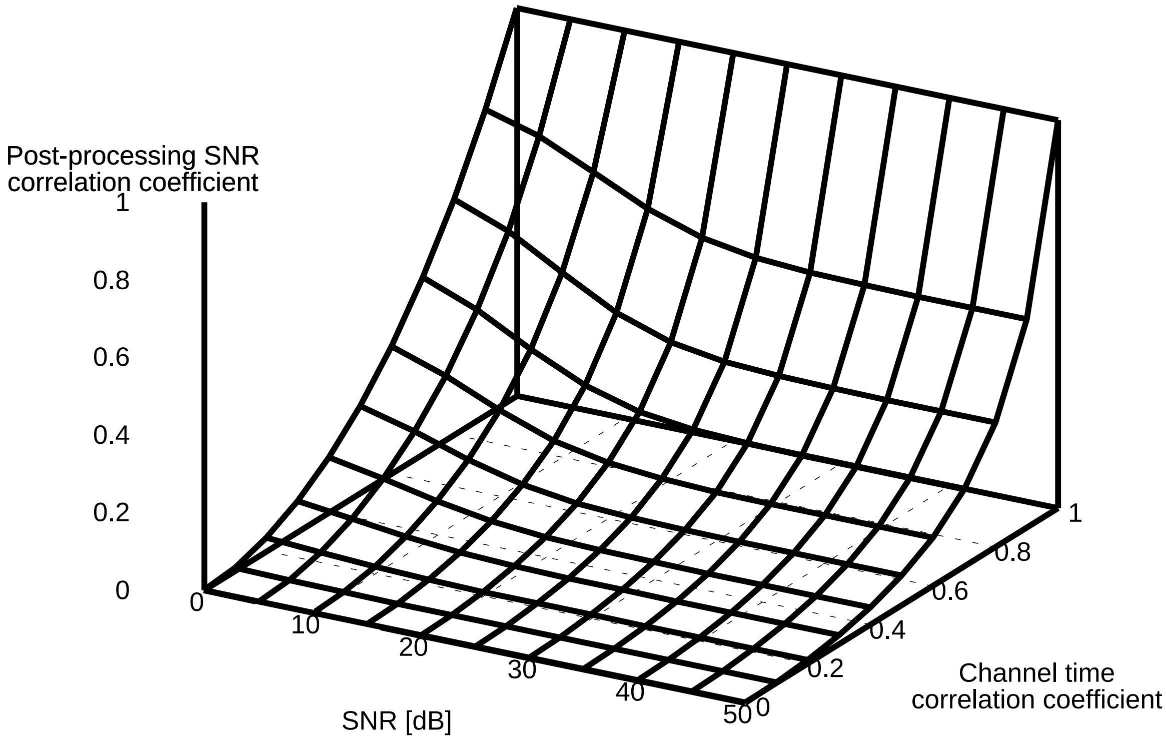

Figure 8.2: Post-processing SNR correlation coefficient vs. channel time correlation coefficient and SNR level for 4×4 antenna link with MMSE receiver

reception the opposite turns out to be the case: the first one is bad, and the second one is good.

Therefore, for the case of SU-MIMO transmission, the correlation coefficient of the sorted post-processing SNR values is measured and presented in Figure 8.4. The figure illustrates that the sorted post-processing SNR is highly correlated even without the channel time correlation. The reason is the same average SNR value. However, the post-processing SNR correlation coefficient increases with the channel time correlation faster in SU case than in MU case, and it is also higher in low SNR region due to MMSE receiver algorithm.

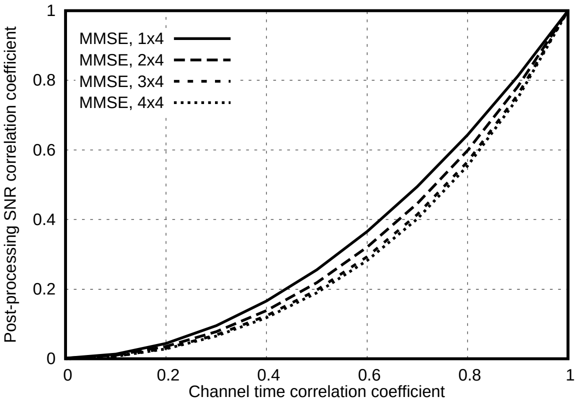

(a) SNR= 5 dB

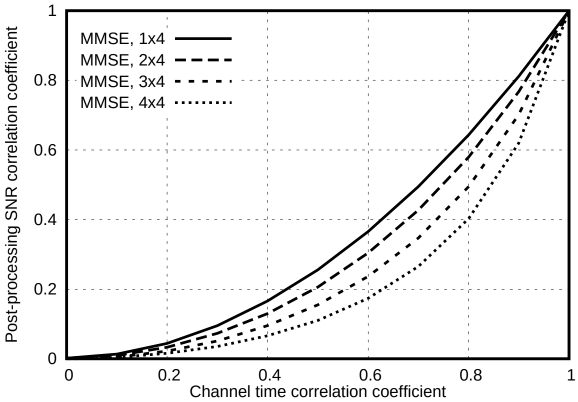

(b) SNR= 15 dB

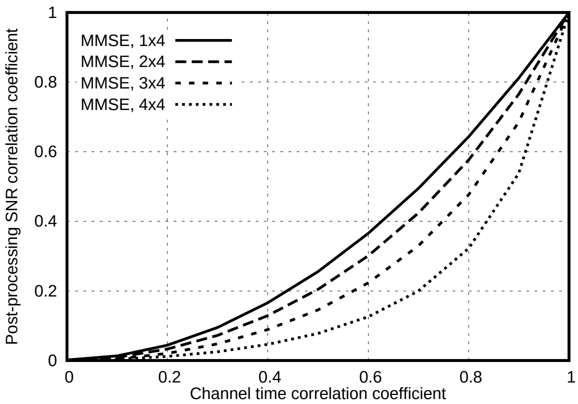

(c) SNR= 40 dB

Figure 8.3: Post-processing SNR correlation coefficient of 1×4, 2×4, 3×4 and 4×4 links vs. channel time correlation coefficient at different SNR levels

8.3 Channel-Aware Scheduling with Fixed PHY modes

In this section channel aware scheduler algorithms applying a fixed PHY mode are described and their performance is studied. The two algorithms build MIMO frames with SU and MU strategy, respectively.

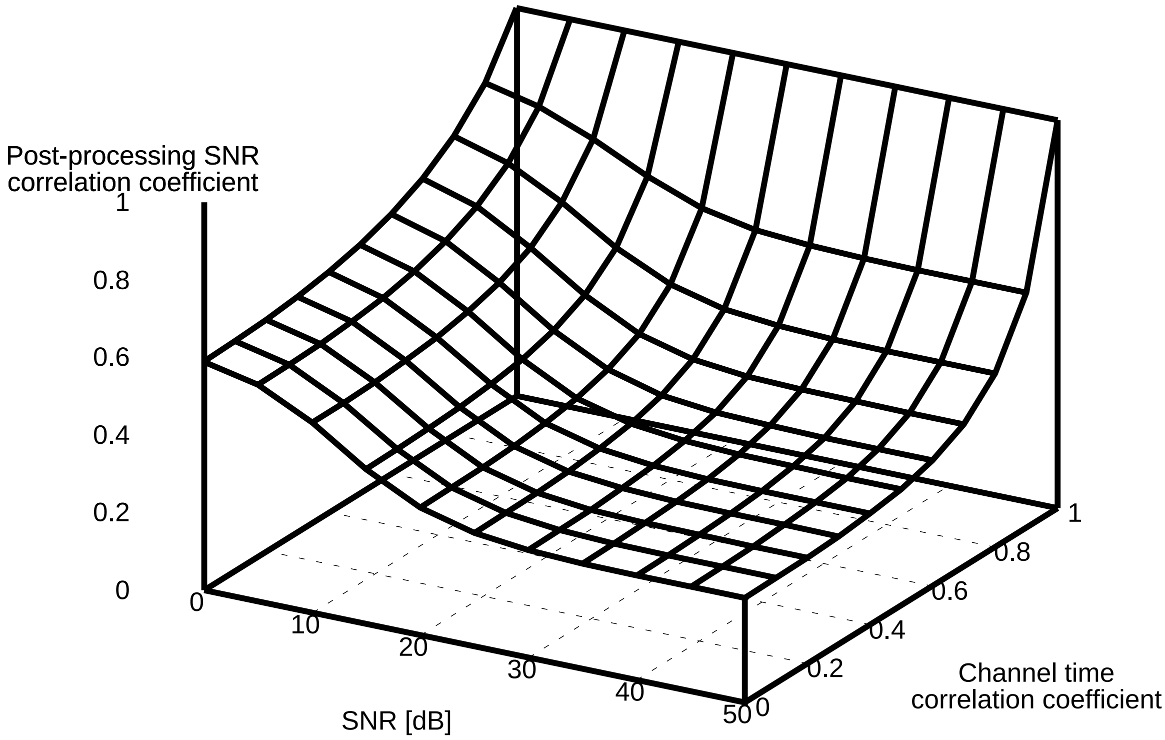

Figure 8.4: Post-processing SNR correlation coefficient vs. channel time correlation coefficient and SNR level for 4×4 antenna link with MMSE receiver in SU case

8.3.1 Algorithm Description

The basic principle over which the scheduler works is to make a binary decision about usability of the post-processing SNR to keep the previously chosen PHY mode. After collecting the channel information from the receivers, the scheduling module of the transmitter makes the decision which station have a good channel and which packets will be transmitted in the upcoming transmission. In this analysis the scheduler always creates a MIMO frame of size equal to the number of transmit antennas. The focus is on the evaluation of the capacity gain bound in multiuser environment.

The algorithms for SU and MU transmission strategies are described in the following.

SU Mode

In Figure 8.5 the decision making of the scheduler operating in SU mode is illustrated. The algorithm takes as input values the estimated post-processing SNRs for each stream and for each user, and chooses the one with the potential for the highest throughput. Since the spatial subchannel can be characterized either as "good" or as "bad", this practically reduces to counting the good subchannels for each user.

In Figure 8.5 the transmitter has three established connections, and the CSI for all the tree stations. Since the receiver station `Rx3` has the highest number of spatial subchannels (three) with post-processing SNR acceptable for the used PHY mode, packets to that station are scheduled for the transmission within the next MIMO frame.

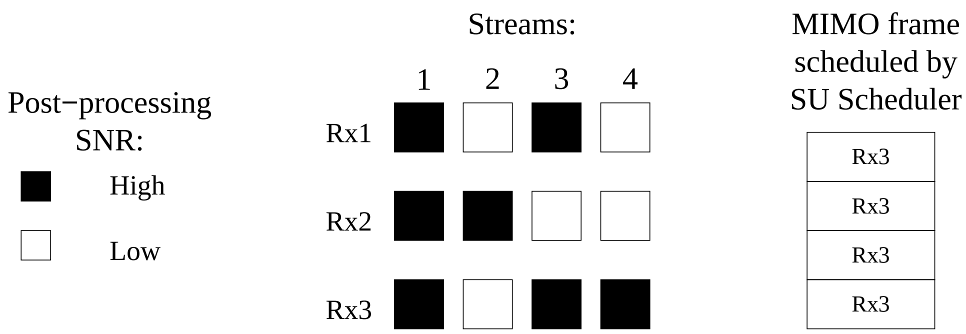

Figure 8.5: SU scheduler with fixed PHY mode

The previous example is simplified by assuming that the transmitter has CSI for all the associated station, which may not be the case. A more detailed description of the scheduler procedure applying SU transmission strategy with fixed PHY mode is presented with pseudocode in Algorithm 8.1.

The transmitter may not have the CSI for all the receivers with which it has established connections and the procedure treats the two groups differently. First, the groups of receivers with and without the CSI are identified. Only the receivers with enough packets in the corresponding data queues to form a MIMO frame are processed. Next, in the first group of receivers the one which has the potential to achieve the highest throughput in the upcoming transmission window. Analytically formulated, the

Algorithm 8.1 SU scheduler with fixed PHY mode

```
Collect CSI;

for (each receiver Rx_i) do
   if (queue length(Rx_i) ≥ MIMO frame size) then
      if (there is CSI feedback from Rx_i) then
         put Rx_i into group I
      else
         m_i = time when the HoL packet of the FIFO queue
                  corresponding to Rx_i was created
         put Rx_i into group II
      end if
   end if
end for

s = arg max_i(n_{i,good streams}), Rx_i ∈ group I
if n_{s,good streams} < threshold then
   s = arg min_i(m_i), Rx_i ∈ group II
end if

Schedule packets from receiver Rx_s for transmission
```

chosen station s is the one which satisfies:

$$s = \arg\max_i(n_{i,\text{good streams}}) \tag{8.2}$$

where i traverses all the receivers. The metric used for channel quality is the number of streams over which the post-processing SNR has the value that guarantees the transmission of packets of certain length with maximum predefined PER.

If the post-processing SNR for receivers represented by their CSI at the transmitter is not higher then some threshold, then the scheduler chooses a receiver from the second group whose packet would be the HoL of the FIFO queue common for all the stations in the second group.

After the receiver has been identified, only the packets that have that station's address as the destination, are scheduled for the following transmission.

MU Mode

When MU transmission is allowed, the scheduler has more flexibility in resource allocation. This is illustrated in the example in Figure 8.6.

The MU scheduler makes a decision for each spatial subchannel separately. Each antenna has a set of candidate receivers, and that are the stations with high post-processing SNR on the corresponding spatial subchannel. The HoL of the FIFO queue common to those stations is selected for the transmission from that antenna. In the example in Figure 8.6 for the first antenna there are three candidate stations, whereas for the last antenna only `Rx3` has the acceptable post-processing SNR.

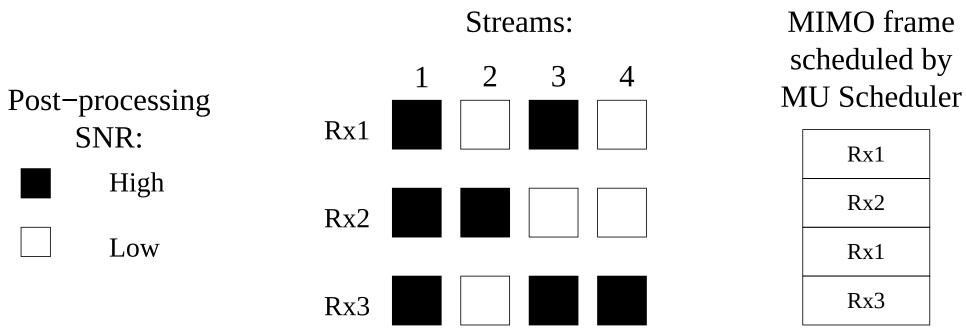

Figure 8.6: MU scheduler with fixed PHY mode

The MU scheduling algorithm is described with pseudocode in Algorithm 8.2. Same as in the previously described SU scheduler, the procedure starts with collecting CSI information from the receivers, and differentiating among the ones whose CSI is present at the transmitter and whose is not.

After that for each antenna the following procedure is repeated: the receiver with the highest post-processing SNR of the signal from that antenna is selected with a packet in the transmitter's data queue for that receiver. If the post-processing SNR is lower than the predefined threshold SNR corresponding to maximum tolerable PER, this receiver is not considered. The scheduler in this case schedules the oldest packet addressed to the receiver from the group of the receivers whose CSI is not known. After a packet has been scheduled, if the transmitter has no remaining packets in the queue for some receiver it is not considered in the next iterations.

Algorithm 8.2 MU scheduler with fixed PHY mode

```
Collect CSI;

for (each receiver Rx_i) do
  if (queue length(Rx_i) ≥ 1) then
    if (there is CSI feedback from Rx_i) then
      put Rx_i into group I
    else
      m_i = time when the HoL packet of the FIFO queue
              corresponding to Rx_i was created
      put Rx_i into group II
    end if
  end if
end for

for (each transmit antenna j) do
  s = arg max_i(ppSNR_{i,j}), Rx_i ∈ group I
  if ppSNR_{s,j} > threshold then
    Schedule the packet for Rx_s
    if Rx_s has no more packets in the queue then
      Remove Rx_s from group I
    end if
  else
    s = arg min_i(m_i), Rx_i ∈ group II
    Schedule the packet for Rx_s
    if Rx_s has no more packets in the queue then
      Remove Rx_s from group II
    else
      m_i = time when the next packet of the FIFO queue
              corresponding to Rx_i was created
    end if
  end if
end for
```

There are several open questions in the described scheduling algorithms. Concerning the threshold SNR in MU mode, a restrictive approach of tolerating very low PER might disqualify all the receivers, and a too high value may lead to frequent retransmissions. In SU mode the receiver CSI threshold for potential link capacity, below which it would be better to use some other link instead, is related to the average performance of the other links. Next, if for a particular user not all the streams have good CSI, the question arises whether it would be better to transmit on all the streams, since transmitting via a bad stream may also lead to a successfull transmission, or to serve just the good streams, which makes the transmission more robust (this question will actually be answered in Section 8.4 that deals with spatial adaptation).

The answers to these questions also depend on the application: if it is data transmission, then the robustness is more important than in case of streaming applications, where sometimes even in case of erroneous receptions, retransmissions are not necessary. This has already been observed in [Vornefeld et al., 1999].

8.3.2 Performance Analysis

The downlink of the AP scenario is used for the performance evaluation of channel aware schedulers with fixed PHY mode. All the stations are assumed located at the same distance from the AP, thus the probability of starvation is minimized since the stations have the same average fading levels. It is assumed that the channel state information of all the users is present at the receiver; at first, the overhead produced for feedback of that information is not considered, but it is treated in detail in Section 8.5.

The maximum tolerable PER is set to 10^{-2}, and the capacity threshold is set to 0. The simulations are done for the number of connections varying from 1 to 20 in overload conditions. The distance between the AP and the other stations is varied in a way that the average SNR at the receiver takes values from 5 dB to 50 dB. The 54 Mb/s PHY mode is used for both SU and MU transmission strategies.

SU-DCF

The throughput in SU-DCF is plotted in Figure 8.7. Dependency on the average input SNR varies with the number of users, since multiuser diversity is exploited.

In the low SNR region, transmissions are not possible since the probability that the post-processing SNR on the channel reaches the threshold value is very low. As the SNR grows, more packets are correctly received.

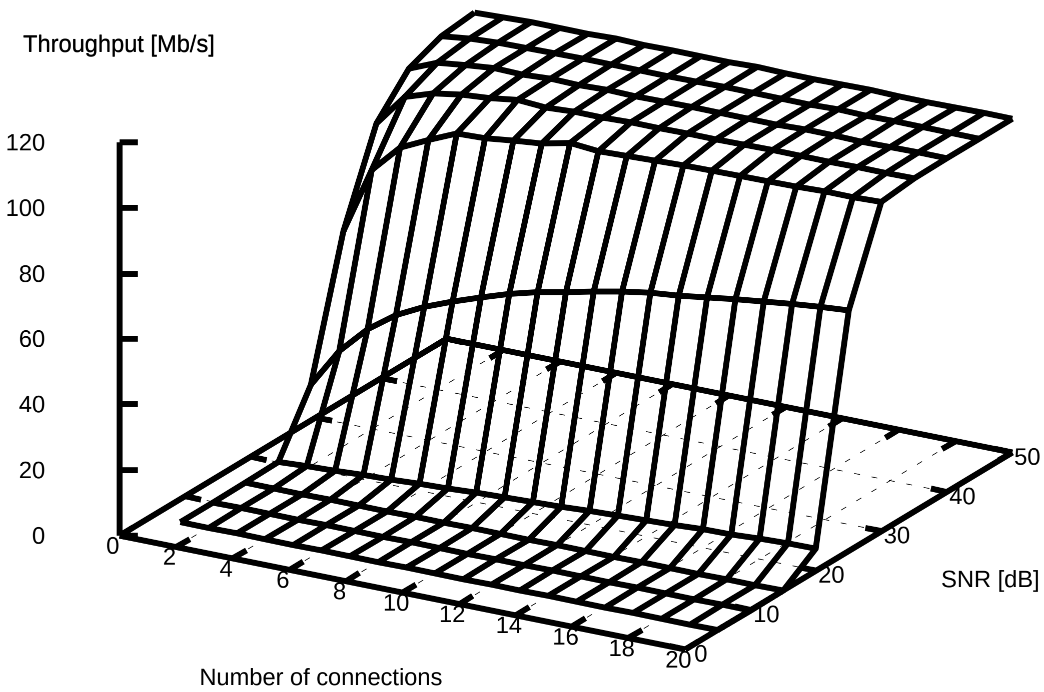

Figure 8.7: Throughput for SU-DCF with channel aware scheduler with fixed PHY modes in case of perfect channel knowledge

By applying the channel aware scheduler, multiuser diversity is exploited, therefore with an increased number of users the performance is significantly improved. This effect is particularly strong at 25 dB.

As the SNR further grows, the throughput reaches the values derived in Section 7.2.2, independently on the number of users, since for all of them the channel is with very high probability in good state.

MU-DCF

The results in case of MU-DCF are presented in Figure 8.8 under OFDMA signaling, and in Figure 8.9 for TDMA signaling.

Same as in SU-DCF, the throughput under extremely low SNR is zero, and under high SNR it reaches the theoretical capacity. However, the performance at moderate SNR differs from that of SU-DCF.

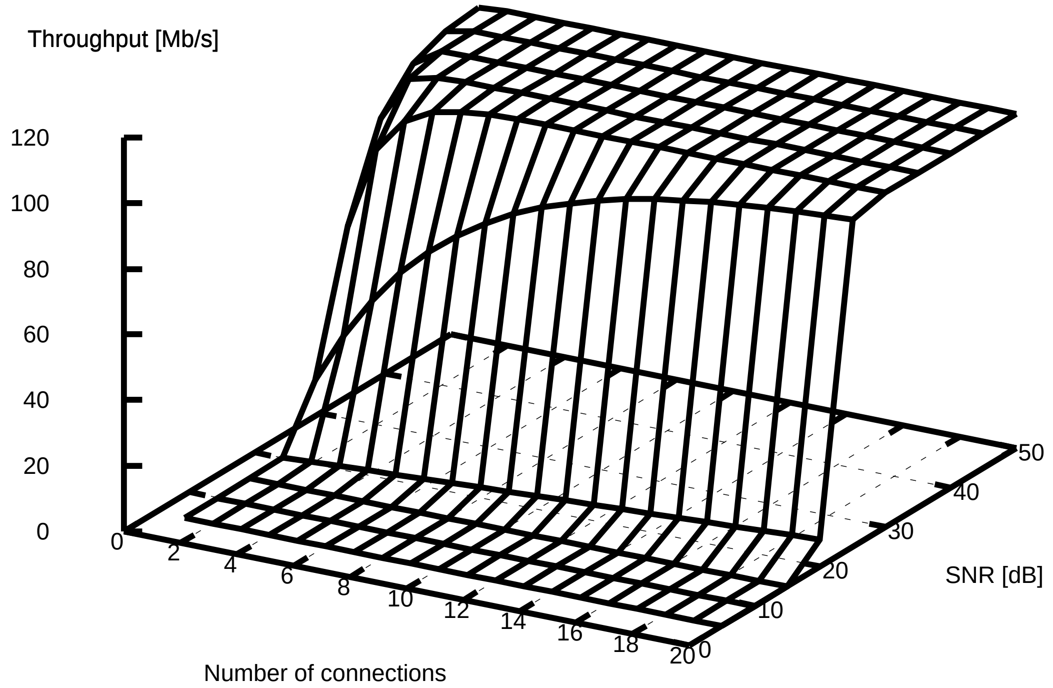

Figure 8.8: Throughput for MU-DCF with OFDMA signaling with channel aware scheduler with fixed PHY modes in case of perfect channel knowledge

With MU transmission, the number of users has more impact on the performance of the system. The throughput grows much faster in MU-DCF than in SU-DCF. The reason is that when the SNR level is not very high, the probability that all the post-processing SNR values of one receiver are also high is not big, and that determines the performance in SU case. On the other hand, in MU case the resolution of exploiting the multiuser diversity is higher: each antenna is transmitting a data packet to the receiver which can hear that antenna with the highest SNR, and the receiver is not unique.

MU-DCF with OFDMA signaling performers better than SU-DCF. However, the performance of MU-DCF with TDMA is somewhat different. As for the scheduler algorithm, it gives the identical decisions in both cases, thus that is not the source of difference.

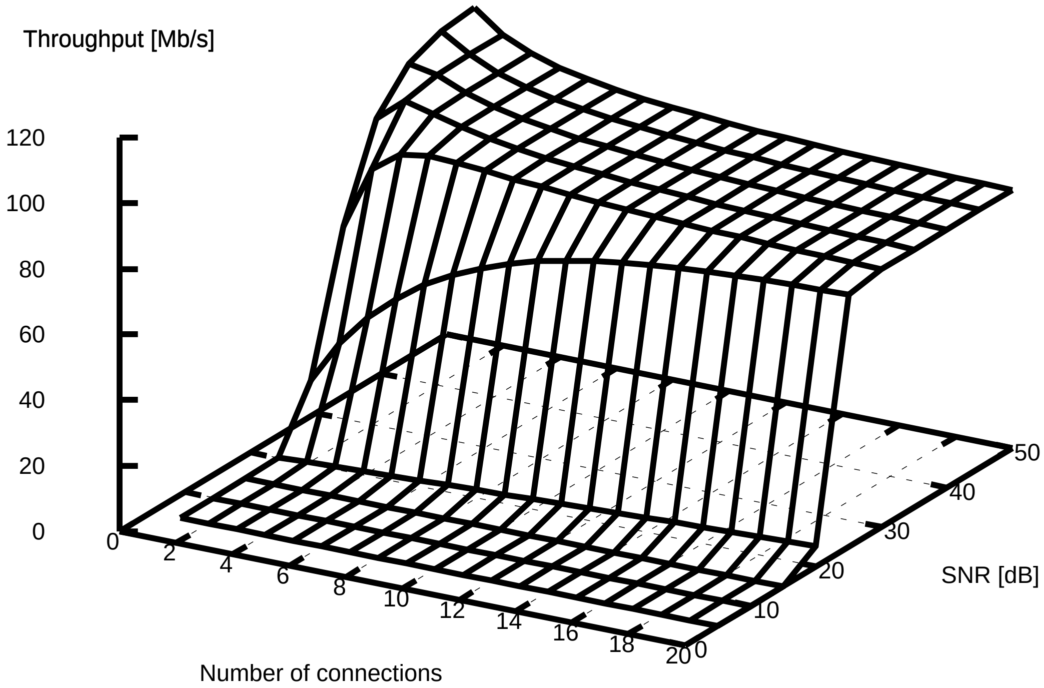

Figure 8.9: Throughput for MU-DCF with TDMA signaling with channel aware scheduler with fixed PHY modes in case of perfect channel knowledge

In previous chapters it has been shown that the overhead with TDMA signaling can be very high, particularly when the number of distinct receivers of a MIMO frame is high, since all have reply to an M-RTS message. When the number of connections in the system grows, the average number of distinct receivers of a MIMO frame also grows and so does the signaling overhead. Therefore the slope of throughput vs. number of connections in moderate SNR level is not as steep as in case of OFDMA signaling. Also, when SNR is high the throughput decreases with the number of connections owing to high signaling overhead. This effect has been shown also in Section 7.2.2. Besides this, high overhead with TDMA signaling contributes to channel incertainty.

For more detailed and quantitative comparison of the analyzed algorithms, their throughput vs. number of connections is plotted in Figure 8.10 at 25 dB and 30 dB SNR. At 25 dB, MU-DCF with OFDMA signaling performs best. The difference in the throughput compared to SU-DCF is more than 30 Mb/s. As for MU-DCF with TDMA signaling, although it exploits the multiuser diversity in the same manner and degree as MU-DCF with OFDMA signaling, on the MAC lever its throughput is less then 10 Mb/s higher than that of SU-DCF.

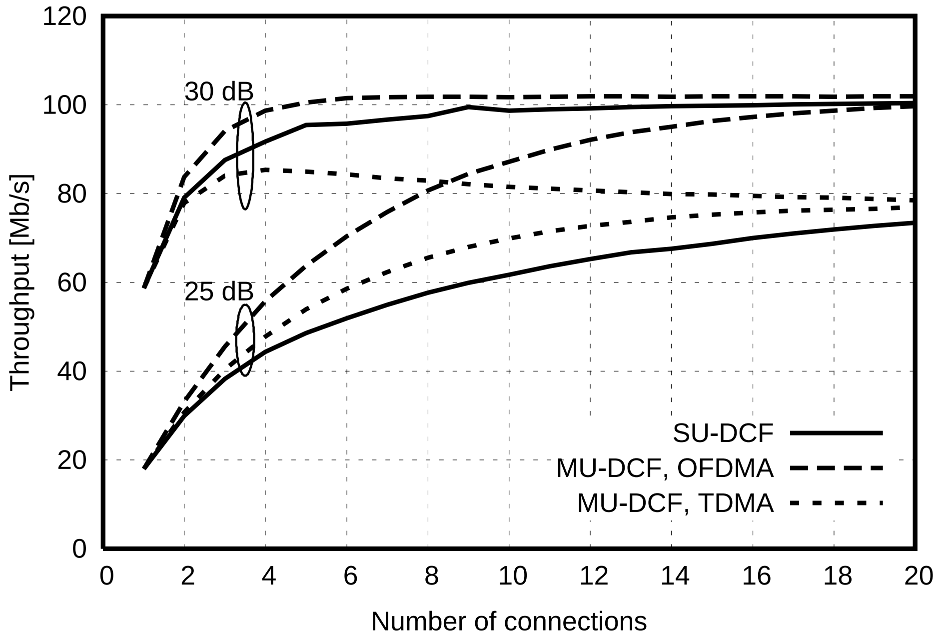

Figure 8.10: Throughput of SU-DCF, and MU-DCF with OFDMA and TDMA signaling at 25 dB and 30 dB SNR in case of perfect channel knowledge

At 30 dB the performance looks different: SU-DCF becomes significantly better then MU-DCF with TDMA signaling, since the average number of “good” streams for the “best” user is increased. However, MU-DCF with OFMDA signaling still performs better due to the higher scheduler flexibility, particularly when the number of stations is small. MU-DCF with TDMA has about 20 dB lower performance due to the high overhead.

For practical systems that, typically, are not operated in overload condition, MU-DCF with OFDMA signaling appears preferable to SU-DCF also from the reason that under SU there might not always be enough packets ready to fill a MIMO frame.

8.3.3 The Impact of CSI Uncertainty

In Section 8.2 it was described how the time varying fading impacts the accuracy of the post-processing SNR in the feedback from the receivers. The performance analysis of the channel aware scheduler operating on these inaccurate values is presented in this section.

In Figures 8.11(a) and 8.11(b) the levels of the throughput at 25 dB and 30 dB SNR are presented for SU-DCF and both versions of MU-DCF when the channel time correlation function is 0.0 and 0.75, respectively. In the first case, SU-DCF throughput does not depend on the number of stations (in case of MU-DCF it reduces due to the higher overhead), since there is no scheduling gain. This performance also corresponds to the case without channel aware scheduling. Hence, figure 8.11(a) can be used as a reference for the scheduling gain.

The throughput in case of a channel time correlation 0.75 (Figure 8.11(b)) is naturally smaller than in case of perfect channel knowledge. MU diversity can still be exploited, but to a smaller degree, thus the steepness on the throughput vs. number of connections curves is smaller compared to Figure 8.10.

In Figure 8.12 the performance of SU-DCF and OFDMA based MU-DCF is compared in the presence of 20 connections with varying channel time correlation. It is interesting to notice that in case of no correlation the performance is practically the same in SU and MU mode. Fine grained scheduling does not bring any benefit since the expectation of the post-processing SNR is the same in both cases. With increasing correlation of the estimated and used channel, throughput increases as well.

The throughput values are listed in Table 8.1 for two cases, perfect channel knowledge and no CSI at the transmitter, with 20 connections. The scheduling gain is particularly high at 25 dB SNR for MU-DCF, where the throughput is increased five-fold with the channel aware scheduler.

In case of low correlation of the estimated and used channel, high PER degrades throughput, but also time is wasted for unsuccessfull transmissions. Thus service time increases.

In Figure 8.13 service time at 25 dB SNR in case of perfect and no channel knowledge is depicted. The service time remains low in case of

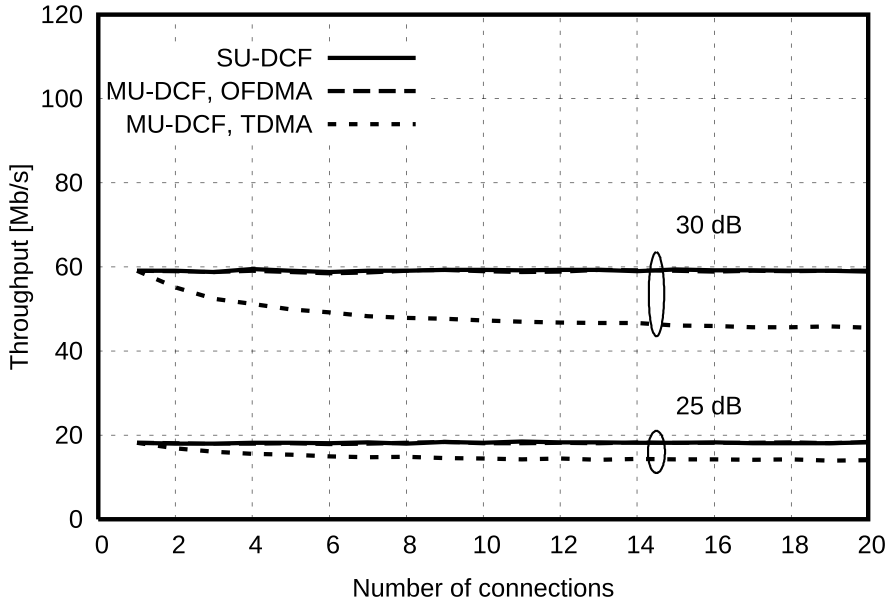

(a) $R(T) = 0.0$

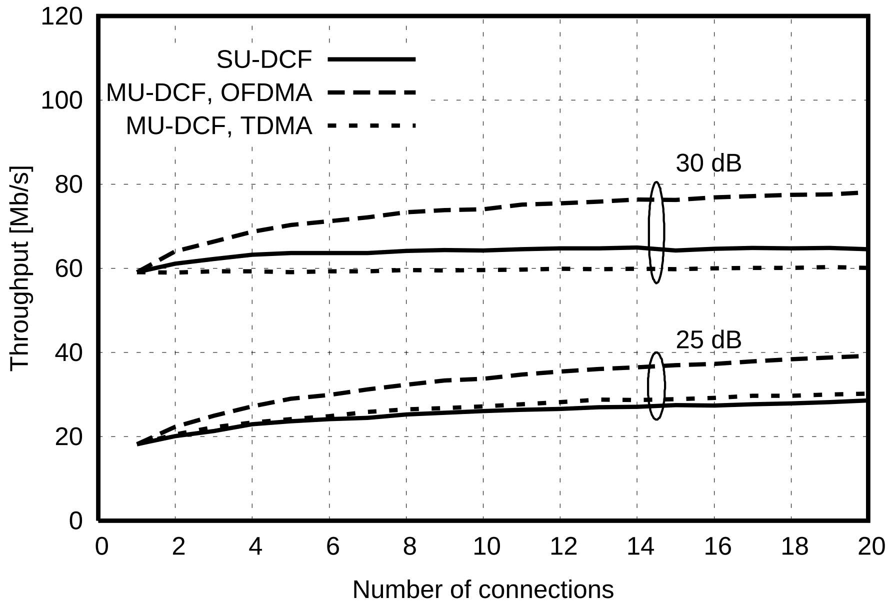

(b) $R(T) = 0.75$

Figure 8.11: Throughput of SU-DCF, and MU-DCF with OFDMA and TDMA signaling at 25 dB and 30 dB SNR, with different channel time correlation coefficient

perfect channel knowledge, particularly in MU case; on the other hand,

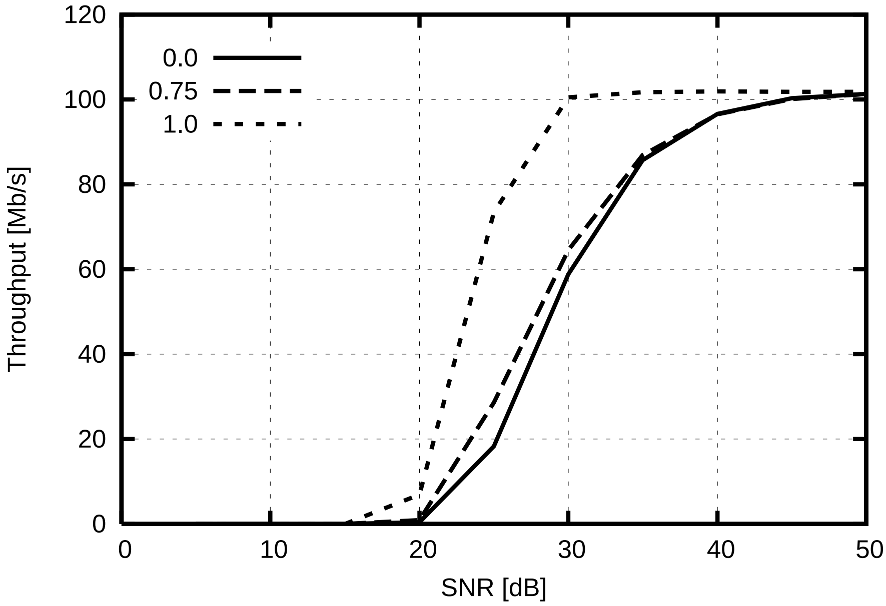

(a) SU-DCF

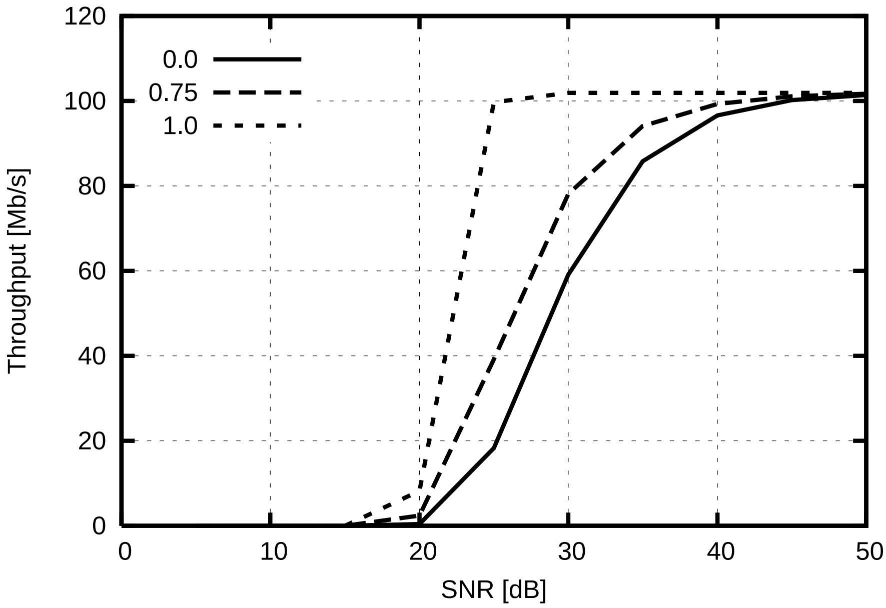

(b) MU-DCF with OFDMA signaling

Figure 8.12: Throughput for different channel time correlation coefficient

with no correlation between the estimated and used channel matrix the service time grows linearly with the number of stations, in both SU and MU cases. Besides high service time, high PER introduces unpredictable

Table 8.1: Throughput in the network with 20 connections

SNR	25 dB	30 dB
Perfect CSI		
SU-DCF	73.42 Mb/s	100.45 Mb/s
MU-DCF, TDMA	76.93 Mb/s	78.53 Mb/s
MU-DCF, OFDMA	99.69 Mb/s	101.89 Mb/s
No CSI		
SU-DCF	18.25 Mb/s	59.08 Mb/s
MU-DCF, TDMA	13.25 Mb/s	42.96 Mb/s
MU-DCF, OFDMA	18.18 Mb/s	59.03 Mb/s

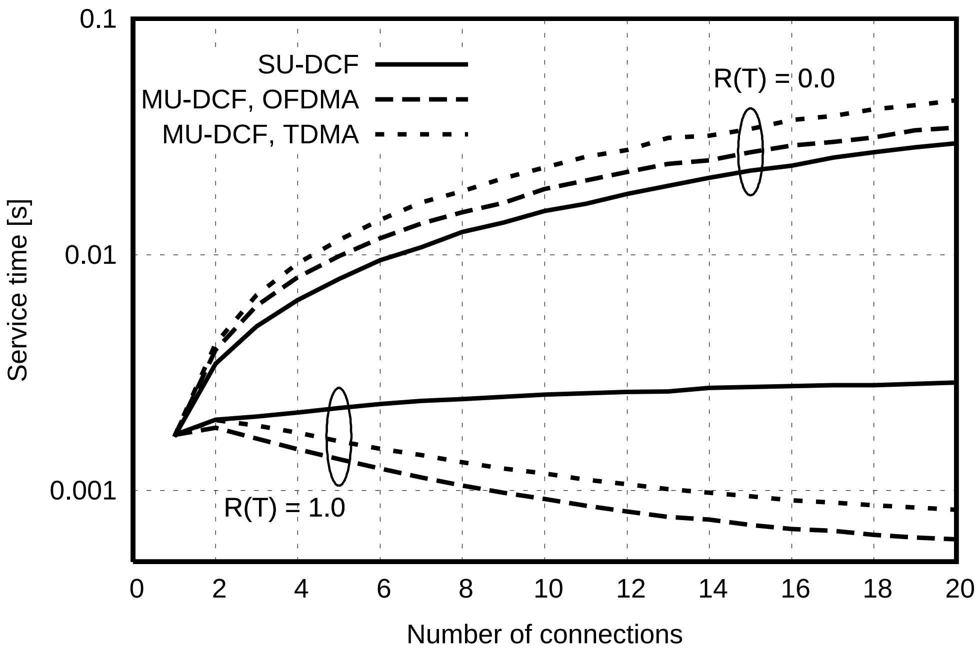

Figure 8.13: Service time of SU-DCF, and MU-DCF with OFDMA and TDMA signaling at 25 dB SNR at different channel time correlation coefficient

delay on higher layers, as well as low channel efficiency.

8.4 Channel-Aware Scheduling with Adaptive Modulation and Coding (AMC)

In this section more degrees of freedom are given to the channel aware scheduler. Instead of only deciding if the particular spatial subchannel is in good state, or how many good subchannels a station can establish, and then use the channel with the predefined PHY mode, the improved scheduler can choose the optimum PHY mode for the given channel realization.

Additional degrees of freedom are added gradually: in the first step, the scheduler performs only AMC on each stream, while the number of streams, and thus the MIMO scheme is fixed. In the second step, the scheduler determines the optimum number of streams for the given channel realization. There, the so called Spatially Adaptive Modulation and Coding (SAMC) is performed prior to applying per-stream AMC.

At first, only link level performance is analyzed, followed by investigation of MU diversity gain on the system level.

8.4.1 Link Level Study

AMC with Fixed MIMO scheme

AMC for a MIMO link is described in Algorithm 8.3. The algorithm operates as a conventional AMC algorithm, with the difference that is uses post-processing SNR values as input parameters to assign the PHY mode for each transmit antenna.

In case that PHY modes can vary on each stream, the lowest chosen PHY mode will determine the duration of the MIMO frame transmission. From the PHY modes defined in IEEE 802.11a standard (Table 4.2), only a subset is used: 12 Mb/s, 24 Mb/s, 36 Mb/s and 48 Mb/s. In order to have a fair comparison, all the MIMO frames are built in a way that their length corresponds to the length of a frame transmitted at 12 Mb/s, even if that is not the lowest used PHY mode. Using the MIMO frame structure as shown in Figure 8.14, the number of packets transmitted with bitrate r on a certain transmit antenna is $\frac{r}{12\,Mb/s}$. It should be noted that this MIMO frame structure has the potential to achieve substantially lower effective overhead than previously analyzed scheme, where only one packet per transmit antenna was scheduled within one transmission window, thus direct comparison of these schemes is not possible.

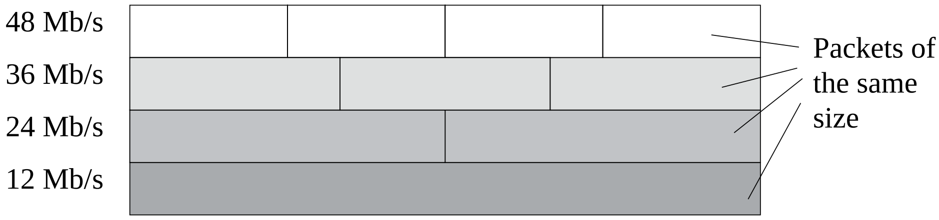

Figure 8.14: MIMO frame structure with variable PHY mode of individual data streams; only a subset of IEEE 802.11a PHY modes is used

---

Algorithm 8.3 AMC for a MIMO link

---

for (each transmit antenna j) **do**
  ppSNR_j = post-processing SNR for antenna j
  Assign the highest PHY mode r_j to antenna j, so that PER $<$ PER_{max}
  Schedule $\frac{r_j}{12\,Mb/s}$ packets for transmission from antenna j
end for

In Figure 8.15 MAC level data rate vs. SNR over a single link using a fixed number of streams and AMC is presented. Links with 1, 2, 3 and 4 transmit antennas are analyzed under a maximum tolerable PER 10^{-2}. The data rate with AMC is plotted with solid lines, whereas the other line styles correspond to fixed PHY modes. One would expect that the solid line would be exactly the envelope of the other ones. However, it can be seen that in all cases the solid line outperforms the fixed PHY mode policy, particularly in SNR regions where the curves corresponding to neighboring PHY modes intersect.

The reason for this is the following: when PHY modes are fixed, the same PHY mode is used for each channel realization, independently of the post-processing SNR level. With AMC over a MIMO link, adaptation is done over the post-processing SNR level of each stream individually. If the adaptation had been done over the average SNR value, thus the same PHY mode would have been assigned to each transmit antenna, then the solid line would have matched the envelope of the data rate achieved by fixed PHY mode assignment. It can also be seen that the gain grows with

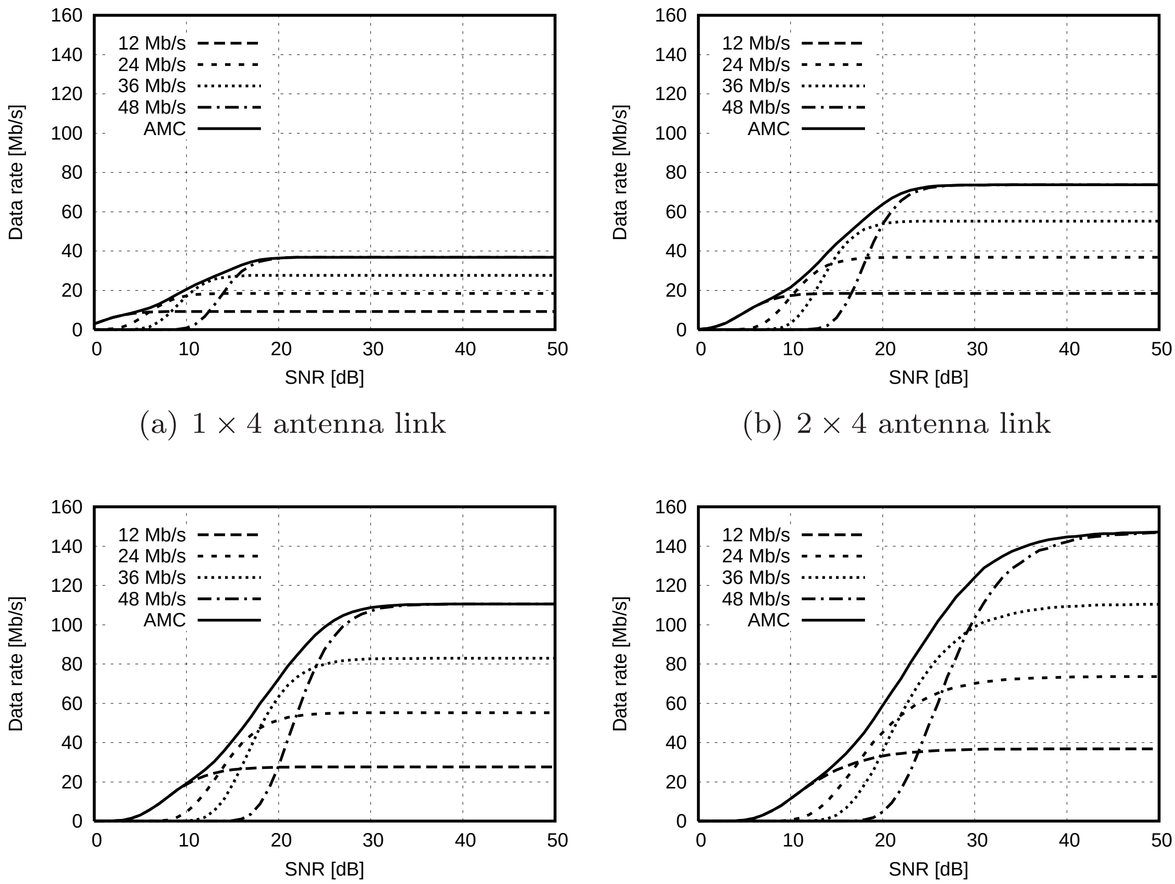

(a) 1×4 antenna link

(b) 2×4 antenna link

(c) 3×4 antenna link

(d) 4×4 antenna link

Figure 8.15: Data rate with AMC with varying number of transmit antennas

the number of used spatial subchannels; the reason is that the variance of post-processing SNR is higher in pure multiplexing schemes, as shown in Section 6.1.3.

The capacity gain over fixed PHY mode assignment is plotted in Figure 8.16 for different maximum tolerable PER values: 10^{-1}, 10^{-3} and 10^{-5}. The first thing to notice is the shape of the curves: there are three peaks, each corresponding to a switching point between two neighboring PHY modes, and they happen at approximately same SNR. The higher the data rate of these PHY modes is, the higher is also the gain: it goes beyond 25 Mb/s at about 29 dB with 10^{-1} maximum tolerable PER.

The shapes of the curves corresponding to different maximum tolerable PER levels are the same. However, the exploited capacity gain grows with that level because of less restrictive PHY mode assignment. However, the number of packet errors also grows, increasing retransmission frequency and degrading the performance of higher layers.

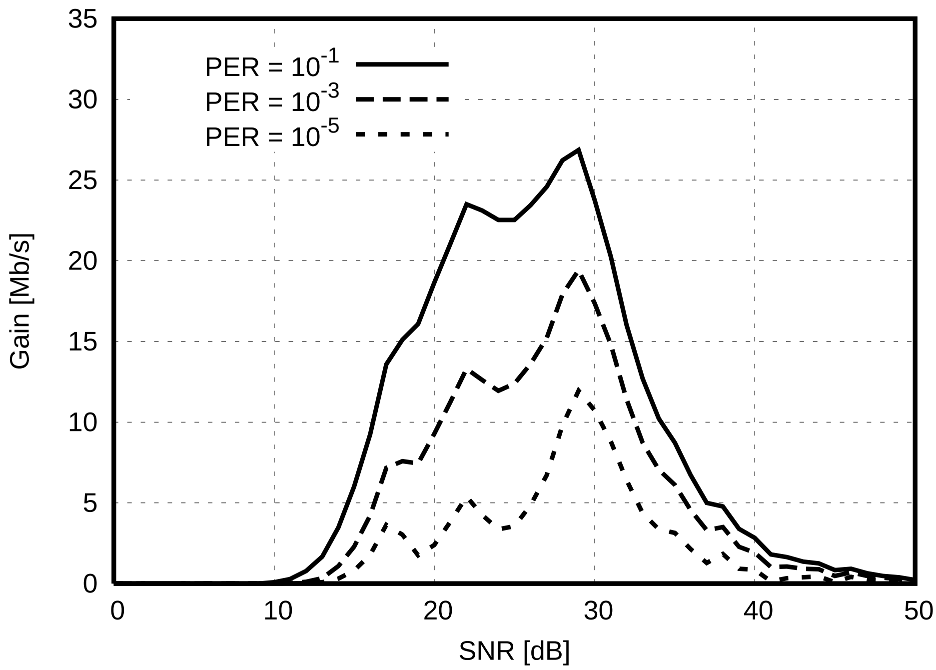

Figure 8.16: Capacity gain achieved with AMC under fixed MIMO (4×4 antenna link)

Spatially Adaptive Modulation and Coding (SAMC)

By relaxing the constraint about the fixed MIMO scheme, the adaptive scheduler applies so called SAMC, that is described in Algorithm 8.4. The algorithm compares the post-processing SNR and related PHY modes over all possible $\binom{M_t}{k}$ k-combinations of transmit antennas, with $k = 1 \cdots M_t$, and the combination that achieves the maximum data rate is selected. This is a combination of antenna selection and AMC.

Figure 8.17 compares AMC over 1×4, 2×4, 3×4 and 4×4 antenna links to the SAMC algorithm at PER 10^{-2}. In the figure, the data rate vs. SNR is presented. Again, the SAMC curve does not match the envelope of AMC curves with fixed MIMO scheme, but more flexibility in the scheduling algorithm brings additional capacity gain.

It is also interesting to compare the data rate achievable with SAMC using different maximum tolerable PER levels as presented in Figure 8.18.

Algorithm 8.4 SAMC for a MIMO link

for $(k = 1,\ k <= M_t,\ k++)$ **do**
  for (each k-combination $C_{k,c}$ of transmit antennas, $R(T) = 1 \cdots \binom{M_t}{k}$) **do**
    for (each active transmit antenna j) **do**
      $\mathrm{ppSNR}_{k,c,j}$ = post-processing SNR for antenna j
      Assign the highest PHY mode $r_{k,c,j}$ to antenna j, so that PER < PER_{max}
      Allocate antenna j for transmission of $\frac{r_{k,c,j}}{12\,Mb/s}$ packets
    end for
    Aggregate bitrate for combination $C_{k,c}$ is calculated as $r_{k,c} = \sum_j r_{k,c,j}$
  end for
end for
Choose the combination of antennas C_{n_s,k_s}, $(n_s, k_s) = \arg\max_{k,c}(r_{k,c})$, and the corresponding PHY modes for data transmission

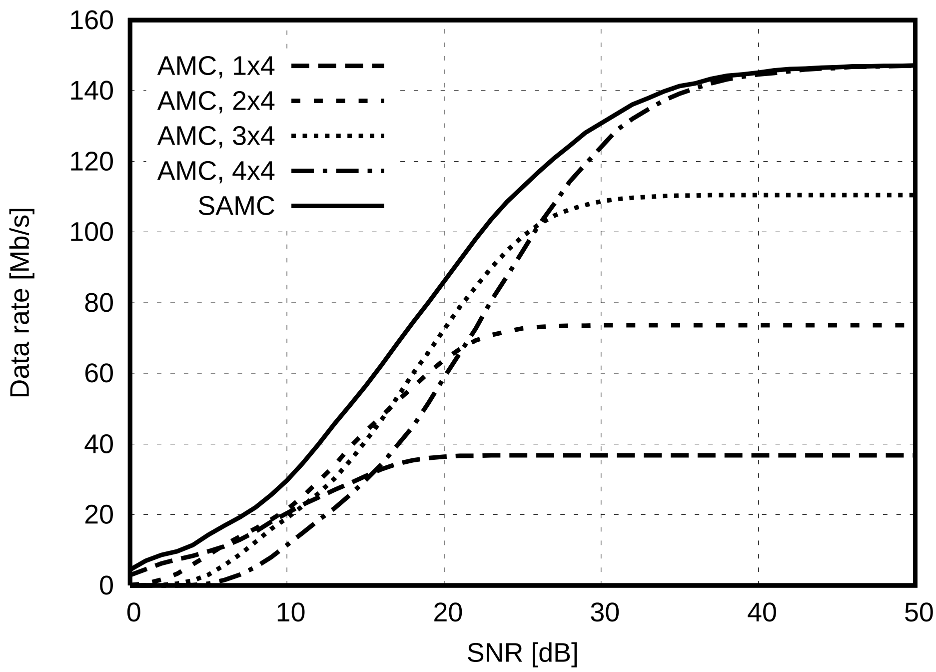

Figure 8.17: AMC with fixed MIMO scheme compared to SAMC at PER = 10^{-2}

The highest data rate is achieved with the highest tolerable PER: the difference at 20 dB SNR for the PER values considered is more than 20 Mb/s.

In Figure 8.19 SAMC capacity gain over corresponding AMC is plotted for different maximum tolerable PER levels. The capacity gain is approx-

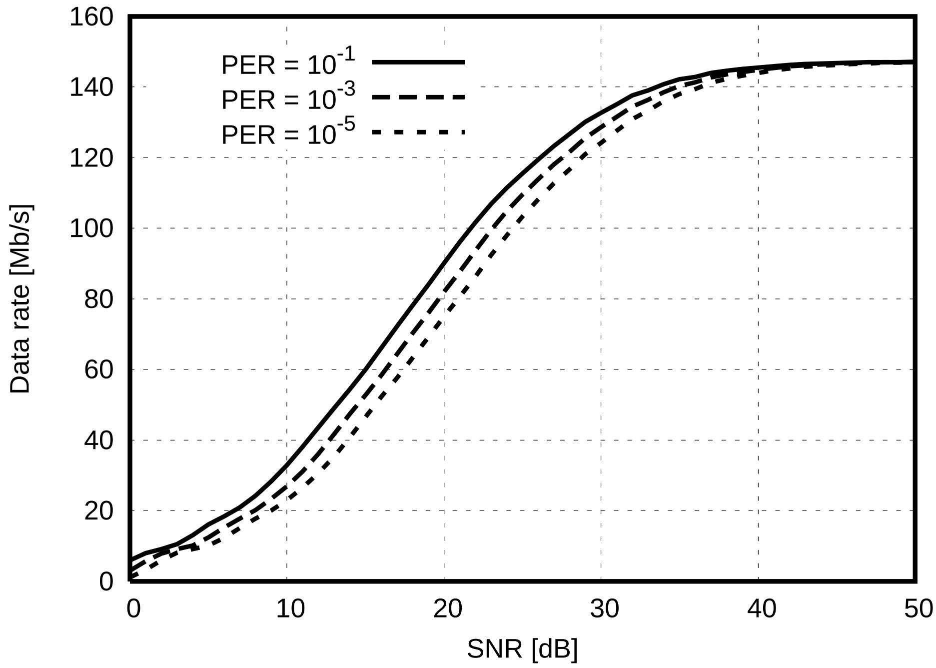

Figure 8.18: Data rate with SAMC algorithm with different maximum tolerable PER levels

imately the same for all the cases analyzed, but it is shifted in SNR, so that the same gain is achieved earlier in case of higher tolerable PER than in case of lower tolerable PER.

It should be also noted that with AMC, the exact values of achieved gain highly depend on PHY modes over which the adaptation is done; however, the conclusions made here still apply in general.

In Figure 8.19 the average number of used transmit antennas with SAMC is plotted. It shows the tendency of using larger number of spatial streams when the SNR value grows. Occasional stagnation intervals occur due to the selected subset of PHY modes: for a certain SNR value using less streams with higher PHY mode yields higher data rate then using more streams with lower PHY mode.

The Impact of Channel Uncertainty

The accuracy of channel knowledge impacts the scheduler performance with both AMC and SAMC algorithms. Figure 8.20 compares SAMC and AMC with fixed MIMO and PER $= 10^{-2}$ when the used and estimated

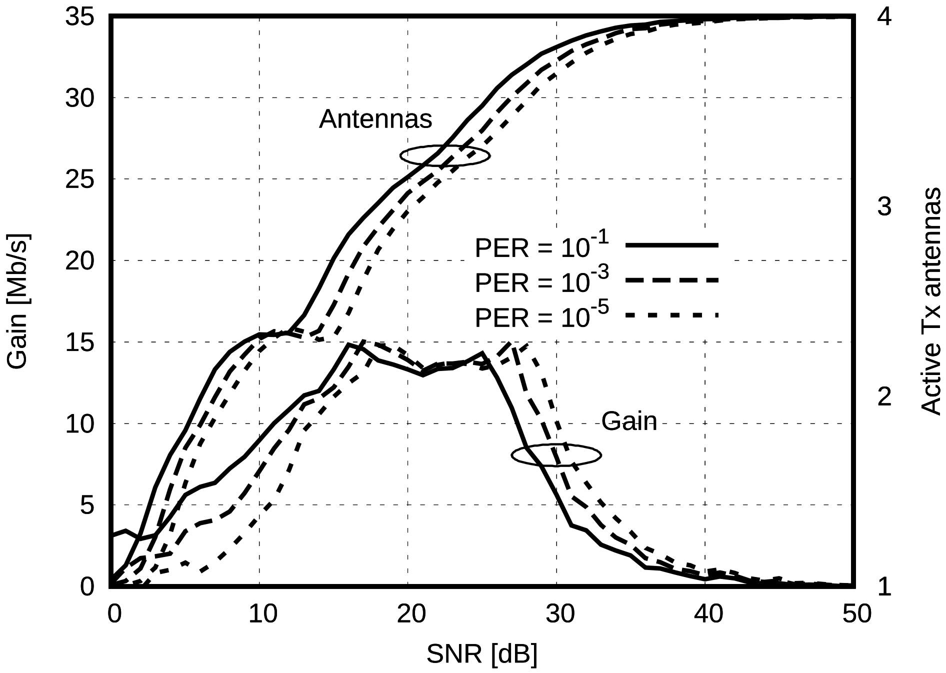

Figure 8.19: Capacity gain and the mean number of transmit antennas with SAMC algorithm with different maximum tolerable PER levels

channels are uncorrelated (outdated channel knowledge).

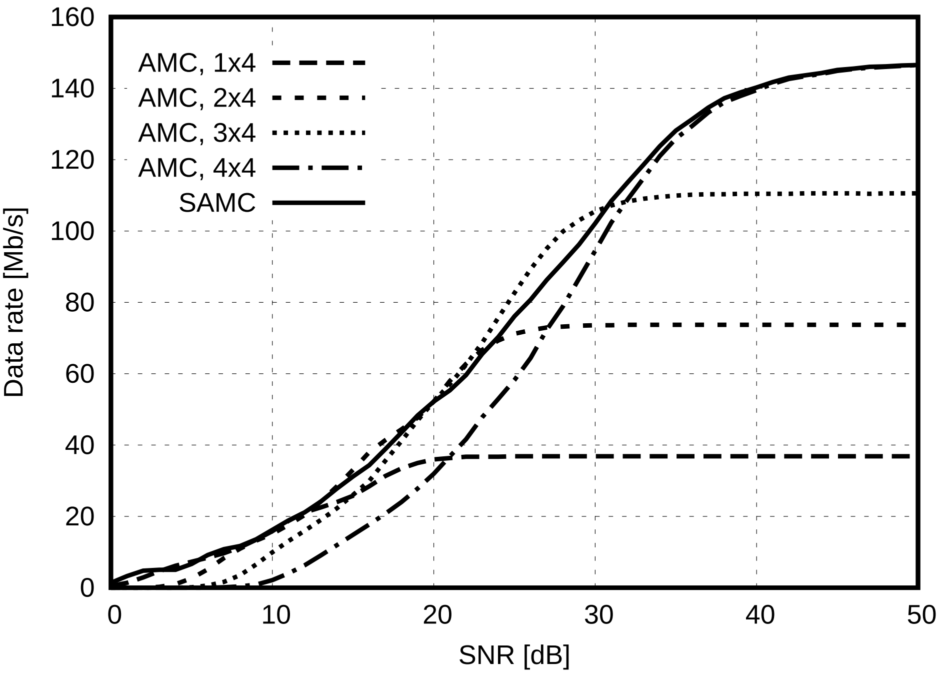

Figure 8.20: AMC data rate with fixed MIMO scheme compared to SAMC at $R(T) = 0$ and PER $= 10^{-2}$

Under this condition, a spatial adaptation deteriorates the performace, because of the “greedy” behavior of the scheduler: e.g. at 23-30 dB SNR, the SAMC scheduler performs worse than the AMC scheduler with fixed 3×4 antenna scheme. The reason is the following: as depicted in Figure 8.19, spatially adaptive scheduler chooses preferentially the 4×4 antenna scheme, that leads to lower average post-processing SNR than 3×4 antenna scheme. If the AMC algorithm is applied on these estimated post-processing SNR values, although they will differ from the actual post-processing SNR values, with 3×4 antenna scheme the probability is higher that the actual post-processing SNR level will not drop below the threshold for the chosen PHY mode.

In Figures 8.21(a) and 8.21(b) the data rate with SAMC algorithm under variable degree of channel uncertainty in terms of channel time correlation is presented, for a maximum tolerable PER of 10^{-1} and 10^{-5}, respectively. The performance is evaluated for the channel time correlation coefficients of value 1.0, 0.75 and 0.0. It can be seen that the difference among the curves with the higher PER threshold is much larger than for of lower PER thresholds. The reason is that under high PER, the choice of PHY mode is more sensitive to channel estimation inaccuracy: a small decrease of post-processing SNR might push PER to very high values, whereas under low PER threshold even if the corresponding post-processing SNR decreases, PER remains low.

8.4.2 System Level Study

Previously described link adaptation methods are applied in the schedulers, that are specified by Algorithms 8.5, 8.6 and 8.7. The first one applies AMC for each stream in SU mode, and chooses the user that maximizes the data rate; Algorithm 8.6 applies AMC in MU mode, and Algorithm 8.7 applies the SAMC in SU mode. SAMC in MU mode is not considered due to complexity; however, in MU mode the presence of MU diversity is expected to compensate for incomplete adaptivity.

The main goal of the analysis in this chapter is the comparison of capacity gains achieved on the system level with spatial adaptation and SU transmission on one hand, and MU diversity on the other. The performance evaluation is done for the AP scenario, for a variable number of stations, under varied distance from the AP. For the fixed MIMO scheme

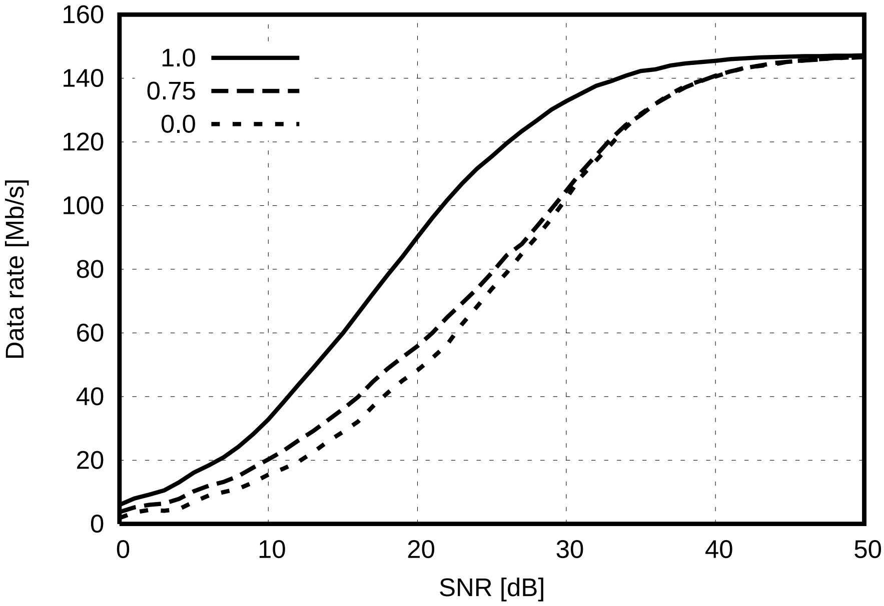

(a) Maximum tolerable PER 0.1

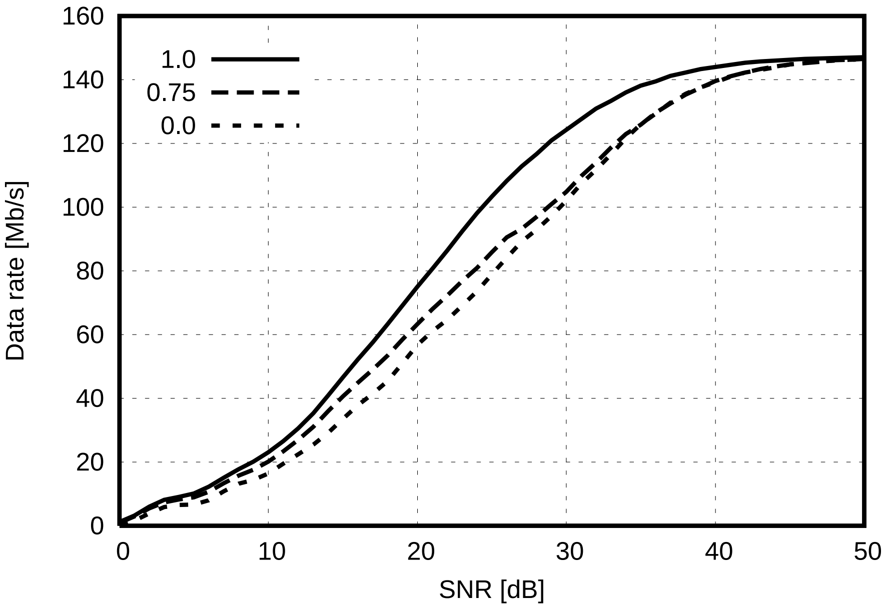

(b) Maximum tolerable PER 10^{-5}

Figure 8.21: Data rate with SAMC for different channel time correlation levels with different maximum tolerable PER

schedulers, the 4×4 antenna scheme is used.

Algorithm 8.5 SU scheduler with AMC and fixed MIMO scheme

Collect CSI;

for (each receiver $\mathrm{Rx_i}$) **do**
  if (there is CSI feedback from $\mathrm{Rx_i}$) **then**
    for (each transmit antenna j) **do**
      Assign the highest PHY mode r_j to antenna j, so that PER < PER_{max}
    end for
    Calculate the aggregate bitrate r_i for receiver $\mathrm{Rx_i}$
    Put $\mathrm{Rx_i}$ into group I
  else
    $m_i =$ time when the HoL packet of the FIFO queue corresponding to $\mathrm{Rx_i}$ was created
    Put $\mathrm{Rx_i}$ into group II
  end if
end for

$s = \arg\max_i(r_i)$, $\mathrm{Rx_i} \in$ group I
if $r_i >$ threshold **then**
  for (each transmit antenna j) **do**
    Schedule $\frac{r_{s,j}}{12\,Mb/s}$ packets for transmission from antenna j
  end for
else
  $s = \arg\min_i(m_i)$, $\mathrm{Rx_i} \in$ group II
  For each transmit antenna schedule one packet from user s for transmission using the lowest PHY mode
end if

In Figure 8.22 throughput vs. SNR with the described scheduling algorithms is presented. Four cases are observed: 1 and 10 connections, both in case of perfect channel knowledge at the transmitter, and in case of no correlation between the estimated and used channel.

Figure 8.22(a) shows the throughput in case of 1 connection and perfect channel knowledge. Naturally, schedulers with fixed MIMO scheme with 1 connection only have the same performance in MU and SU mode. The scheduler with SAMC has significantly better performance, particularly when SNR is between 15 dB and 25 dB, since the MIMO scheme is adapted.

Algorithm 8.6 MU scheduler with AMC and fixed MIMO scheme

```
Collect CSI;

for (each receiver Rx_i) do
   if (there is CSI feedback from Rx_i) then
      for (each transmit antenna j) do
         Assign the highest PHY mode r_{i,j} to antenna j, so that PER <
         PER_max
      end for
      put Rx_i into group I
   else
      m_i = position of the oldest packet for Rx_i in the queue
      put Rx_i into group II
   end if
end for

for (each transmit antenna j) do
   among the receivers that achieve the rate max_i(r_{i,j}), Rx_i ∈ group I,
   find the receiver Rx_s with the oldest packet in the data queue
   if r_{s,j} > threshold then
      Schedule the r_{s,j} / (12 Mb/s) packets for Rx_s
      if Rx_s has no more packets in the queue then
         Remove Rx_s from group I
      end if
   else
      s = arg min_i(m_i), Rx_i ∈ group II
      Schedule the packets for Rx_s
      if Rx_s has no more packets in the queue then
         Remove Rx_s from group II
      else
         m_i = position of the next oldest packet for Rx_i in the queue
      end if
   end if
end for
```

In the presence of MU diversity with 10 connections in Figure 8.22(b), all the algorithms show better performance. However, the schedulers with fixed MIMO scheme benefit more from MU diversity, thus the difference in performance of the three algorithms is decreased. The scheduler with the fixed MIMO scheme operating in SU mode has the poorest performance.

Algorithm 8.7 Scheduler with SAMC

Collect CSI;

for (each receiver $\mathrm{Rx_i}$) **do**
  for ($k = 1$, $k <= M_t$, $k++$) **do**
    for (each k-combination $C_{k,c}$ of Tx antennas, $R(T) = 1 \cdots \binom{M_t}{k}$) **do**
      for (each active transmit antenna j) **do**
        Assign the highest PHY mode $r_{i,k,c,j}$ to antenna j,
        so that PER $<$ PER$_{max}$
        Allocate antenna j for transmission of $\frac{r_{i,k,c,j}}{12\,Mb/s}$ packets
      end for
      Aggregate bitrate for combination $C_{k,c}$ is calculated as
      $r_{i,k,c} = \sum_j r_{i,k,c,j}$
    end for
  end for
  Choose the combination of antennas C_{i,n_s,k_s}, $(n_s, k_s) = \arg\max_{k,c}(r_{i,k,c})$,
  and the corresponding PHY modes
end for

Schedule packets to the receiver p for transmission, $p = \arg\max_i C_{i,n_s,k_s}$

With 10 connection, when SNR is high, MU scheduler has the lowest throughput due to higher overhead.

The performace in the two analyzed scenarios in the presence of high channel uncertainty is illustrated in Figures 8.22(c) and 8.22(d). Although performance is degraded with both scenarios (1 and 10 connections), it can be seen that with 10 connections the throughput is reduced more. The reason is that under MU diversity the transmitter sees the equivalent channel better than it really is. Therefore, the scheduler with adaptive MIMO scheme wrongly chooses a MIMO scheme with more spatial streams as visible from the average number of active transmit antennas vs. SNR for variable number of connections in Figure 8.23. Moreover, the scheduler tends to apply higher valued PHY modes. However, since the estimated channel is not correlated with the channel at the time it is used, "bigger" mistake is made than if more robust MIMO scheme and PHY had been chosen.

This effect is also visible from Figure 8.24, where throughput vs. number of connections at 20 dB SNR is shown, for three values of channel

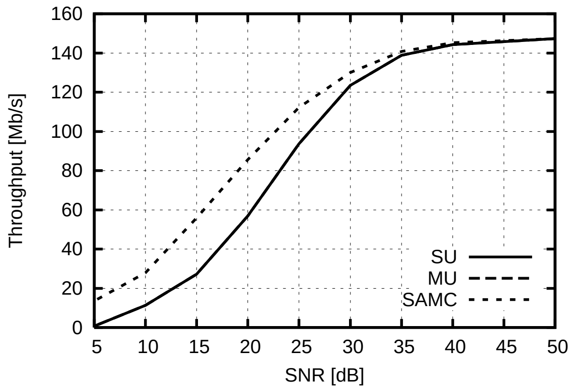

(a) 1 connection, $R(T) = 1.0$

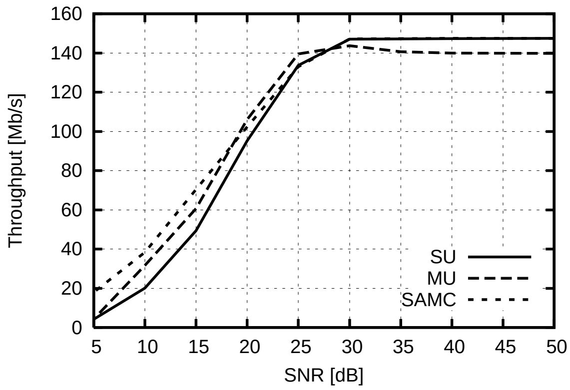

(b) 10 connections, $R(T) = 1.0$

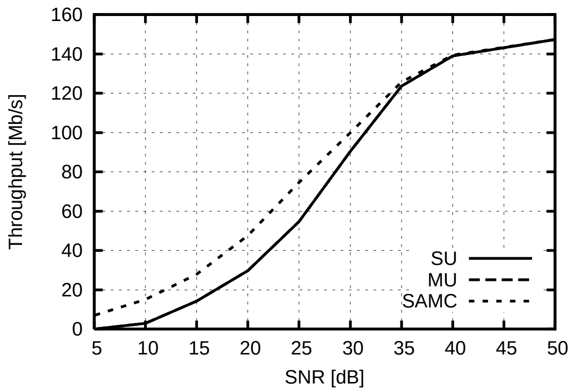

(c) 1 connection, $R(T) = 0.0$

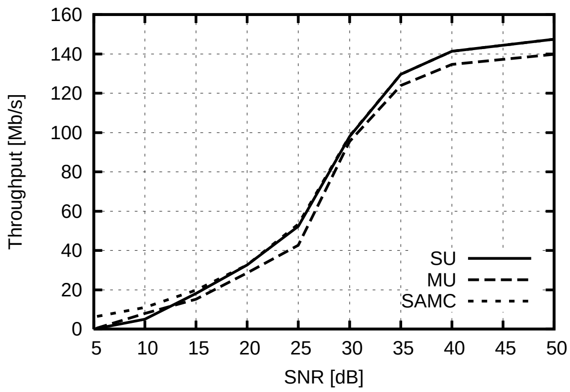

(d) 10 connections, $R(T) = 0.0$

Figure 8.22: Throughput with different scheduling policies vs. SNR, for varying number of stations with perfect ($R(T) = 1.0$) and outdated ($R(T) = 0.0$) CSI

correlation function $R(T)$: 1.0, 0.75 and 0.0. With perfect channel knowledge (Figure 8.24(a)), the capacity gain due to MU diversity can be seen. Since the SNR is not very high, the best performance is achieved by the MU scheduler.

However, when $R(T)$ reduces to 0.75, the performance dramatically deteriorates (Figure 8.24(b)). It can be seen that the scheduler with SAMC gives much better performace than the other ones, since it uses more robust MIMO schemes. The performance in this case is closer to the performance of no correlation of estimated and used channel (Figure 8.24(c)) than to that of perfect channel knowledge.

Therefore, channel aware schedulers should be applied with caution,

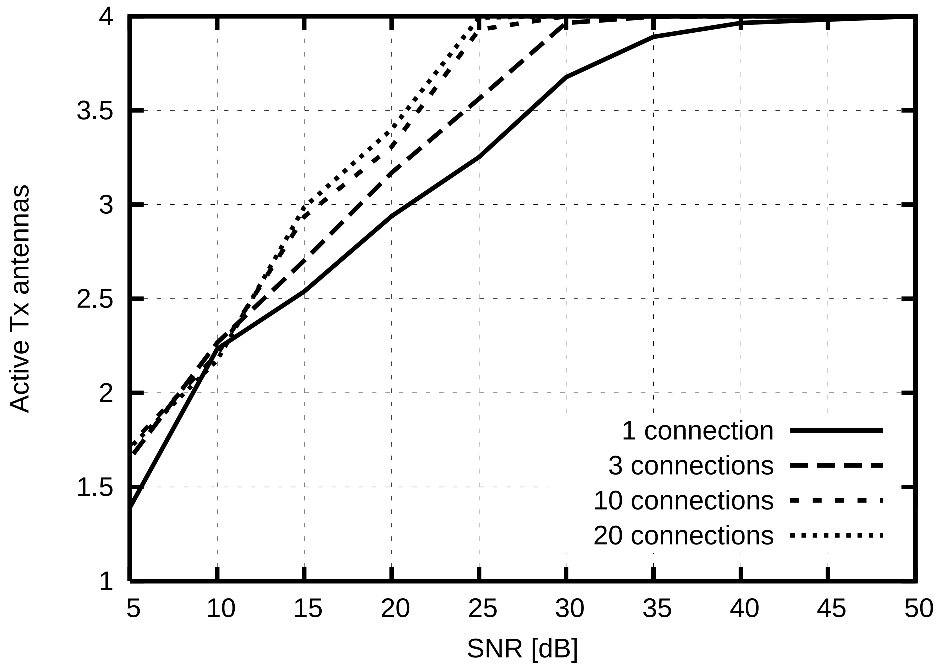

Figure 8.23: The average number of transmit antennas selected by SAMC algorithm depending on the number of connections

as already suggested when discussing the standard deviation of post-processing SNR given in Figure 6.5. Not only that channel aware scheduling does not provide any gain in case of low correlation of estimated and used channel, but it may even lead to worse performance than schedulers that do not take into account any CSI.

8.5 CSI Feedback Provision

In the foregoing analysis it has been assumed that the CSI is known at the transmitter. In this section the focus is on the overhead produced when providing this information by the receiver.

The first question which is naturally raised is related to the number of the stations which are to send their channel feedback. either in TDMA or in OFDMA manner. More precisely, when does the overhead for providing channel feedback to the transmitter cost more than what is gained by applying channel aware scheduling?

Transmitting in OFDMA manner increases the complexity of the sys-

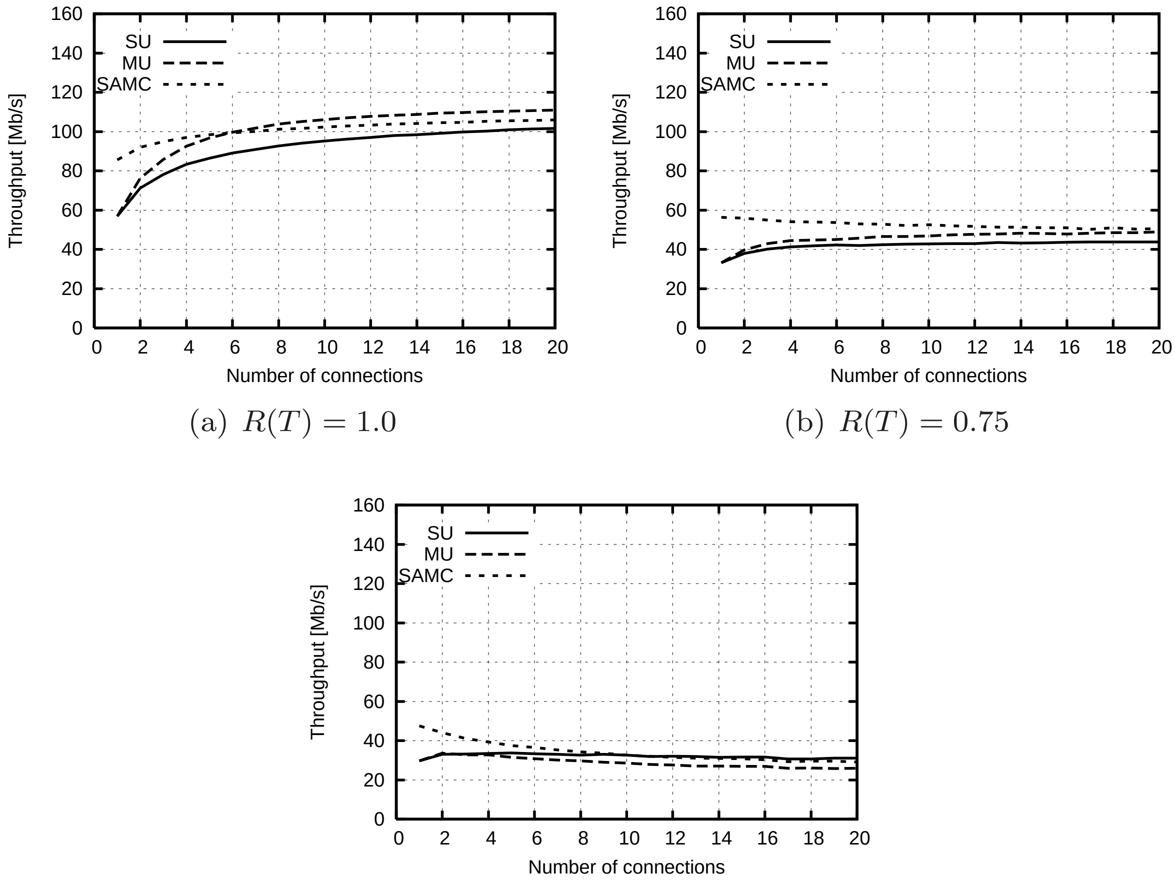

(a) $R(T) = 1.0$

(b) $R(T) = 0.75$

(c) $R(T) = 0.0$

Figure 8.24: Throughput with different scheduling policies at 20 dB SNR vs. number of connections, varying channel time correlation

tem, but significantly reduces the time needed for the stations addressed by MU-RTS to transmit their CSI within M-CTS frames. Figure 8.25 gives the minimum factor by which the throughput should increase with channel aware scheduling in order to justify the time needed by the transmitter to collect the CSI from 1, 5 and 10 stations for a duration of the transmission window in the range from 0 to 1 s. Clearly, there is no interest in all parameter combinations where the increase factor is 1.0 or below

The figure shows that using the channel knowledge for very short transmission windows requires very high scheduling gain, particularly with TDMA signaling. On the other hand, the longer the transmission window is, the less reliable is the CSI, particularly at the end of the transmission,

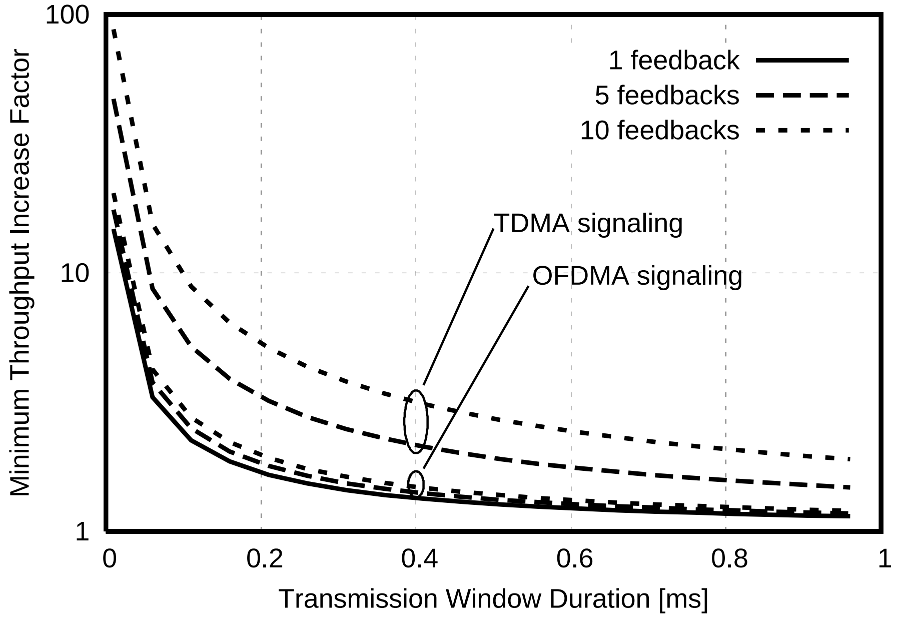

Figure 8.25: Overhead produced by CSI feedback

due to time variant channel fading.

This leads to another advantage of OFDMA compared to TDMA signaling, and that is the fact that since the transmission of CSI lasts shorter, the time between the channel estimation and its usage is shorter, too, thus the post-processing SNR correlation is expected to be higher.

Referring to Figure 8.1, since the the duration of one M-RTS - M-CST - data - M-ACK cycle is about 400 μs with data frame length of 1024 byte at 54 Mb/s, channel aware scheduling can be applied only in prevailingly stationary scenarios. Otherwise, the estimated channel matrix will not be up-to-date and the scheduler decision will be far from optimum. This applies for both higher terminal speeds and higher frequencies.

8.6 Summary

This chapter gave some important insights on channel aware scheduling in MU environment under channel uncertainty. In the first step, the analysis of the post-processing SNR correlation revealed high sensitivity to imperfect correlation of estimated and used channel matrix. Then, channel aware scheduling with different degrees of freedom are analyzed, on the link and system level, and with perfect and outdated CSI.

SU schedulers generally fail to exploit MU diversity in the same extent as MU schedulers. However, even in the presence of MU diversity, in low SNR range spatial adaptation proves to be better approach, by trading multiplexing gain for diversity.

Outdated CSI that affects the accuracy of estimated post-processing SNR also translates to degraded performance of schedulers. That applies in particular in the presence of MU diversity, since in that case the scheduler sees that channel better that it actually is and wrongly assigns more streams and applies higher valued PHY modes.

CHAPTER 9

Conclusion

MIMO communications are globally seen as a key technology for the next generation wireless networks (e.g. 3GPP LTE, IEEE 802.16 and IEEE 802.11n), because of their potential to dramatically increase the system performance (such as capacity or robustness of transmissions) without the additional power of bandwidth.

This thesis deals with higher layer aspects of MIMO systems, in particular MAC layer. The performance of different MIMO schemes, with different system parameters varied is investigated on the proposed IEEE 802.11 based MAC protocol with support for spatial multiplexing using multiple antennas.

The analyzed protocol allows for freedom in transmission strategies. The comprehensive analysis given in this thesis has shown the benefits and drawbacks of SU and MU transmission strategies. It has been shown that the system performace highly depends on the traffic characteristics and the network size. It can be summarized that SU mode is preferable in systems with smaller number of stations and connections, with applications that are not delay-sensitive, and that produce relatively monotonous traffic. In case of real-time applications, and with higher number of connections, although providing lower saturation throughput, MU mode has higher potential for providing timely packet delivery.

The performance of the protocols is also compared in the presence of channel aware scheduler. Fine-grained MU adaptation algorithms have higher potential for better performance than the coarse-grained SU or non-adaptive ones, for the price of higher complexity. However, when the MIMO scheme is also a subject to adaptation algorithm, it gives better performance than MU schedulers, particularly in low SNR range.

Analysis in the presence of channel uncertainty has shown high sensitivity of the analyzed algorithms to imperfect correlation of estimated and used channel matrix. Not only that channel aware scheduling does not provide any gain in case of low correlation of estimated and used channel, but it may lead to worse performance than schedulers that do not take into account CSI. That applies in particular in the presence of MU diversity, since this improves the quality of the channel seen by the transmitter, and leads to choosing higher and less robust PHY modes. This indicates the importance of accuracy of CSI on both sides on communication link, which is one of the biggest challenges in approaching the theoretical MIMO channel capacity.

APPENDIX A

Description of MACNET2 Simulation Tool

MACNET2 [Peetz, 2003, Orfanos, 2006] is an event driven simulation tool developed at the Chair of Communication Networks, RWTH Aachen, for the performance evaluation of HiperLAN/2 and IEEE 802.11 MAC protocols, including MC-CDMA based IEEE 802.11. As a part of this thesis, SU-DCF and MU-DCF protocols, as well as a detailed channel model have been implemented in the simulator.

An overview of the structure of the MACNET2 simulation tool is given in Figure A.1. The protocol is implemented in Specification and Description Language (SDL)[1] and C++ is used, primarily for the channel model and simulation control.

The MIMO channel model, including the receiver algorithms have been implemented in C++ and form a separate module. The SDL module Terminal contains the MAC protocol functionality, and an interface to PHY. SDL graphical representation is translated to phrase representation and converted to C++ code. Besides implementing the standard functions such as channel sensing, this module contains the scheduler algorithm implementations. Different traffic types are provided in the traffic Load Generator module, and the flow of the simulation is managed by the Simulation Control module.

MACNET2 is a system level simulator, and as such allows for setting up scenarios with arbitrary number of stations and their positions (high number of stations, however, increases the simulation time). In the following, more detailed description of MACNET2 is given: protocol implementation is addressed in Sections A.1 and channel modeling in Section A.2.

[1] SDL is a specification language standardized as International Telecommunication Union (ITU) Recommendation Z.100.

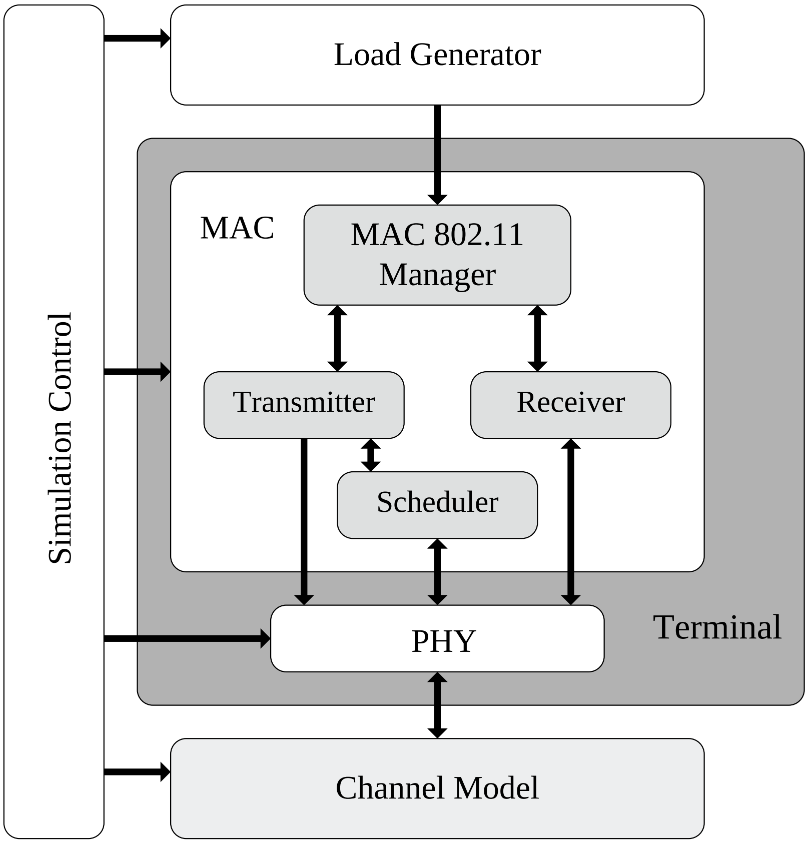

Figure A.1: MACNET2 Simulator

Section A.3 gives an overview of the implementation of channel aware schedulers, including channel uncertainty.

A.1 Protocol Specification

SU-DCF and MU-DCF are implemented in the SDL part of the simulator, including the control frame exchange as described in Section 5, and TDMA and OFDMA based signaling. Both transmitter and receiver modules are affected: the transmitter transmits a set of data packets combined into a MIMO frame, which are separated at the receiver. The receiver uses the information about the receive SNR that is encoded in each data packet to evaluate the correctness of reception. In case of operating in MU mode, the transmitter has to decide which receivers to poll in the MU-RTS frame, as well as which data frames to combine in a MIMO frame. This is implemented according to the scheduling algorithms described in

Section 8.

A.2 Channel Model

In order to model MIMO communication on PHY, MIMO channel matrix is generated between each transmitter-receiver pair. Dimensions of the matrix depend on the number of antennas that are present at the stations, which is a simulation parameter. Channel transfer functions between each transmit/receive antenna pair are independent and identically distributed zero-mean circularly symmetric complex Gaussian random variables with unity variance, constant over the time of one channel access, change though for each channel use and are uncorrelated in time, as described in Section 3.2.1.

Post-processing SNR, calculated using MMSE of ZF algorithm, that corresponds to a certain stream is associated with all the packets that are transmitted on that stream, i.e. for the given transmitter, to the receiver and using the corresponding transmit antenna.

A.3 Scheduling Algorithms

Channel aware scheduling algorithms are specified in SDL. The scheduler module receives from all the stations their CSI in the form of corresponding post-processing SNR. In case of SAMC algorithm, the station feeds back the optimum MIMO scheme together with the corresponding SNR. Then, CSI feedbacks are processed together with the state of queues containing data packets ready for transmission, in order to generate a MIMO frame and transmit it.

A.3.1 Channel Uncertainty Modeling

With perfect channel knowledge at the transmitter, CSI, i.e. post-processing SNR at the time of channel estimation is the same as that at the time of reception. The case of channel uncertainty is somewhat more complex than the case of perfect channel knowledge.

When the channel matrix at the time of channel estimation is generated, another channel matrix, corresponding to the time of data transmission is also generated. The entries of the second channel are correlated with the corresponding entries from the first one, and the correlation is specified by the correlation coefficient that is an input parameter.

When the receiver sends CSI feedback, it does not send only the post-processing SNR values at the time of channel estimation, but also those at the time of MIMO frame reception. The scheduling algorithm then uses the first set for making a scheduling decision after the given algorithm, and the second set of post-processing SNR values is associated with packets depending on the receiver, and antenna it is transmitted from.

List of Figures

List of Tables

LIST OF ABBREVIATIONS

3GPP	3rd Generation Partnership Project
ACK	Acknowledgment
AIFS	Arbitration Interframe Space
A-MPDU	MAC Protocol Data Unit Aggregation
A-MSDU	MAC Service Data Unit Aggregation
AMC	Adaptive Modulation and Coding
AoA	Angle-of-Arrival
AP	Access Point
ARQ	Automatic Repeat Request
AWGN	Additive White Gaussian Noise
BA	Block Acknowledgment
BER	Bit Error Rate
BLAST	Bell Labs Layered Space Time
BR	Bit-by-Bit Round Robin
BSS	Basic Service Set
CD	Colision Detection
CDF	Cumulative Distribution Function
CDMA	Code Division Multiple Access
CoV	Coefficient of Variation
CSI	Channel State Information
CSMA/CA	Carrier Sense Multiple Access with Collision Avoidance
CTS	Clear-to-Send
CW	Contention Window
DCF	Distributed Coordination Function
DIFS	Distributed Coordination Function Interframe Space
DLL	Data Link Layer
DLP	Direct Link Protocol
DSSS	Direct-Sequence Spread-Spectrum
EDCF	Enhanced Distributed Coordination Function
EIFS	Extended Interframe Space
ESS	Extended Service Set
FCS	Frame Check Sequence
FHSS	Frequency-Hopping Spread-Spectrum
FIFO	First In - First Out
HCCA	Hybrid Coordination Function-Controlled Channel Access
HCF	Hybrid Coordination Function
HoL	Head-of-Line
HR/DSSS	High Rate / Direct Sequence Spread Spectrum
HSPA+	High-Speed Packet Access Evolution

IBSS	Independent Basic Service Set
IFS	Interframe Space
IP	Internet Protocol
IR	Infrared
ISI	Inter-Symbol Interference
ISO	International Organization for Standardization
LAN	Local Area Network
LDPC	Low-Density Parity-Check
LoS	Line-of-Sight
LLC	Logical Link Control
LTE	Long Term Evolution
MAC	Medium Access Control
MAN	Metropolitan Local Area Network
M-ACK	MIMO-ACK
MC-CDMA	Multi-Carrier Code Division Multiple Access
MCS	Modulation and Coding Scheme
M-CTS	MIMO-CTS
MIMO	Multiple Input - Multiple Output
MISO	Multiple Input - Single Output
ML	Maximum Likelihood
MMSE	Minimum Mean Square Error
MPDU	MAC Protocol Data Unit
M-RTS	MIMO-RTS
MRC	Maximum Ratio Combining
MSDU	MAC Service Data Unit
MSI	Multi-Stream Interference
MU	Multi-User
MU-DCF	Multi-User - Distributed Coordination Function
NAV	Network Allocation Vector
OFDM	Orthogonal Frequency Division Multiplexing
OFDMA	Orthogonal Frequency Division Multiple Access
OSI	Open Systems Interconnection
OSTBC	Orthogonal Space-Time Block Coding
PAN	Personal Area Network
PCF	Point Coordination Function
PDF	probability density function
PDU	Protocol Data Unit
PER	Packet Error Rate
PHY	Physical Layer
PIFS	Point Coordination Function Interframe Space
PLCP	Physical Layer Convergence Procedure
PLR	Packet Loss Rate
PMD	Physical Medium Dependent

QoS	Quality of Service
RF	Radio Frequency
RIFS	Reduced Interframe Space
RR	Round Robin
RTS	Request-to-Send
SAMC	Spatially Adaptive Modulation and Coding
SAP	Service Access Point
SCM	Spatial Channel Model
SDIV	Spatial Diversity
SDL	Specification and Description Language
SDMA	Space Division Multiple Access
SER	Symbol Error Rate
SIFS	Short Interframe Space
SIMO	Single Input - Multiple Output
SINR	signal-to-Interference-plus-Noise Ratio
SISO	Single Input - Single Output
SNR	Signal-to-Noise Ratio
SMUX	Spatial Multiplexing
ST	Space-Time
STC	Space-Time Coding
STBC	Space-Time Block Coding
STTC	Space-Time Trellis Coding
SU	Single-User
SUC	Successive Cancellation
SU-DCF	Single-User - Distributed Coordination Function
SVD	Singular Value Decomposition
TC	Traffic Class
TCP	Transmission Control Protocol
TDMA	Time Division Multiple Access
TGn	IEEE 802.11n Task Group
TXOP	Transmission Opportunity
VoIP	Voice-over-IP
WiMAX	Worldwide Interoperability for Microwave Access
WLAN	Wireless Local Area Network
WMAN	Wireless Metropolitan Area Network
ZF	Zero Forcing

Bibliography

[3GPP, 2007] 3GPP (2007). *Spatial Channel Model for Multiple Input Multiple Output (MIMO) simulations (Release 7)*. 3rd Generation Partnership Project, Technical Specification Group Radio Access Network. 26

[Alamouti, 1998] Alamouti, S. (1998). A simple transmit diversity technique for wireless communications. *Selected Areas in Communications, IEEE Journal on*, 16(8):1451–1458. 30

[Anton-Haro et al., 2006] Anton-Haro, C., Svedman, P., Bengtsson, M., Alexiou, A., and Gameiro, A. (Sept. 2006). Cross-Layer Scheduling for Multi-User MIMO Systems. *Communications Magazine, IEEE*, 44(9):39–45. 114

[Berger-Sabbatel et al., 2004] Berger-Sabbatel, G., Duda, A., Gaudoin, O., Heusse, M., and Rousseau, F. (29 Nov.-3 Dec. 2004). Fairness and its Impact on Delay in 802.11 Networks. In *Global Telecommunications Conference, 2004. GLOBECOM '04. IEEE*, volume 5, pages 2967–2973 Vol.5, Dallas, TX, USA. 99

[Bianchi, 2000] Bianchi, G. (2000). Performance Analysis of the IEEE 802.11 Distributed Coordination Function. *IEEE Journal on Selected Areas in Communications*, 18(3):535–547. 84, 91

[Bianchi, 1998] Bianchi, G. (Dec 1998). IEEE 802.11-saturation throughput analysis. *Communications Letters, IEEE*, 2(12):318–320. 84

[Bianchi and Tinnirello, 2005] Bianchi, G. and Tinnirello, I. (2005). Remarks on IEEE 802.11 DCF Performance Analysis. *IEEE Communications Letters*, 9(8):765–767. 84, 85, 90, 91

[Biglieri et al., 1998] Biglieri, E., Proakis, J. G., and Shamai, S. (1998). Fading Channels: Information-Theoretic and Communications Aspects. *IEEE Transactions on Information Theory*, 44. 25

[Cao and Li, 2001] Cao, Y. and Li, V. (2001). Scheduling Algorithms in Broadband Wireless Networks. *Proceedings of the IEEE*, 89(1):76–87. 114

[Ci and Sharif, 2005] Ci, S. and Sharif, H. (2005). Improving Goodput in IEEE

802.11 Wireless LANs by Using Variable Size and Variable Rate (VSVR) Schemes. *Wirel. Commun. Mob. Comput.*, 5(3):329–342. 61

[Clarke, 1968] Clarke, R. H. (1968). A Statistical Theory of Mobile Radio Reception. *Bell Labs Technical Journal*, 47:957–1000. 14, 115

[Cooklev, 2004] Cooklev, T. (2004). *Wireless Communications Standards: A Study of IEEE 802.11, 802.15 and 802.16.* Standards Information Network, IEEE Press, New York, NY, USA. 41

[Cover and Thomas, 1991] Cover, T. M. and Thomas, J. A. (1991). *Elements of information theory.* John Wiley and Sons, Inc. 23

[Demers et al., 1989] Demers, A., Keshav, S., and Shenker, S. (1989). Analysis and Simulation of a Fair Queueing Algorithm. *ACM SIGCOMM Computer Communication Review*, 19(4):1–12. 100

[Dianati et al., 2005] Dianati, M., Shen, X. S., and Naik, S. (2005). A New Fairness Index for Radio Resource Allocation in Wireless Networks. *IEEE Wireless Communications and Networking Conference, 2005*, 2:712–717 Vol. 2. 101

[Durgin and Rappaport, 1998] Durgin, G. D. and Rappaport, T. S. (1998). Basic Relationship between Multipath Angular Spread and Narrowband Fading in Wireless Channels. *Electronics Letters*, 34(25):2431–2432. 15

[Ertel et al., 1998] Ertel, R., Cardieri, P., Sowerby, K., Rappaport, T., and Reed, J. (1998). Overview of Spatial Channel Models for Antenna Array Communication Systems. *Personal Communications, IEEE [see also IEEE Wireless Communications]*, 5(1):10–22. 26

[Farsakh and Nossek, 1994] Farsakh, C. and Nossek, J. (1994). Application of Space Division Multiple Access to Mobile Radio. *Personal, Indoor and Mobile Radio Communications, 1994. Wireless Networks - Catching the Mobile Future., 5th IEEE International Symposium on*, pages 736–739 vol.2. 36

[Fincke and Pohst, 1985] Fincke, U. and Pohst, M. E. (1985). Improved Methods for Calculating Vectors of Short Length in a Lattice, Including a Complexity Analysis. In *Mathematics of Computation*, volume 44, pages 463–471. 33

[Foschini, 1996] Foschini, G. J. (1996). Layered Space-Time Architecture For Wireless Communication in a Fading Environment when Using Multi-Element Antennas. *Bell Labs Technical Journal*, pages 41–59. 1, 22, 32

[Gallager, 1963] Gallager, R. G. (1963). *Low Density Parity Check Codes*. MIT Press, Cambridge, MA, USA. 48

[Gans, 1972] Gans, M. J. (1972). A Power-Spectral Theory of Propagation in the Mobile-Radio Environment. *IEEE Transactions on Vehicular Technology*, 21(1):27–38. 15

[Gast, 2002] Gast, M. S. (2002). *802.11 Wireless Networks: The Definitive Guide*. O'Reilly & Associates, Inc., Sebastopol, CA, USA. 40, 41

[Godara, 1997a] Godara, L. C. (1997a). Application of Antenna Arrays to Mobile Communications, Part I: Performance Improvement, Feasability and System Considerations. *Proceedings of the IEEE*, 85(7):1031–1060. 36

[Godara, 1997b] Godara, L. C. (1997b). Application of Antenna Arrays to Mobile. Communications, Part II: Beam-Forming and Direction-of-Arrival Considerations. *Proceedings of the IEEE*, 85(8):1195–1245. 36

[Golub and Loan, 1989] Golub, G. H. and Loan, C. F. V. (1989). *Matrix Computations*. The Johns Hopkins University Press, Baltimore, MD, USA. 23, 34

[Gore et al., 2002] Gore, D., Heath, R. J., and Paulraj, A. (2002). On Performance of the Zero Forcing Receiver in Presence of Transmit Correlation. *IEEE International Symposium on Information Theory*, pages 159–159. 34

[Gore et al., 2000] Gore, D., Nabar, R., and Paulraj, A. (2000). Selecting an Optimal Set of Transmit Antennas for a Low Rank Matrix Channel. *Acoustics, Speech, and Signal Processing, 2000. ICASSP '00. Proceedings. 2000 IEEE International Conference on*, 5:2785–2788 vol.5. 114

[Hata, 1980] Hata, M. (1980). Empirical Formula for Propagation Loss in Land Mobile Radio Services. *IEEE Transactions on Vehicular Technology*, 29(3):317–325. 9, 11

[Heath Jr and Love, 2005] Heath Jr, R. and Love, D. (2005). Multimode Antenna Selection for Spatial Multiplexing Systems with Linear Receivers. *Signal Processing, IEEE Transactions on [see also Acoustics, Speech, and Signal Processing, IEEE Transactions on]*, 53(8 Part 2):3042–3056. 114

[Heath Jr and Paulraj, 2002] Heath Jr, R. and Paulraj, A. (2002). Linear Dispersion Codes for MIMO Systems Based on Frame Theory. *Signal Processing, IEEE Transactions on [see also Acoustics, Speech, and Signal Processing, IEEE Transactions on]*, 50(10):2429–2441. 21

[Heath Jr et al., 2001] Heath Jr, R., Sandhu, S., and Paulraj, A. (2001). Antenna Selection for Spatial Multiplexing Systems with Linear Receivers. *Communications Letters, IEEE*, 5(4):142–144. 114

[Hosein, 2006] Hosein, P. (April 2006). On the Optimal Scheduling of Uplink Resources in OFDMA-Based Wireless Networks. In *Proceedings of the 12th European Wireless Conference*, Athens, Greece. 114

[Huang et al., 2002] Huang, Z., Shen, C.-C., Srisathapornphat, C., and Jaikaeo, C. (2002). A Busy-Tone Based Directional MAC Protocol for Ad Hoc Networks. *MILCOM 2002. Proceedings*, 2:1233–1238 vol.2. 36

[IEEE, 2003] IEEE (2003). *Information Technology- Telecommunications and Information Exchange between Systems- Local and Metropolitan Area Networks- Specific Requirements- Part 11: Wireless LAN Medium Access Control (MAC) and Physical Layer (PHY) Specifications.* 802.11 WG. 39

[IEEE, 2004a] IEEE (2004a). *IEEE Standard for Local and Metropolitan Area Networks Media Access Control (MAC) Bridges.* 802.1D WG. 46

[IEEE, 2004b] IEEE (2004b). *TGn Channel Models.* 802.11 WG. 26

[IEEE, 2005] IEEE (2005). *IEEE Std 802.3 - 2005 Part 3: Carrier Sense Multiple Access with Collision Detection (CSMA/CD) Access Method and Physical Layer Specifications.* 802.3 WG. 39, 49

[IEEE, 2007a] IEEE (2007a). *IEEE P802.11n/D2.02 Draft STANDARD for Information Technology- Telecommunications and Information Exchange Between Systems- Local and Metropolitan Area Networks- Specific Requirements- Part 11: Wireless LAN Medium Access Control (MAC) and Physical Layer (PHY) Specifications: Enhancements for Higher Throughput.* 802.11 WG. 47

[IEEE, 2007b] IEEE (2007b). *IEEE P802.11n/D2.04 Draft STANDARD for Information Technology- Telecommunications and Information Exchange Between Systems- Local and Metropolitan Area Networks- Specific Requirements- Part 11: Wireless LAN Medium Access Control (MAC) and Physical Layer (PHY) Specifications: Enhancements for Higher Throughput.* 802.11 WG. 48, 49

[IEEE, 2007c] IEEE (2007c). *IEEE Standard for Information Technology- Telecommunications and Information Exchange between Systems-Local and Metropolitan Area Networks-Specific Requirements - Part 11: Wireless LAN*

Medium Access Control (MAC) and Physical Layer (PHY) Specifications. 802.11 WG. 39, 45

[Jain et al., 1998] Jain, R. K., Chiu, D.-M. W., and Hawe, W. R. (1998). A Quantitative Measure Of Fairness And Discrimination For Resource Allocation In Shared Computer Systems. *The Computing Research Repository, CoRR*, cs.NI/9809099. 101

[Jakes, 1974] Jakes, J. W. C. (1974). *Microwave Mobile Communications.* A Wiley Interscience Publication, New York, NY, USA. 14, 116

[Kannan, 1983] Kannan, R. (1983). Improved Algorithms for Integer Programming and Related Lattice Problems. In *STOC '83: Proceedings of the fifteenth annual ACM symposium on Theory of computing*, pages 193–206, New York, NY, USA. ACM. 33

[Kelly et al., 1998] Kelly, F., Maulloo, A., and Tan, D. (1998). Rate Control in Communication Networks: Shadow Prices, Proportional Fairness and Stability. In *Journal of the Operational Research Society*, volume 49, pages 237–252. 99, 114

[Ko et al., 2000] Ko, Y.-B., Shankarkumar, V., and Vaidya, N. H. (March 2000). Medium Access Control Protocols using Directional Antennas in Ad Hoc Networks. In *INFOCOM*, pages 13–21, Tel-Aviv, Israel. 36

[Koutsopoulos and Tassiulas, 2002] Koutsopoulos, I. and Tassiulas, L. (2002). Adaptive Resource Allocation in SDMA-Based Wireless Broadband Networks with OFDM Signaling. *INFOCOM 2002. Twenty-First Annual Joint Conference of the IEEE Computer and Communications Societies. Proceedings. IEEE*, 3:1376–1385 vol.3. 36

[Kuppa and Dattatreya, 2006] Kuppa, S. and Dattatreya, G. (June 2006). Modeling and Analysis of Frame Aggregation in Unsaturated WLANs with Finite Buffer Stations. In *Communications, 2006. ICC '06. IEEE International Conference on*, volume 3, pages 967–972, Istanbul, Turkey. 51

[Larson and Shubert, 1979] Larson, H. and Shubert, B. (1979). *Probabilistic Models in Engineering Sciences.* John Wiley and Sons, New York, NY, USA. 29

[Larsson and Stoica, 2003] Larsson, E. G. and Stoica, P. (2003). *Space-Time Block Coding for Wireless Communications.* Cambridge University Press, Cambridge, UK. 23, 25, 29, 31, 32

[Law and Kelton, 2000] Law, A. and Kelton, W. (2000). *Simulation Modeling and Analysis*. Mc Grawn Hill. 77

[Lee et al., 2006] Lee, J.-W., Chiang, M., and Calderbank, A. (2006). Price-Based Distributed Algorithms for Rate-Reliability Tradeoff in Network Utility Maximization. *Selected Areas in Communications, IEEE Journal on*, 24(5):962–976. 114

[Liberti and Rappaport, 1999] Liberti, J. C. and Rappaport, T. S. (1999). *Smart Antennas for Wireless Communications*. Prentice Hall, Inc., Upper Saddle River, NJ, USA. 15

[Lin and Wong, 2006] Lin, Y. and Wong, V. W. S. (November 2006). Frame Aggregation and Optimal Frame Size Adaptation for IEEE 802.11n WLANs. In *Global Telecommunications Conference, 2006. GLOBECOM '06. IEEE*, pages 1–6, San Francisco, CA, USA. 51, 61

[Lu et al., 1999] Lu, S., Bharghavan, V., and Srikant, R. (1999). Fair Scheduling in Wireless Packet Networks. *Networking, IEEE/ACM Transactions on*, 7(4):473–489. 114

[McKenney, 1991] McKenney, P. E. (1991). Stochastic Fairness Queuing. *Internetworking: Theory and Experience*, 2:113–131. 100

[Michalke et al., 2006] Michalke, C., Zimmermann, E., and Fettweis, G. (Sept. 2006). Linear Mimo Receivers vs. Tree Search Detection: A Performance Comparison Overview. *Personal, Indoor and Mobile Radio Communications, 2006 IEEE 17th International Symposium on*, pages 1–7. 35

[Mirkovic, 2008] Mirkovic, J. (2008). Fairness and Delay in MU-MIMO WLANs. In *Proceedings of 5th IEEE Consumer Communications & Networking Conference 2008*, Las Vegas, USA. 98

[Mirkovic et al., 2006] Mirkovic, J., Orfanos, G., and Reumerman, H.-J. (2006). MIMO Link Modeling for System Level Simulations. In *Proceedings of the 17th Annual IEEE International Symposium on Personal, Indoor and Mobile Radio Communications*, Helsinki, Finland. 63

[Mirkovic et al., 2007a] Mirkovic, J., Orfanos, G., Reumerman, H.-J., and Denteneer, D. (2007a). A MAC Protocol for MIMO Based IEEE 802.11 Wireless Local Area Networks. In *Proceedings of Wireless Communications and Network Conference (WCNC) 2007*, Hong Kong, China. IEEE Communication Society. 53

[Mirkovic and Walke, 2008b] Mirkovic, J. and Walke, B. (2008b). Theoretical Analysis of Saturation Throughput in MU-DCF. In *Proceedings of IEEE 67th Vehicular Technology Conference: VTC2008-Spring*, page 5, Singapore. 75

[Mirkovic and Walke, 2008a] Mirkovic, J. and Walke, B. (October 2008a). On Performance of MIMO Link Adaptation in the Presence of Channel Uncertainty. In *IEEE International Conference on Wireless and Mobile Computing, Networking and Communications - IEEE WiMob 2008*, page 6, Avignon, France. 113

[Mirkovic et al., 2008] Mirkovic, J., Walke, B., and Garcia, J. G. (October 2008). Channel Aware Scheduling in MIMO Based WLANs in the Presence of Channel Uncertainty. In *IEEE International Symposium on Wireless Communication Systems 2008 - IEEE ISWCS 2008*, page 5, Reykjavik, Iceland. 113

[Mirkovic et al., 2007b] Mirkovic, J., Walke, B., and Zhao, J. (2007b). Channel Aware Scheduling in MU-DCF WLANs. In *Proceedings of International Conference on Wireless Communications, Networking and Mobile Computing (WiCOM) 2007*, Shanghai, China. IEEE Communication Society. 113

[Mirkovic et al., 2007c] Mirkovic, J., Zhao, J., and Denteneer, D. (2007c). A MAC Protocol with Multi-User MIMO Support for Ad-Hoc WLANs. In *Personal, Indoor and Mobile Radio Communications, 2007. IEEE 18th International Symposium on*, Athens, Greece. 53

[Nagle, 1987] Nagle, J. B. (1987). On Packet Switches with Infinite Storage. *IEEE Transactions on Communications [legacy, pre - 1988]*, 35(4):435–438. 100

[Nasipuri et al., 2000] Nasipuri, A., Ye, S., You, J., and Hiromoto, R. (2000). A MAC Protocol for Mobile Ad Hoc Networks Using Directional Antennas. 36

[Ng et al., 1998] Ng, T. S. E., Stoica, I., and Zhang, H. (1998). Packet Fair Queueing Algorithms for Wireless Networks with Location-Dependent Errors. *INFOCOM '98. Seventeenth Annual Joint Conference of the IEEE Computer and Communications Societies. Proceedings. IEEE*, 3:1103–1111 vol.3. 114

[Okumura et al., 1968] Okumura, Y., Ohmori, E., Kawano, T., and Fukuda, K. (1968). Field Strength and its Variability in VHF and UHF Land Mobile Service. *Rev. Elec. Comm. Lab*, 16:825. 9, 11

[Orfanos, 2006] Orfanos, G. (2006). *Development and Performance Evaluation of an MAC Protocol for MC-CDMA Wireless LANs with QoS Support.* PhD thesis, Aachen University, Aachen, Germany. 153

[Ozarow et al., 1994] Ozarow, L. H., Shamai, S., and Wyner, A. D. (1994). Information Theoretic Considerations for Cellular Mobile Radio. *IEEE Transactions on Vehicular Technology*, 43(2):359–378. 25

[Park et al., 2007] Park, M., Chae, C., and Heath, R. (2007). Ergodic Capacity of Spatial Multiplexing MIMO Systems with ZF Receivers for Log-Normal Shadowing and Rayleigh Fading Channels. In *Personal, Indoor and Mobile Radio Communications, 2007. PIMRC 2007. IEEE 18th International Symposium on*, pages 1–5, Athens, Greece. 34

[Paulray et al., 2004] Paulray, A. J., Gore, D. A., Nabar, R. U., and Bölcskei, H. (2004). An overview of MIMO communications - A Key to Gigabit Wireless. *Proceedings of the IEEE*, 92(2):198–218. 18

[Paulray et al., 2003] Paulray, A. J., Nabar, R. U., and Gore, D. A. (2003). *Introduction to Space-Time Wireless Communications.* Cambridge University Press, Cambridge, UK. 15, 18, 23, 24, 26, 28, 29, 33, 34, 35

[Peetz, 2003] Peetz, J. (2003). *Multihop-Ad-hoc-Kommunikation mit dynamischer Frequenzwahl, Leistungssteuerung und Ratenanpassung für drahtlose Netze im 5 GHz Band.* PhD thesis, Aachen University, Lehrstuhl für Kommunikationsnetze. 153

[Piolini and Rolando, 1999] Piolini, F. and Rolando, A. (1999). Smart channel-assignment algorithm for SDMA systems. *Microwave Theory and Techniques, IEEE Transactions on*, 47(6):693–699. 36

[Pohl et al., 2003] Pohl, V., Nguyen, P. H., Jungnickel, V., and von Helmolt, C. (December 2003). How Often Channel Estimation is Needed in MIMO Systems. In *Global Telecommunications Conference, 2003. GLOBECOM '03. IEEE*, volume 2, pages 814–818 Vol.2, San Francisco, CA, USA. 115

[Proakis, 2001] Proakis, J. G. (2001). *Digital Communications.* Mc Grawn Hill. 9, 22, 28, 32

[Rappaport, 2001] Rappaport, T. (2001). *Wireless Communications: Principles and Practice.* Prentice Hall PTR, Upper Saddle River, NJ, USA. 7, 12, 14, 15

[Roy et al., 1986] Roy, R., Paulraj, A., and Kailath, T. (Oct 1986). ESPRIT–

A Subspace Rotation Approach to Estimation of Parameters of Cisoids in Noise. *Acoustics, Speech, and Signal Processing [see also IEEE Transactions on Signal Processing], IEEE Transactions on*, 34(5):1340–1342. 1

[Schmidt, 1986] Schmidt, R. (Mar 1986). Multiple emitter location and signal parameter estimation. *Antennas and Propagation, IEEE Transactions on [legacy, pre - 1988]*, 34(3):276–280. 1

[Shad et al., 2001] Shad, F., Todd, T., Kezys, V., and Litva, J. (2001). Dynamic Slot Allocation (DSA) in Indoor SDMA/TDMA Using a Smart Antenna Basestation. *Networking, IEEE/ACM Transactions on*, 9(1):69–81. 36

[Shannon, 1948a] Shannon, C. E. (1948a). A Mathematical Theory of Communication. *Bell System Technical Journal*, 27:379–423. 22

[Shannon, 1948b] Shannon, C. E. (1948b). A Mathematical Theory of Communication. *Bell System Technical Journal*, 27:623–656. 22

[Shreedhar and Varghese, 1995] Shreedhar, M. and Varghese, G. (1995). Efficient Fair Queueing Using Deficit Round Robin. *ACM SIGCOMM Computer Communication Review*, 25(4):231–242. 100

[Sklar, 1997a] Sklar, B. (1997a). Rayleigh Fading Channels in Mobile Digital Communication Systems. I. Characterization. *Communications Magazine, IEEE*, 35(9):136–146. 9, 10, 12, 14

[Sklar, 1997b] Sklar, B. (1997b). Rayleigh Fading Channels in Mobile Digital Communication Systems .II. Mitigation. *Communications Magazine, IEEE*, 35(7):102–109. 14

[Sklar, 2001] Sklar, B. (2001). *Digital Communications: Fundamentals and Applications (2nd ed.)*. Prentice-Hall, Inc., Upper Saddle River, NJ, USA. 8, 9, 10, 11, 12, 13, 14, 116

[Skordoulis et al., 2008] Skordoulis, D., Ni, Q., Chen, H.-H., Stephens, A. P., Liu, C., and Jamalipour, A. (2008). IEEE 802.11n MAC Frame Aggregation Mechanisms for Next-Generation High-Throughput WLANs. *Wireless Communications, IEEE [see also IEEE Personal Communications]*, 15(1):40–47. 51

[Tarokh et al., 1999a] Tarokh, V., Jafarkhani, H., and Calderbank, A. (1999a). Space-time block codes from orthogonal designs. *Information Theory, IEEE Transactions on*, 45(5):1456–1467. 1, 32

[Tarokh et al., 1999b] Tarokh, V., Naguib, A., Seshadri, N., and Calderbank, A. R. (1999b). Space-Time Codes for High Data Rate Wireless Communication: Performance Criteria in the Presence of Channel Estimation Errors, Mobility, and Multiple Paths. *IEEE Transactions on Communications*, 47(2):199–207. 33

[Tarokh et al., 1998] Tarokh, V., Seshadri, N., and Calderbank, A. R. (1998). Space-Time Codes for High Data Rate Wireless Communication: Performance Criterion and Code Construction. *IEEE Transactions on Information Theory*, 44(2):744–765. 33

[Telatar, 1999] Telatar, E. (1999). Capacity of Multi-Antenna Gaussian Channels. *European Transactions on Telecommunications*, 10(6):585–596. 1, 22

[Titus, 1999] Titus, L. (1999). Maximum Ratio Transmission. *IEEE Transactions on Communications*, 47(10):1458–1461. 29

[Tobagi and Kleinrock, 1975] Tobagi, F. and Kleinrock, L. (1975). Packet Switching in Radio Channels: Part II–The Hidden Terminal Problem in Carrier Sense Multiple-Access and the Busy-Tone Solution. *Communications, IEEE Transactions on [legacy, pre - 1988]*, 23(12):1417–1433. 36

[van de Beek et al., 1999] van de Beek, J.-J., Borjesson, P., Boucheret, M.-L., Landstrom, D., Arenas, J., Odling, P., Ostberg, C., Wahlqvist, M., and Wilson, S. (Nov 1999). A Time and Frequency Synchronization Scheme for Multiuser OFDM. *Selected Areas in Communications, IEEE Journal on*, 17(11):1900–1914. 58

[Vornefeld et al., 1999] Vornefeld, U., Walke, C., and Walke, B. (1999). SDMA-Techniques for Wireless ATM. *IEEE Communications Magazine*, 0:2–7. 125

[Walke, 1999] Walke, B. (1999). *Mobile Radio Networks: Networking and Protocols*. John Wiley & Sons, Inc. New York, NY, USA. 40

[Winters, 1984] Winters, J. (1984). Optimum Combining in Digital Mobile Radio with Cochannel Interference. *Selected Areas in Communications, IEEE Journal on*, 2(4):528–539. 1

[Winters et al., 1994] Winters, J. H., Salz, J., and Gitlin, R. D. (1994). The Impact of Antenna Diversity on the Capacity of Wireless Communication Systems. *IEEE Transactions on Communications*, 42:1740–1751. 34

[Yin et al., 2004] Yin, J., Wang, X., and Agrawal, D. (March 2004). Optimal Packet Size in Error-Prone Channel for IEEE 802.11 Distributed Coordination Function. *Wireless Communications and Networking Conference, 2004. WCNC. 2004 IEEE*, 3:1654–1659 Vol.3. 61

[Yoo et al., 2004] Yoo, T., Yoon, E., and Goldsmith, A. (2004). MIMO Capacity with Channel Uncertainty: Does Feedback Help? In *Global Telecommunications Conference, 2004. GLOBECOM '04. IEEE*, volume 1, pages 96–100 Vol.1, Dallas, TX, USA. 115

[Ziouva and Antonakopoulos, 2002] Ziouva, E. and Antonakopoulos, T. (2002). CSMA/CA performance under high traffic conditions: throughput and delay analysis. *Computer Communications*, 25(3):313–321. 84

ACKNOWLEDGMENT

Completing this PhD thesis in a little bit more than five years at the Department of Communication Networks (ComNets) at RWTH Aachen University I owe most to my supervisor Prof. Bernhard Walke. I wish to express to him my sincere gratitude for the provided opportunity as well as for all the discussions, advices and the given freedom throughput my research work.

Also, I would like to thank Prof. Friedrich Jondral from the University of Karlsruhe for his kind support as the second examiner.

Thanks to both scientific and non-scientific, former and present members of ComNets, for accompanying, supporting when needed, and for making a motivating work environment; let me mention only some of them: Fahad Aijaz, Daniel Bültmann, Martha Lucia Clavijo-Velasco, Michael Einhaus, Guido R. Hiertz, Ralf Jennen, Ole Klein, Georgios Orfanos, Arif Otyakmaz, Doro Pawelzick, Benedikt Wolz, Yunpeng Zang. I would also like to express my appreciation to Hans-Jürgen Reumermann and Dee Denteneer from Philips Eindhoven in the Netherlands for the great cooperation during our common project work. Many thanks I owe to my students Javier Cerezuela, Jing Zhao, Minh Phu Doan and Jordi Gomez Garcia, whose contributions helped my research work as well.

Special thanks I owe to following people: to my parents Slavica and Novica Mirković, my sister Natasa Mirković Letourneut, my brother in law Leonardo Letourneaut, my friends, in particular to Boris Pijetlović, Jelena Tepavac and Bane Timotijević, and last, but certainly not least to Michael Einhaus. To them I express here once again my true appreciation and endless gratefulness. I would kindly ask for forbearance people whose generous support made my dissertation possible, but who were not explicitly mentioned here. My endless gratitude extends also to you.

CURRICULUM VITAE

Name:	Jelena Mirković
Date of birth:	December 19^{th}, 1978
Place of birth:	Kikinda, Serbia
Nationality:	Serbian

09/1993 - 06/1997	Gymnasium "Dušan Vasiljev", Kikinda, Serbia
10/1997 - 06/2003	Studies of Electrical Engineering at the University of Belgrad, Serbia
10/2001 - 12/2001	Internship at the University of Malaga, Spain
08/2003 - 10/2008	Research engineer at the Department of Communication Networks, RWTH Aachen University